# THE USE OF CARBONATION AND FRACTIONAL EVAPORATIVE CRYSTALLIZATION IN THE PRETREATMENT OF HANFORD NUCLEAR WASTES

A Thesis
Presented to
The Academic Faculty

By

George Pierre Dumont Jr.

In Partial Fulfillment
Of the Requirements for the Degree
Master of Science in Chemical and Biomolecular Engineering

Georgia Institute of Technology

August, 2007

**THE USE OF CARBONATION AND FRACTIONAL EVAPORATIVE CRYSTALLIZATION IN THE PRETREATMENT OF HANFORD NUCLEAR WASTES**

Approved by:

Dr. Ronald W. Rousseau, Chair and Advisor
School of Chemical and Biomolecular Engineering
*Georgia Institute of Technology*

Dr. Amyn S. Teja
School of Chemical and Biomolecular Engineering
*Georgia Institute of Technology*

Dr. Wm. James Frederick, Jr.
School of Chemical and Biomolecular Engineering
Director, Institute of Paper Science and Technology
*Georgia Institute of Technology*

Date Approved: June 27, 2007

## PREFACE

There are currently 53 million gallons of hazardous and highly radioactive wastes awaiting treatment at the Hanford site in the State of Washington. These wastes are stored in 177 underground shielded tanks, partitioned into 18 tank farms. Wastes have accumulated at the site since World War II and are a result of more than fifty years of nuclear materials production.

Waste is a term referring to liquids and solids that are radioactive and/or hazardous [DOE/EM-0319, 1997]. Department of Energy wastes awaiting disposal are accumulated in containers, tanks, silos, buildings, and other structures along with the wastes that have been retrieved in site cleanups. All waste that falls under the responsibility of the US Department of Energy (DOE) is measured in terms of volume and radioactivity content [DOE/EM-0319, 1997]. "Approximately two-thirds of the legacy of waste managed by the Department of Energy was generated from nuclear weapons production. Some waste has been generated as a result of other DOE programs in basic research, nuclear power research, and other applied research and development activities. Additionally, some waste was generated as a result of producing nuclear fuel for the NNPP (Naval Nuclear Propulsion Program) and commercial nuclear power reactors" [DOE/EM-0319, 1997].

At the Hanford site, nuclear wastes have been generated by activities like those described above and include such as purification and chemical separation, mining, milling and refining, reactor operations, research, development and testing, fuel and target fabrication, enrichment, and finally weapons components fabrication. Activities

related to weapons production are responsible for 220,000 $m^3$ of the 239,000 $m^3$ of the total volume of high-level liquid wastes inventoried at the Hanford site. In terms of radioactivity, the nuclear weapons activities generated 320 million curies among the total 347 million curies disposed at Hanford [DOE/EM-0319, 1997].

Isotopes responsible for the radioactivity of the waste stored at Hanford are mainly uranium fission products. Hence, a methodology was developed in order to select the most important radionuclides present in the Hanford waste along with their concentrations [Cowley W.L, 1998]. This methodology facilitated the identification of cesium [Lewis R.E, 1965], technetium [Vance E.R, 1998] and strontium [Fullam H.T, 1976] as radioactive species present in Hanford waste. Among these radioactive isotopes, $^{137}Cs$ (cesium 137) has been identified as the major isotope remaining in the low and medium curie wastes that must be removed before immobilization.

However, radioactive isotopes represent only a small fraction of the waste. The bulk of the waste is composed of non-radioactive inorganic chemicals issued from the fuel reprocessing operations. More recently, the characterization of the solid phases in the waste have focused not only on quantifying amounts but also in speciation. Speciation studies showed the importance of the presence of several sodium double salts and of certain heavy elements [Herting Dan, 2003].

Since limited thermodynamic information was available for these sodium double salts at the conditions present in the Hanford tanks, there was a need for simulation tools in order to predict their thermodynamic behavior. The Environmental Simulation Program (developed by OLI Systems Inc.) was chosen in order to simulate the salt cake dissolution, tank retrieval, and pipeline transfer operations. Experimental measurements

of phase equilibrium were performed for 9 saltcakes in the high ionic strength inorganic system conditions of the Hanford waste tanks and compared to simulations. This allowed examining of the predictive aspect of the simulation program [Toghiani Rebecca K., 2002].

The treatment of both Low Level Liquid Waste (LLLW) and High Level Liquid Waste (HLLW) accumulated at Hanford site was initially intended to be performed by a single structure called the Waste Treatment and Immobilization Plant (WTP). It is intended to immobilize the liquid waste in borosilicate glass cast into stainless steel canisters. The filled canisters will be disposed of in a federal geologic repository.

The waste treatment plant facility was originally intended to integrate three main processes. A pretreatment unit would reduce the volume of HLLW to be treated. Then the liquid waste would be sent to the melter feed vitrification system. Among the different technologies possible for the vitrification process we can mention the “in-can melter”, the “Pt Crucible” and the “Joule-heated” melter [Chapman C.C, 1979]. The vitrification plant at Hanford would use a continuous feed melter technology [Smith Robert. A, 1990] where the feed is introduced continuously inside the melter box with a water-cooled nozzle. The refractory-lined melter box is equipped with a stainless steel cooling water jacket, heating electrodes, and off-gas vent. The off-gas system is positioned from the exhaust opening in the melter cell to the exhaust duct of the plant’s building. Its aim is to remove the particulates, the radionuclides, and reactive gases that have formed in the melter so that the exhaust gas meets regulations. The glass formed is then transferred to the canister by introducing vacuum inside the canister and using a canister-to-melter spout. The filled canister is then cooled on a stainless steel turntable and stored in the

appropriate repository site. The melter cell is equipped with a closed circuit television in order to control the process.

The vitrification process is a common technique used for the HLLW treatment and has been used successfully in several other U.S. Department of Energy sites [Carreon Rudy, 2002], [Rabiger K., 1995], [Colombo, P., 2003]. This technology, which consists of the immobilization of the liquid waste into a borosilicate glass, has been investigated thoroughly during the years.

To demonstrate the feasibility of vitrification and the durability of the high-level waste glass, a high level waste sample from Hanford tank AZ-101 was processed to glass and analyzed with respect to chemical composition, radionuclide content, and waste loading capacity [Hrma P., Crum J.V, Bates D.J, 2005]. The vitrified borosilicate glass was then tested to demonstrate its compliance with regulatory requirements. Crystallinity testing was performed by quantitative X-Ray Diffraction (XRD) and image analysis was performed with scanning electron microscopy (SEM) micrographs. Glass leachability was measured with the product consistency test and the toxicity characteristic leaching procedure [Hrma P., Crum J.V, Bredt P.R, 2005]. These results were compared with the non-radioactive simulant glass results and models were used in order to identify the impact of spinels on glass composition and leachability [Wilson B.K, 2002], [Mika M., 2001].

In 2000, the U.S. Department of Energy awarded a 14 billion dollar contract for the construction of the WTP and the cleaning of the Hanford site by the year 2030 [Smith Robert A., 1990]. However, contractor and DOE Management issues have led to higher costs, construction delays, and safety concerns. Since the WTP construction contract was

awarded in 2000, the estimated building cost has increased more than 150 %, from 4.3 to 11 billion dollars. In addition, the completion date for the building of the WTP has been postponed by 6 years or more [Aloise Gene, 2006]. These issues were attributed to insufficient contractor performance in implementing the adequate nuclear safety requirements and in its project estimate, the DOE management issues, and technical challenges that arose.

Safety issues were also raised as an effect of extended storage time at Hanford site [DOEM/EM-0266, 1996], [DOEM/EM-0232 and DOEM/EM-0290, 1995-1996], [DOE, 1996]. Many of Hanford's older single shell tanks have leaked and some one million gallons of waste are believed to have leaked from these tanks in the last fifty years [DOE/EM-0319, 1997]. The double shell tanks, some of these having been built in the early 80's, were constructed to last for 50 years. However, the extension in the project completion time increased the risks of liquid waste or flammable gases leaking due to the aging of the waste [Bryan Sam, 2003]. Three additional main releases of radioactive materials have occurred since 1944. More than 200 million gallons of slightly radioactive water have been routinely discharged in Hanford soil leading to soil and groundwater contamination since 1951. Between 1944 and 1947 Iodine-131, a radioactive isotope with a half-life of eight days, was directly released into the atmosphere. Finally, between 1944 and 1971, radionuclides were directly released to the Columbia River through contaminated cooling water used for the fuel elements in the reactor core [DOE/EM-0319, 1997].

Based on this information related to cost, time, and environmental issues, the U.S. Department of Energy has determined that the preferred alternative to remediate the

Hanford tank waste would be to submit it to a pretreatment process. This process would separate the waste into Low Activity Waste (LAW) and High Level Waste (HLW), which would both be vitrified into borosilicate glasses [Carreon Rudy, 2002].

The LAW would be immobilized through bulk vitrification for on-site disposal, contrary to the HLW that would be immobilized as glass through the WTP for ultimate disposal in the national repository. The bulk vitrification process is well known at the Hanford site and experiments at the engineering scale have been performed with simulated waste solutions [Tyree Geoff.], [Kaldor R.A, 1985], [Huang Frank, 1994]. In these experiments, simulant was mixed with soil and small amounts of chemical additives before being melted at 1300 degrees centigrade. The melter used for the bulk vitrification process also acts as the final container for the immobilized waste and can be stored in situ. This vitrification method, by supplementing the WTP, would greatly decrease the final repository and overall project costs while accelerating the treatment of Hanford wastes [Thompson L.E, 2003].

Several methods have been proposed and studied for use in removing cesium from Hanford wastes. Such methods include ion exchange, solvent extraction, tetraphenylborate precipitation, nanofiltration-complexation and evaporative fractional crystallization. Ideally, the selected technology will remove at least 99% of the cesium from the waste and add no additional waste streams to the process [Carreon Rudy, 2002].

The proposed ion exchange process uses a SuperLig® 644 resin material containing a poly (hydroxyarlyne) ligand, which is highly selective for the cesium cation. Research has proven that by operating two ion exchange columns in series, cesium removal yields can range from 99.4-99.98%. The reason for the range in cesium yields

was found to be the potassium concentration in the feed stream; potassium competes with cesium for the ligand sites on the resin. This process is very attractive since the resin can be reused by eluting the column with nitric acid (removing the cesium) and regenerating the resin with sodium hydroxide. The downside to this technology is that it introduces an acid and base stream to the process, which could increase the total waste volume [Hassan N.M, 2002].

A second possible method for removing cesium from Hanford wastes is an extraction process using magnetic microparticles. These particles are composed of magnetite ($Fe_3O_4$), crystalline silicotitanate (CST), and polyacrolein, and are known by the trade name MagAcryl$^{TM}$-CST. During the process cesium binds to the CST in the micropores and after an appropriate contact time a high gradient magnetic separator is used to separate the particles from the liquid stream. This method has proven to remove between 90-98% of the cesium in a single stage. The major drawback to this method is that magnetite is susceptible to dissolution under extreme conditions, and since the magnetic separation step relies on magnetite, dissolution would ruin this process [Kaminski Michael D., 2002].

Tetraphenylborate (TPB) precipitation is another alternative for cesium removal from Hanford wastes. To begin this process, aqueous NaTPB is mixed with the cesium containing waste. Ion exchange occurs between sodium and cesium and insoluble CsTPB is precipitated from the solution. This cesium precipitate is then separated, dissolved in a propylene carbonate stream, and sent to a three phase extraction. The extraction step involves an upper layer of tripropylamine, a middle layer of aqueous $NaNO_3$, and a lower layer of cesium-containing propylene carbonate. During the extraction process, ion

exchange occurs again between cesium and sodium, with aqueous $CsNO_3$ being the final product of interest. TPB precipitation has proven to have a cesium removal yield of at least 99.8%, but there are several drawbacks to this method. These drawbacks include the additional process streams necessary for the separation process and the potential decomposition of TPB into benzene and other flammable organics [Ponder Sherman M., 2001].

The fourth alternative method discussed here is nanofiltration-complexation. This process utilizes a cesium-selective ligand to form a cesium-ligand complex in the waste stream, which is then sent to a nanofiltration step. The ligand chosen for testing was tetrahydroxylated bis-crown-6 calix[4]arene. This process is attractive since it does not add additional wastes to the process, but studies have shown that a single stage of complexation-nanofiltration only removes 90% of the cesium in the feed stream [Chitry Frederic, 2001].

The pretreatment method selected and investigated in this thesis is fractional crystallization. This method "was already demonstrated in the laboratory for separating clean, virtually non-radioactive sodium nitrate from Hanford tank waste". Flowsheet modeling has shown that the process could reduce the volume of vitrified low activity waste (LAW) by 80% to 90%, reducing disposal costs by an estimated $240 million, and would eliminate the need for building a $2.2 billion large scale vitrification plant [Herting Daniel L., 1997].

The evaporative crystallization method uses experimental solubility data obtained for three main sodium salts present in the simulant solutions. The solubilities of sodium nitrate, sodium nitrite, and sodium aluminate were obtained as functions of the

temperature and concentration of sodium hydroxide, nitrate, nitrite and aluminate. The effects of the other species present in simulated waste solutions were found to be negligible [Reynolds D.A, 1985].

A general procedure for the evaporative fractional crystallization of simulated Hanford waste solutions was established. It concerns the crystal formation of burkeite and other sodium salts. This method would decrease the volume of radioactive waste, but also the sodium-to-sulfate molar ratio in the WTP feed, which may limit the formation of stable glass matrices during vitrification [Geniesse Donald James, 2004].

The crystal identification of the solid phases issued from research on Hanford simulated wastes are performed through Polarized Light Microscopy (PLM). For each of the different crystalline species commonly obtained from processes involving Hanford wastes (or simulated wastes), a listing of characteristics and full-color photographs was established. The crystalline characteristics described were the extinction position, the crystal morphology, the optic and elongation signs, the interference figure and birefringence [Herting D.L, 1992]. The precise inventory and importance of the data collected on inorganic species likely to crystallize made this technique the preferred method for crystal characterization.

The simulants used in testing were developed from available analysis data. Tests on simulated waste are to be performed before tests on the actual radioactive wastes. Laboratory testing with the radioactive wastes are to be handled under hot cell environment. The specific hot cell equipment to be used for the cesium removal pretreatment process testing has been already developed [Hammit A.P, 1979].

## ACKNOWLEDGEMENTS

I would like to acknowledge the financial support for this research project provided by the U.S. Department of Energy's Office of Environmental Management (EM-21 – Office of Cleanup Technology) through CH2M HILL and COGEMA, Inc. The interaction with Eric Nelson has been beneficial in keeping the activities moving forward and focused on the project objectives.

Guidance from Dr. Daniel L. Herting of CH2M HILL provided very helpful insights to many of the issues concerning fractional crystallization from the Hanford solutions. In addition, his knowledge and willingness to help the project team learn to use polarized light microscopy in studying crystals produced in this work were invaluable.

Don Geniesse of COGEMA, Inc. provided knowledgeable and timely guidance with his simulations of fractional crystallization. He did not mind answering even the most mundane questions regarding the systems with which we worked, and he was especially helpful in responding to "what if" questions regarding process modifications.

The work benefited considerably from discussions with Tim Nordahl, President of Swenson Inc. He provided perspectives and suggestions regarding the most important data for taking the results of our work to a scaled-up process.

We express appreciation to Jeff Dillener of Galbraith laboratories for his diligence in working with us to provide analytical results that were as useful as possible. We also would like to thank Mike Buchanan at the IPST Center at Georgia Tech for his assistance with chemical analyses.

Jeff Andrews and Brad Parker of the machine shop in the School of Chemical & Biomolecular Engineering provided careful and timely work in constructing parts of the assembled apparatus.

I would also like to acknowledge past and present members of Dr. Rousseau's research group for their support and assistance in day-to-day activities. These members include Karsten Bartling, Stephanie Barthe, Cosmas Bayuadri, Krystle Chavez, Young-soo Kim, Quinta Nwanosike, and "Ov" Apichit Svang-Aryaskul.

Finally, I would like to give special thanks to those whom I worked with closely on this project. I would like to thank my advisor Dr. Ronald W. Rousseau for his guidance and support and my team members Dr. Hatem Alsyouri and Laurent Nassif for their hard work in the experiments and analyses involved in this project.

## TABLE OF CONTENTS

## LIST OF TABLES

## LIST OF FIGURES

# LIST OF ABBREVIATIONS

## Abbreviations and Acronyms

| | |
|---|---|
| ACS | American Chemical Society |
| ASTM | American Society of Testing Materials |
| CD | compact disk |
| CSD | crystal size distribution |
| DAQ | data acquisition |
| DF | Decontamination Factor |
| DST | Double-Shell Tank |
| MW | molecular weight |
| OD | outside diameter |
| PLM | Polarized Light Microscopy |
| PTFE | poly tetrafluoroethylene |
| SST | Single-Shell Tank |
| WTP | Waste Treatment and Immobilization Plant |

## Units

| | |
|---|---|
| ft | foot |
| g | gram |
| °C | degrees centrigrade |
| wt% | weight percent |
| mol | mole |
| M | molar |
| L | Liter |
| mL | milliliter |
| ppm | parts per million |
| Ci | curies |
| mm | millimeter |
| mA | milliampere |
| Ω | ohms |
| pH | potential of Hydrogen – measure of acidity or alkalinity |
| in | inch |
| µm | micrometer |
| h | hour |
| min | minute |

## SUMMARY

The purpose of this work was to explore the use of fractional evaporative crystallization as a technology that can be used to separate medium-curie waste from the Hanford Site tank farms into a high-curie waste stream, which can be sent to a Waste Treatment and Immobilization Plant (WTP), and a low-curie waste stream, which can be sent to Bulk Vitrification. Experimental semi-batch crystallizations of sodium salts from simulant solutions of double-shell tank (DST) feed demonstrated that the recovered crystalline product met the purity requirement for exclusion of cesium and nearly met the requirement on sodium recovery.

Batch fractional evaporative crystallization involves the removal of multiple solutes from a feed solution by the progressive achievement of supersaturation (through evaporation) and concomitant nucleation and growth of each species. The slurry collected from each of these crystallization stages was collected and introduced to filtration and washing steps. The product crystals obtained after washing were sampled for analysis by polarized light microscopy (PLM), dried, and sieved. The PLM results aided in identification of species crystallized in each stage.

Carbonation was used as a supplemental method to evaporative crystallization in order to increase the sodium recovery in DST experiments. Carbonation was necessary due to the high aluminum ion concentration in the solution, which leads to formation of a viscous gel during evaporation. This gel was avoided by reacting carbon dioxide with hydroxyl ions, which modified the system behavior. Through two stages of carbonation, each followed by evaporation, the effect of carbonation on sodium recovery was demonstrated.

# CHAPTER 1: INTRODUCTION

The purpose of the work described in this thesis was to determine whether or not fractional crystallization is a feasible technology that can be used to condition double-shell tank (DST) wastes from the Hanford Site tank farms for the CH2M Hill Low Activity Waste (LAW) supplemental treatment system. Apparatus and procedures used during crystallization runs are presented and results from the DST Certification Run are compared to process criteria.

## 1.1 PROCESS CRITERIA

The fundamental objective of the CH2M Hill LAW supplemental treatment system is to separate the input waste stream into two output streams; one stream will be concentrated in the radioactive elements (primarily $^{137}Cs$), while the other will contain the majority of sodium and sulfate ions. The concentrated $^{137}Cs$ stream will be sent to a Waste Treatment and Immobilization Plant (WTP) for further processing, while the relatively low radioactive stream will be sent to a bulk vitrification plant in preparation for long-term storage.

Minimum separation goals for the supplemental treatment system were provided (in order of priority) in the Statement of Work for $^{137}Cs$ activity in the stream going to the bulk vitrification facility (<0.05 Ci/L or 2.89E-03 g/L in a 5 molar sodium solution, based on 20% $^{137}Cs$ to total cesium), input sodium recovered in the stream sent to bulk vitrification (>50%), and sulfate-to-sodium molar ratio in the stream going to the WTP (<0.01). The preliminary thermodynamic models applied by COGEMA, Inc. for each of the simulant feeds indicated that these goals can theoretically be met by fractional

crystallization. The models further indicated that it was possible to approach the desired removal levels (<0.0012 Ci/L or 6.93E-05 g/L, 90%, and ≤ 0.0022, respectively). These are to be achieved by crystallization of sodium salts, especially those containing nitrate, carbonate, and sulfate ions, while leaving the highly soluble cesium in solution.

In the case of fractional crystallization, the stream corresponding to the WTP feed is the liquid filtrate recovered during solid-liquid separation and the bulk vitrification feed corresponds to the crystalline product. The minimum and desired separation goals listed above translate to fractional crystallization as follows:

- Obtain a crystalline product that upon dissolution in water to a 5 M sodium concentration has a Cs content low enough to produce a specific activity of less than 0.05 Ci/L, and preferably less than 0.0012 Ci/L.
- Recover at least 50% of the sodium from the feed solution as crystalline product, and preferably at least 90%.
- Produce a filtrate that has a molar ratio of sulfate to sodium less than 0.01, and preferably less than 0.0022.

## 1.2 FRACTIONAL CRYSTALLIZATION

When a solution has a single species that can be crystallized by cooling, evaporation, addition of a non-solvent or some other means of concentrating the solution, such an operation may be thought of as simple crystallization. However, when a solution contains multiple solutes, solutes may be expected to come out of solution (crystallize) when each has reached its solubility limit. For example, suppose a solution contains three solutes (A, B, and C) that all saturate the solution as solvent is evaporated from a

solution, and the solution also contains additional solutes whose concentrations increase as evaporation occurs, but do not reach saturation. Figure 1 illustrates the hypothetical distribution of products if the solution is progressively saturated with A, then B, and finally C in the course of evaporating solvent from the solution. The unique behavior of each solute is readily apparent: in this example species A is a double salt containing species B and the stoichiometry of A limits its production after one of its constituents is depleted. The mass of crystalline B accumulates rapidly immediately after it saturates the solution, but its production decreases slowly thereafter. The mass of crystalline C builds slowly after saturation and then rapidly as the end of the operation is approached. Clearly, the point at which the slurry is sent to a solid-liquid separator will influence the composition of the final product and, concomitantly, the characteristics of the separation.

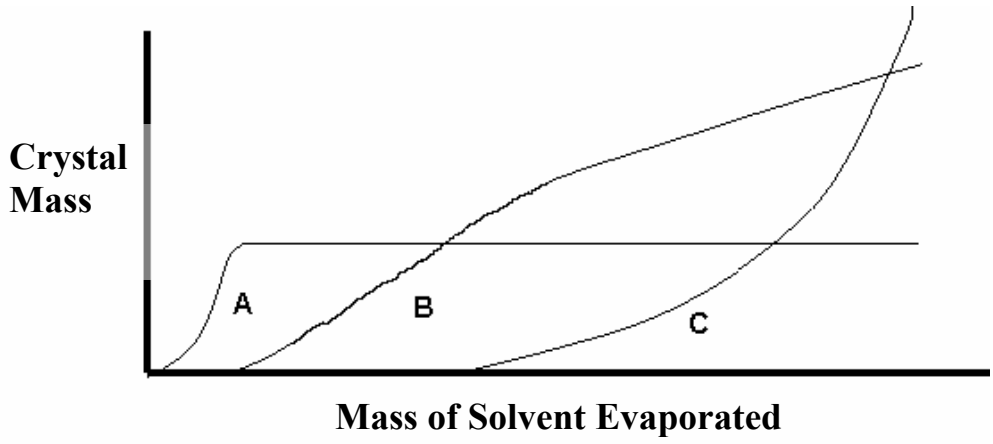


**Figure 1. Hypothetical Product Distribution from Fractional Crystallization: Solution Becomes Saturated with Solutes at Different Times in the Evaporation.**

Now consider a different situation, one in which the solutes achieve saturation at roughly the same time in process. Assuming that all nucleate and grow as such conditions are achieved, the product generation is expected to look more like that in Figure 2. In this situation, separation of species from one another by simple fractional crystallization is not possible; instead, this instance of fractional crystallization only facilitates separation of a physical mixture of the crystalline solutes from the residual mother liquor.

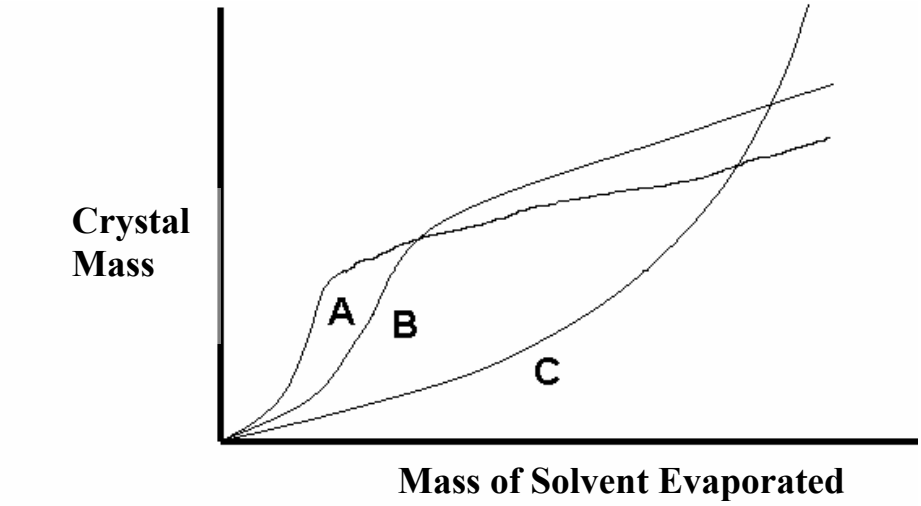


**Figure 2. Hypothetical Product Distribution from Fractional Crystallization: Solution Becomes Saturated with Solutes at Roughly the Same Times in the Evaporation.**

Figure 3 shows the results of simulation LAB3_Test.XLS, provided by COGEMA, Inc. In the simulation, the feed contained sodium carbonate (36.05 g), sodium sulfate (11.69 g), sodium nitrate (195.39 g), sodium hydroxide (56.18 g), aluminum hydroxide (15.92 g), and water (675.02 g) in proportions similar to Single-Shell Tank (SST) Early Feed Solution. The total solute concentration was adjusted so that the

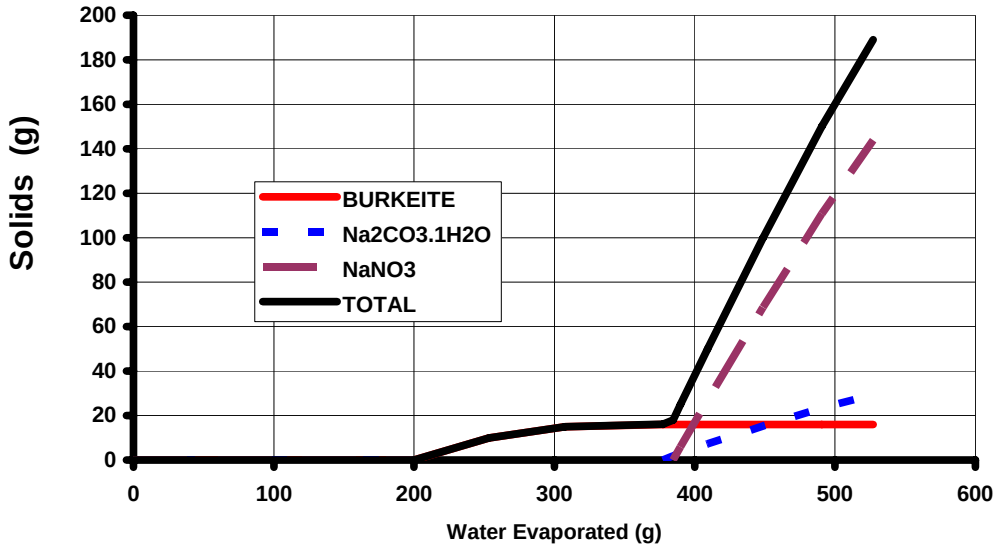


**Figure 3. Mass of Crystals Produced in Simulated Evaporation of Solutions Containing Sodium Carbonate, Sodium Sulfate, and Sodium Nitrate at 60°C (LAB3_Test.XLS).**

solution would reach saturation at 60°C after 200 g of water had been evaporated. Note that in the figure, burkeite saturates the solution after approximately 200 g of water have been evaporated. At that point in the process, the only solid that forms is burkeite and the mass of crystals of this species continues to grow, without other crystalline material being formed, until approximately 380 g of water have been evaporated. At that point, sodium nitrate begins to come out of solution and the mass of these crystals increases rapidly. At about the same time, sodium carbonate monohydrate saturates the solution and crystals of this species begin to form.

The behavior described is expected to be characteristic of all three simulant solutions: SST Early Feed Solution, SST Late Feed Solution, and Double-Shell Tank

(DST) Feed Solution. Since the objective of the operation is to remove a significant fraction (more than 50%) of the sodium salts from the feed solution, irrespective of the counter ion, this behavior presents no apparent problem.

## 1.3 SEPARATION OF CRYSTALS FROM MOTHER LIQUOR

As described in the preceding section, the formation of crystals removes sodium salts and other species from solution. For this to be an effective separation process, the crystals must then be separated from the residual mother liquor by solid-liquid segregation. It is possible to do this by filtration, centrifugation, or other commonly used techniques. However, the nature of the crystals, in particular their morphology and size distribution, determine how easily they can be segregated from the mother liquor. In general, a narrow crystal size distribution leads to easier separation than one that is broad; bulky crystals as opposed to flakes or needles also mean an easier separation.

For single-solute, simple crystallization the size distribution is determined by the nucleation and growth kinetics of the crystalline species. In fractional crystallization of the type characterized by the behavior in Figure 3, the nucleation and growth kinetics of each species leads to a determination of the final crystal size distribution.

As will be described in later sections of this thesis, considerable effort went into developing a means to segregate the complex crystalline solids from the mother liquor on a laboratory scale. Similar effort led to the development of a means to wash the mother liquor from the interstices of filter cakes produced in the experimental program. A secondary part of this work led to development of washing procedures that allowed sieve

analyses to determine product crystal size distributions without significant distortion by crystal agglomeration.

## 1.4 CARBONATION AND PROCESSING CONCERNS WITH DOUBLE-SHELL FEED SOLUTIONS

As water is evaporated from the feed solutions, soluble species become more and more concentrated, though in the key instance of cesium, saturation is not reached. Aluminum ions are one of those species whose concentrations are increased, and it approaches conditions where the solubility limits of sodium aluminate, $NaAlO_2$, may be reached. Unfortunately, aluminum salts do not crystallize at sufficiently rapid rates; instead, they cause the formation of a viscous gel that is very difficult to handle. Clearly, this is a condition that must be avoided for a successful process.

The concentration of aluminum in the DST Feed Solution is approximately twice that in the SST Early Feed Solution and about an order of magnitude higher than in the SST Late Feed Solution. It is a concern, therefore, that evaporation of DST Feed Solutions to the extent required to meet the requirements on sodium recovery will lead to formation of aluminum-based gels.

One of the methods that have been proposed for addressing the dilemma of dealing with this situation is the use of carbonation to modify the system behavior. Carbonation involves dissolution and reaction of $CO_2$ with hydroxyl ions in the feed solution:

$$CO_2 + 2\ OH^- \rightarrow CO_3^{2-} + H_2O \qquad (1\text{-}1)$$

The consumption of hydroxyl ions by carbonation and their concentration by evaporation are illustrated in Figure 4. In fact, Figure 4 shows two stages of carbonation, each of which is followed by evaporation. Note that the concentration of aluminum and hydroxyl ions remains in a space that is below solubility limits of the two aluminum salts, and therefore should avoid formation of aluminum-based gels. During evaporation, crystals of sodium salts are generated and the concentration of aluminum increases, as illustrated by the solid lines in Figure 4. The use of more than one stage is designed to increase the sodium recovery. The kinetics of carbonation and gel formation are complex phenomena that need rationalization so that operating variables such as the total amount and the rate of $CO_2$ addition can be related to the onset of gel formation.

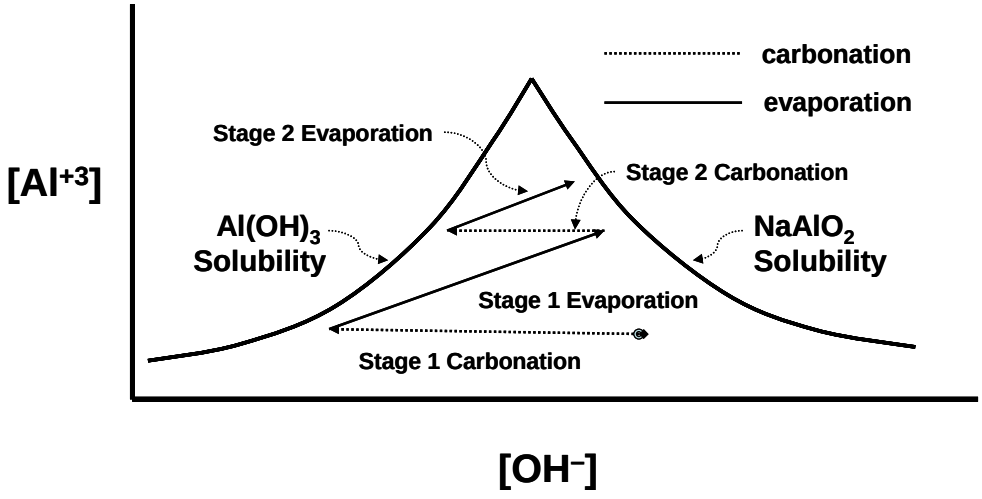


**Figure 4. Illustration of the Use of Two Stages of Carbonation and Evaporation to Maintain Solution Concentrations in a Space that Minimizes Aluminum Gel Formation While Maximizing the Production of Sodium Salts.**

## 1.5 CERTIFICATION RUNS AND CHEMICAL ANALYSES

The culmination of studies leading to process protocols for each of the feed solutions (SST Early Feed, SST Late Feed, and DST Feed) was performance of runs that were designed to test those protocols against the process criteria cited earlier. The masses of each stream were determined carefully, and appropriate samples were sent to Galbraith Laboratories (Galbraith) for analysis. These results, which were obtained using Quality Assurance (QA) certified techniques, form the basis of demonstrating the applicability of the fractional crystallization pretreatment technology.

## 1.6 COMPARING ANALYTICAL RESULTS TO PROCESS CRITERIA

As stated above, the objectives of the technology described in the present thesis involve the cesium content of the recovered crystals, the recovery of sodium in the solid product, and the separation of sulfate ions from the liquid destined for feed to the Waste Treatment and Immobilization Plant.

The analytical results obtained from Galbraith provide compositions of samples in wt % for major components and parts per million (ppm), which is mass of a species per million mass units of the sample. There are at least two ways to use such information to compare the outcome of a fractional crystallization run with Objective 1.

One method uses the compositions of the streams and estimates of the fraction of the total cesium in the streams of interest that is present as $^{137}Cs$. To illustrate the methodology, assume that a sample of the final product crystals has been analyzed and found to contain 25 wt% sodium (Na) and 0.2 ppm cesium (Cs). The basis of calculation for determining if the product meets Objective 1 is to estimate the activity of a solution of

this material containing 5 M Na, which is 5 M Na/L. As specified in the SOW, it may be assumed that there is 1 g $^{137}$Cs/5 g Cs in typical streams at Hanford. It may also be assumed that the activity of $^{137}$Cs is 86.58 Ci per g of $^{137}$Cs. This means, then, that the specific activity associated with the product is

$$5\frac{\text{mol Na}}{\text{L}}\times\frac{23\text{ g Na}}{\text{mol Na}}\times\frac{100\text{ g}}{25\text{ g Na}}\times\frac{0.2\text{ g Cs}}{1{,}000{,}000\text{ g}}\times\frac{86.58\text{ Ci}}{\text{g }^{137}\text{Cs}}\times\frac{1\text{ g }^{137}\text{Cs}}{5\text{ g Cs}}=0.0016\frac{\text{Ci}}{\text{L}} \quad (1\text{-}2)$$

This value can be compared to the criterion in Objective 1.

A second method for estimating the approach to Objective 1 is in terms of a decontamination factor (DF), defined as the activity of $^{137}$Cs in real waste or the total cesium concentration in a simulant feed at 5 M sodium concentration divided by the corresponding activity or concentration in the salt recovered from the fractional crystallization process, also at a 5 M sodium concentration. The decontamination factors corresponding to Objective 1 are as given in Table 1.

**Table 1. Required Decontamination Factors to Meet Objective on $^{137}$Cs Activity.**

| Feed Solution to Fractional Crystallization | $^{137}$Cs activity (Ci/L) | | Decontamination Factor (*DF*) | |
|---|---|---|---|---|
| | Minimum | Desired | Minimum | Desired |
| **SST Early Feed** | **0.05** | **0.0012** | **1.15** | **48** |
| **SST Late Feed** | **0.05** | **0.0012** | **—[1]** | **14** |
| **DST** | **0.05** | **0.0012** | **7.0** | **292** |

The decontamination factors can be estimated from the following relationship:

[1] Activity of feed is below minimum required; therefore minimum DF does not apply.

$$DF = \frac{\left[\text{activity of } {}^{137}\text{Cs (at 5 M Na)}\right]_{\text{feed}}}{\left[\text{activity of } {}^{137}\text{Cs (at 5 M Na)}\right]_{\text{waste}}} = \frac{\left[\dfrac{\text{ppm Cs}}{\text{wt \% Na}}\right]_{\text{feed}}}{\left[\dfrac{\text{ppm Cs}}{\text{wt \% Na}}\right]_{\text{waste}}} \tag{1-3}$$

where the compositions in the term on the farthest right are given by the analyses of crystals produced in the operation. For example, suppose the feed to a process contains 10 wt% sodium and 0.20 ppm Cs, and crystals produced contain 28 wt% sodium and 0.04 ppm Cs. Such results correspond to a DF of 14, which has been calculated as follows:

$$DF = \frac{\left[\dfrac{0.20 \text{ ppm Cs}}{10 \text{ wt\% Na}}\right]_{\text{feed}}}{\left[\dfrac{0.04 \text{ ppm Cs}}{28 \text{ wt\% Na}}\right]_{\text{waste}}} = 14 \tag{1-4}$$

## 1.7 RESEARCH OBJECTIVES LINKED TO HANFORD WASTE PROCESSING

Along with the primary objective of determining whether or not fractional crystallization is a feasible technology to be used in the treatment of Hanford wastes, two underlying phenomena were examined during the present research. One had to do with the solubility of gibbsite ($Al[OH]_3$) and sodium aluminate ($NaAlO_2$), which were illustrated qualitatively in Figure 4. The second concerned the roles of evaporation rate and crystal washing in determining the product purity.

As discussed in Section 1.4, gel formation is a major concern related to DST waste processing. Gel may form during carbonation if the solubility of gibbsite is exceeded or during evaporation if the solubility of sodium aluminate is exceeded. In the present work it was necessary to develop methods to predict the solubility limits of these

two species. These methods were then used along with thermodynamic models to avoid gel formation during carbonation and evaporation of DST solutions. Additionally, it was necessary to determine whether or not any gel formed during carbonation could be dissolved upon addition of NaOH.

Along with the gelation phenomenon, product purity was a large focus of this work. In the case of Hanford wastes, purity relates to the amount of cesium in the product. Process variables such as evaporation rate have an effect on the impurities included within the crystal structures and washing efficiency determines the amount of impurities remaining in the interstitial spaces of the filter cake. Practices and procedures must be developed in order to reduce inclusions within the product crystals and efficiently wash the filter cake, which is composed of multiple crystalline species.

# CHAPTER 2: APPARATUS AND PROCEDURES

The experimental apparatus and procedures used in performing the crystallization and carbonation runs evolved as experience was gained in working with the different solutions comprising SST Early Feed, SST Late Feed, and DST Feed. The evolution resulted from knowledge learned about feed-specific characteristics and interrelationships between solute crystallization and crystallizer configuration. The original system configuration is shown schematically in Figure 5. Although the same basic configuration was used in all runs, several modifications were made to address problems associated with accumulation of crystal encrustations on the walls and baffles of the crystallizer. The key modification was to add the capability of periodic addition of feed solution so that the active volume in the crystallizer could be maintained throughout the run. Figure 6 is a photograph of the modified apparatus with a feed vessel positioned above the crystallizer. Note also that the reflux condenser has been removed from the system as it was considered unnecessary when the system was operated in the constant-volume mode.

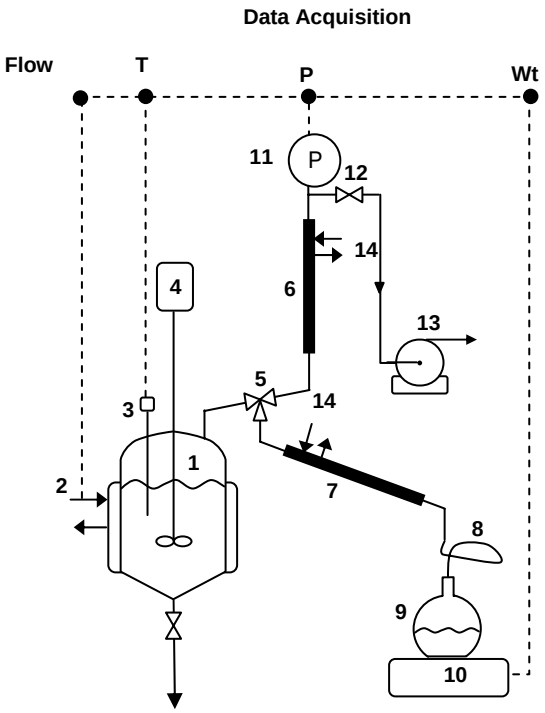


(1) Crystallizer, (2) Heating Fluid/Water, (3) Thermocouple, (4) Motor to Drive Stirrer, (5) 3-Way Valve, , (6) Reflux condenser, (7) Product Condenser, (8) Flexible Tube Adapter, (9) Condensate Collection Flask, (10) Digital Balance, (11) Pressure Sensor, (12) On-Off Valve Plus Metering Valve, (13) Vacuum Pump, (14) Cooling Water.

**Figure 5. Schematic of System Used in Initial Crystallization Runs.**

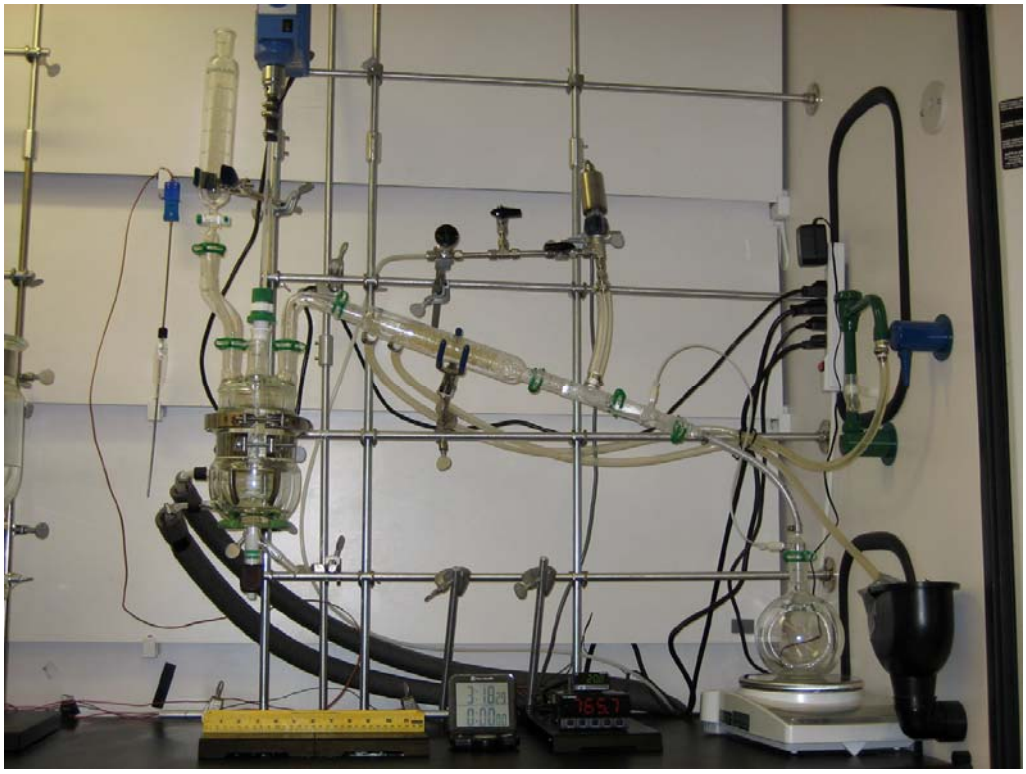

**Figure 6. Evaporative Crystallization System with 300-mL Crystallizer Installed.**

## 2.1 EQUIPMENT

The following items of equipment are described: crystallizers, filtration and crystal-washing apparatus, data-logging software and hardware, carbonation apparatus, and analytical equipment (sieves and ro-tap, polarized light microscope, balances).

### 2.1.1 Crystallizers

The vessels used as crystallizers were of 1-L, 600-mL, 300-mL, and 100-mL nominal sizes, and the 1-L vessel is shown below in Figure 7. The reason different sizes were used was to facilitate multiple-stage batch and semi-batch operations in which the volume of feed available for successive stages was reduced because of the vapor generated in preceding stages. For example, this would mean that if the batch feed was

1 L and 400 mL of condensate were generated in the first stage of operation, the available feed for the second stage would be approximately 600 mL, and so forth for subsequent stages. Use of the smaller sized vessels also allowed significant savings on the amount of feed necessary to perform each run. For example, using the 300-mL and 100-mL crystallizers for a two stage run would only use about one-third the amount of chemicals necessary to operate the same run in the 1-L and 300-mL crystallizers.

The internals of the crystallizers included four equally spaced baffles that were contoured so that they rested on the curved portion of the vessel. The baffle cages for the 1-L, 600-mL, and 300-mL crystallizers are shown in Figure 8. They were manufactured in-house and designed so that they did not interfere with the impeller and accommodated other crystallizer internals. The four metal baffles fit snugly against the crystallizer wall. Baffles were not used in the 100-mL crystallizer due to the reduced dimensions of this vessel.

**Figure 7. 1-L Vessel Used as a Crystallizer**

From Left to Right in Each Photograph: 1-L, 600-mL, and 300-mL Baffle Cages.

**Figure 8. Baffles Used in the Three Crystallizers.**

The heads for each crystallizer had four openings: one was used for the agitator, one for vapor withdrawal, one for insertion of a thermocouple, and one for addition of feed or seed crystals. The feed vessel shown sitting atop the crystallizer in Figure 6 was used to add feed solution during the course of a run. The vessel has a valve that allows regulation of the flow of feed solution into a short length of glass tubing leaving the vessel. A length of tygon tubing was connected to the glass tubing, and the end of the tygon tubing was adjusted so that the feed fell onto the active surface near the agitator in the crystallizer; in other words, the apparatus is designed so that the feed can be rapidly and thoroughly distributed upon entering the crystallizer.

The temperature of the crystallizer contents was measured by the thermocouple and readings were recorded on a computer. Heat was added to the system by a heating fluid that was pumped through the jacket of the crystallizer. The rate of evaporation was manipulated by adjusting the temperature of the heating fluid.

As vapor was generated in the crystallizer, it passed into a heat exchanger where it was condensed. The heat exchanger had cooling water flowing through a jacket. The

condensate flowed from the heat exchanger through a flexible tube to a collection vessel resting on a balance. The condensate collection receiver was equipped with a pressure equalization Teflon tube to prevent accumulation of the condensate on top of the receiver. Readings from the balance were transmitted to and stored on a computer. A vacuum pump reduced the pressure in the system to the desired value.

The agitators used in the crystallizers varied according to the size of the vessel. For the 1-L and 600-mL vessels, two impellers were used. These are shown in Figure 9. For the 300-mL and 100-mL vessels, only one impeller was used, with the one of the left of Figure 9 used in the 100-mL vessel and the one on the right used in the 300-mL vessel. The mixing intensity was controlled by an adjustable speed motor connected by a rubber tube to the glass shaft turning the impellers. It was important to have good mixing to keep the crystals, especially the larger ones, from settling at the bottom of the vessel; on the other hand, excessive intensity subjected crystals in the system to possible attrition (breakage) and splashed liquid on the upper walls of the crystallizer, which contributed to scaling problems.

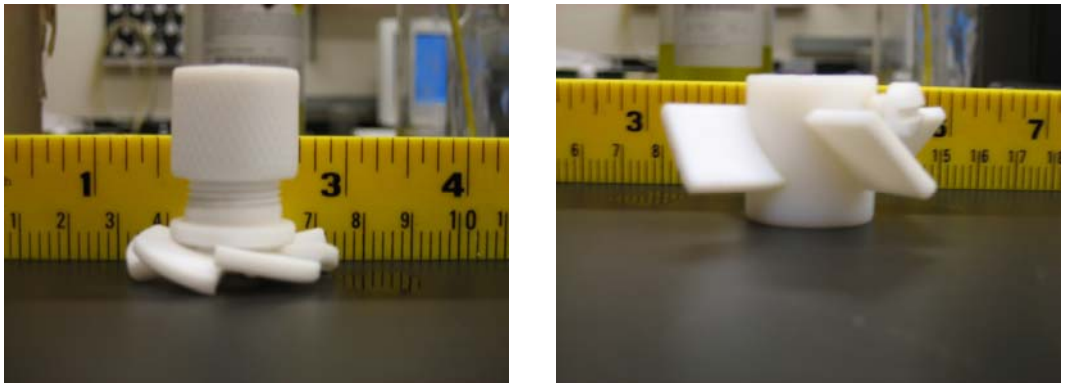

Both impellers were used in the 1-L and 600-mL crystallizers, with the one on the right positioned approximately a few mm from the surface of the slurry, while the one on the left was close to the bottom of the vessel. The impeller on the left was used alone in the 100-mL crystallizer and the one on the right was used alone in the 300-mL crystallizer.

**Figure 9. Impellers Used in the Stirred-Tank Crystallizers.**

### 2.1.2 Filtration and Crystal-Washing

The apparatus used to filter crystals from the slurry and to wash mother liquor from the filter cake is shown in Figure 10. It was designed by the research team at Georgia Tech; the design criteria included (1) a slurry volume of 800 mL, (2) the dimensions of the crystallizer and medium-frit filter previously purchased, and (3) the manufacturing limitations of the provider (Chemglass). The final drawings of the apparatus were sent to Chemglass for a quote and design confirmation, and the details of the apparatus manufactured by Chemglass are provided in Appendix A.

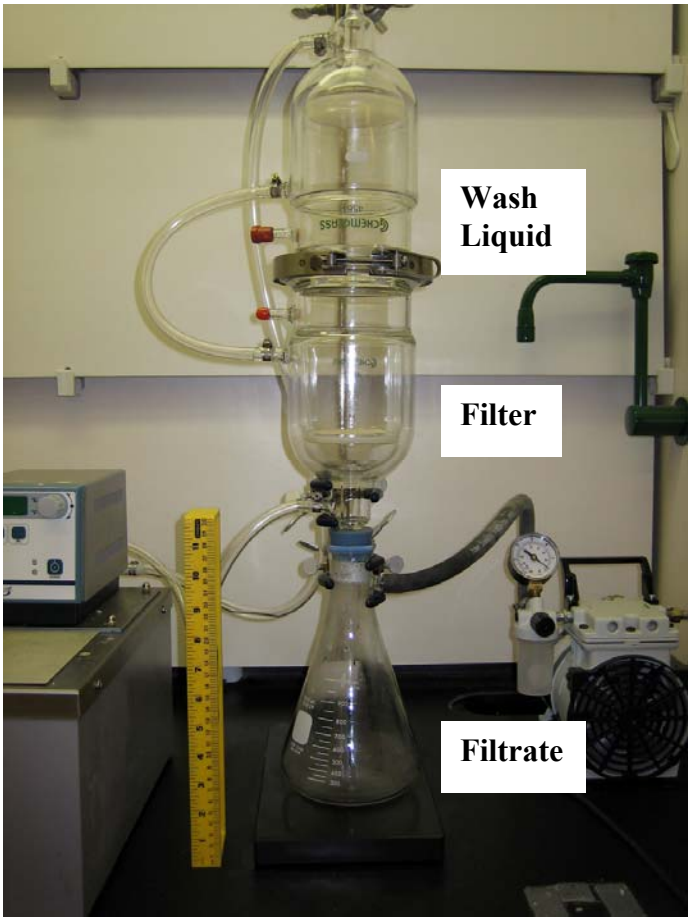


**Figure 10. Apparatus Used for Filtration and Washing.**

The filter has a glass frit onto which the process slurry was poured. It also was possible to transfer the slurry directly from the crystallization vessel to the filter by drawing it through flexible tubing and into an opening just below the clamping ring. A vacuum was drawn on the filtrate receptacle, and the frit captured the crystals and separated them from the filtrate, which flowed through the frit and into the receptacle. At the conclusion of the filtration step, wash liquid (usually an aqueous solution saturated with the major solutes) was added to the upper vessel and then was drawn from the feed vessel through a perforated plate that dispersed the liquid over the filter cake. The filter and wash-liquid receptacles are jacketed and a fluid at a temperature corresponding to

that of the crystallizer flowed through the jacket. The objective was to maintain the temperature of the process slurry at a near-constant value. The vacuum pump in the picture pulled a vacuum in the filtrate receptacle.

This apparatus allowed filtration and washing to be performed under isothermal conditions since both top and bottom parts are jacketed. It also provided good distribution of the washing liquid by forcing it to flow through a plate perforated with holes each having a diameter of 1 mm. The distribution of the wash liquid provided superior washing efficiency. The system can be operated at atmospheric conditions or under vacuum.

### 2.1.3 Data-Logging Software and Hardware

The data-acquisition system monitored temperature and pressure inside the crystallizer, along with the mass of condensate collected on the balance. Temperature was measured with a hastelloy thermocouple (T-type C-276 purchased from Chemglass) while pressure was monitored with an Omega transducer. These sensing devices were connected to meters for direct display of readings; analog temperature controller/display (CNi3253, Omega) and process meter controller (DP25B-E, Omega) for pressure reading. These meters were connected to a data acquisition (DAQ) board (PMD-1208FS, Measurement Computing) for continuous recording of data. This board accepted voltage signals for data storage and connected to the computer through a USB port. The pressure transducer and temperature meter gave current outputs (4-20 mA), so 250 Ω resistors (249XBK-ND, Digi-Key) were used to convert the current signals to voltage signals compatible with the DAQ board. The digital balance used to measure the condensate

mass (PB1502-S Mettler Toledo obtained from VWR) was connected to the computer through a RS-232 port. Due to the fact that multiple RS-232 ports were needed, a computer board was installed that provided four RS-232 connections (PCI-COM232/4-9, Measurement Computing). Readings from the DAQ board and the RS-232 ports were collected in a LabView program and the voltage signals from the DAQ board were calibrated to their corresponding temperature and pressure values. A simplified layout of the DAQ connections is shown in Figure 11.

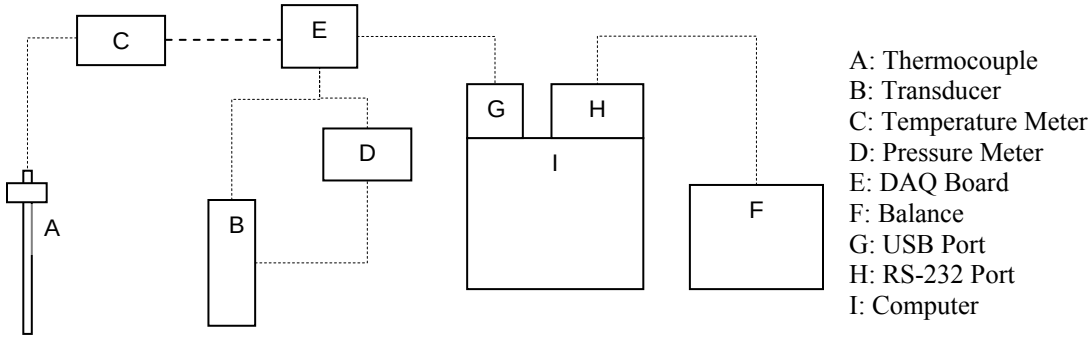


**Figure 11. Data Acquisition System Setup.**

### 2.1.4 Carbonation

Carbonation was performed with the apparatus shown in Figure 12. It consisted of a 1000-mL vessel equipped with a five-neck top. The five neck openings were used for a mechanical stirrer, a pH/temperature probe, a gas input tube, a gas output tube, and feed loading. The tubes used for gas flow were 0.25 in. O.D. and made of rigid PTFE. They were secured to the vessel with glass adapters (thermocouple adapter, 24/40 inner joint, size ¼-in.) purchased from Chemglass. The input tubing was pierced to create two small holes for bubbling gas into the vessel and the bottom opening was plugged with Teflon tape. The vessel was equipped with a baffle cage and two Teflon impellers, separated by

approximately 3 inches. The baffle cage and impellers were used to improve the distribution of gas bubbles inside the vessel. Carbon dioxide was fed from a cylinder purchased from AirGas (research grade 99.998%, product number CD R200). The input flow was adjusted by means of a stainless-steel metering valve (1/4-in. tube fitting, Swagelock) and a flowmeter (300 mL/min air capacity, GF-6541-1210, Accural Gilmont provided by Fisher Scientific). A three-way valve (1/4-in. tube fitting, Swagelok) was downstream from the flowmeter and allowed switching the regulated gas between the vessel for carbonation and a bubble flowmeter for flow measurement and calibration. The input and output flows from the vessel were measured with bubble flowmeters (1-10-100 mL/min capacity, Bubble-O-Meter). A valve allowed control of the gas flow from the $CO_2$ cylinder to the carbonation vessel. A schematic illustration of the apparatus configuration is presented in the review of procedures used for carbonation (Section 2.2.8). Carbonation of DST solutions is also detailed further in Section 3.0.

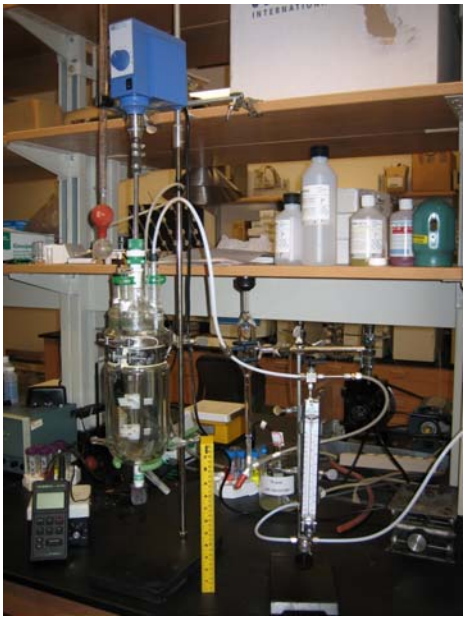

**Figure 12. Vessel Used for Carbonation.**

### 2.1.5 Analytical Equipment

#### 2.1.5.1 Sieves and Ro-Tap

Crystal size distribution (CSD) analysis was conducted by sieving on a Ro-Tap test sieve shaker (RX-29, serial 24210, Tyler) utilizing US standard sieve nests obtained from Dual Manufacturing Co. The sieving apparatus is shown in Figure 13. The shaker features a combination circular motion along with a vertical vibration induced by an upper hammer tapping that allows good size segregation of crystals as they attempt to pass through the sieving apertures. The shaker can accommodate test sieves of 3-in., 6-in., or 8-in. diameter and can be adjusted to fit various numbers of sieves depending on their depth. In the present work, 3-in. diameter x 1-in. depth test sieves were used and the shaker was adjusted to accommodate a stack of 11 sieves, including the pan. Shaking time can be adjusted by turning a thumb screw until the desired value appears in a digital window. The shaker is placed on a stand inside a Ro-Tap sound enclosure cabinet to reduce the noise level.

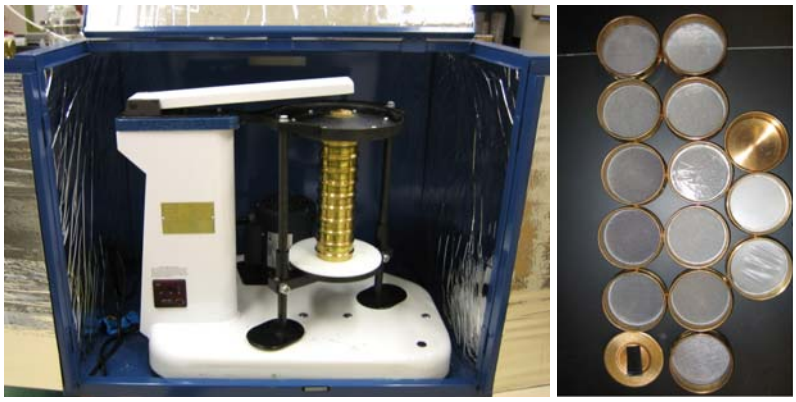

**Figure 13. Ro-Tap Test Sieve Shaker Placed Inside a Sound Enclosure Cabinet (Left) and Test Sieving Nests Top View (Right).**

The test sieves are US standard sieves with brass frames and stainless-steel mesh. Table 2 shows the sieves available for the current analyses; they ranged in nominal aperture from 10 to 1180 μm. They were selected so that the ratio of aperture sizes on consecutive sieves is almost √2. Sieve tests were typically performed using the 38 to 850 μm nests, unless the operation involved particularly large or small crystals. In these cases the 10-, 20-, or 1080-μm sieves were used to provide a more accurate distribution. The sieves can hold about 27 g of sample mass, but only 15 to 20 g were used.

**Table 2. Sieves Used for CSD Analysis.**

| No. | ASTM Sieve No. | Nominal Sieve Opening (μm) |
|---|---|---|
| **1** | **16** | **1180** |
| **2** | **20** | **850** |
| **3** | **30** | **600** |
| **4** | **40** | **425** |
| **5** | **50** | **300** |
| **6** | **70** | **212** |
| **7** | **100** | **150** |
| **8** | **140** | **106** |
| **9** | **200** | **75** |
| **10** | **270** | **53** |
| **11** | **400** | **38** |
| **12** | **635** | **20** |
| **13** | **850** | **10** |

All Sieves From Dual Manufacturing Co.

Crystal agglomeration was the major problem affecting CSD analyses throughout the test runs. Microscopic observation of samples taken directly from the crystallizer proved that agglomeration plaguing CSD analysis was not a result of events within the crystallizer, but rather an artifact associated with filtration and drying of product crystals.

It was caused by residual traces of mother liquor on crystal surfaces after filtration and/or washing that led to crystallization of solute from the mother liquor as the solvent was evaporated; as this material crystallized it bound adjacent crystals into agglomerates. To reduce this phenomenon, two extra steps were introduced to the procedures followed prior to sieving. First, the final washed crystals were flushed with a hydrophilic solvent (acetone) to wash any residual mother liquor from the crystals and reduce the extent of agglomeration. Then after drying, the crystals were subjected to a manual, gentle separation process to disrupt any remaining agglomerates. The overall sieving procedure summarized below was applied to all certification runs.

All of the product crystals that had been washed with saturated solution were placed in the washing/filtration apparatus and washed with an approximately equivalent mass of acetone. The acetone was introduced from the top part of the washing apparatus and was evenly distributed over the crystal sample upon being drawn into the filtering flask. The crystals were then collected, spread wide on a pan and left overnight to allow evaporation of residual solvent.

Washing with acetone did not totally eliminate agglomeration, but significantly reduced it; some crystal agglomerates still appeared in the dried crystals. These agglomerates would contribute significantly to the sieve fraction larger than 500 μm and negligibly to the fraction less than 200 μm. It was found that these agglomerates could be disrupted with gentle manipulation using a spatula. Microscopic observation confirmed that such manipulation did not break the constituent crystals, but it did improve the true representation of single crystals that is required for representative CSD data.

The selection of sieve sizes to use in an analysis depended on the size of crystals generated in a run. Guidance was obtained from the simulation files (e.g., sodium nitrate is often over 100 μm while burkeite is about 20 μm) and from visual observations of crystals grown during the experiment. All sieve analyses were performed with the 38 to 850 μm test sieves. If fine crystals (< 38 μm) were significant in the crystal sample (by having large mass collected in the bottom pan), they were further separated by using 10- and 20-μm sieves in place of the two largest aperture sieves.

Each sieve analysis was performed with 10 sieves in a nest, in addition to the bottom pan and the cover. The sieves were rinsed with hot water and dried in an oven prior to use. The empty weight of individual sieves was recorded and they were stacked in a nest, from top to bottom in order of decreasing openings. A 15 to 20 g sample of the crystals to be analyzed was then added to the top-most sieve and covered. The sieve stack was assembled and loaded in the Ro-Tap. The timer was adjusted to 30 min and the machine was started.

When the operation was completed, the stack was removed and each sieve was weighed; the tare weights of the sieves were subtracted from the final weights to determine the mass of crystals recovered on each sieve. By definition, the crystals collected in each nest ranged in size from the aperture of the sieve opening to that of the sieve above the one being analyzed; for example, crystals collected in the 38-μm sieve were between 38 and 53 μm (the upper nest according to Table 2) in size. These data were then used to evaluate the crystal size distribution, which could be expressed as histograms, density functions, or cumulative distributions. Samples were collected from several of the sieves and held in vials for further analysis by polarized light microscopy.

Such analyses facilitated determination of the crystal composition in each size range and detection of crystal breakage or agglomeration.

#### **2.1.5.2** Polarized-Light Microscope (PLM)

PLM images were obtained on a Meiji Techno trinocular polarizing microscope (Model ML9300), which is illustrated in Figure 14. Images are either observed in the eyepiece and/or acquired on a computer. The source of light in the microscope is provided by a Koehler-type illuminator with intensity controlled by a knob (6). The substage polarizer (5) is fully rotatable, sending polarized light within angles between 0–360 degrees up to the specimen. When the polarizer is swung-out, the light is un-polarized. The analyzer (16) is a slide-in plate mounted in an in-tube slider positioned after the specimen which moves the analyzer in and out of the optical path. When the analyzer is "in" and the polarizer (5) is swung in and set at 0 degrees, the elements are crossed and the field of view is said to be extinguished. In this condition the field of view is dark, except for an optically active specimen in the field path, which rotates the polarization angle and becomes visible against the dark background.

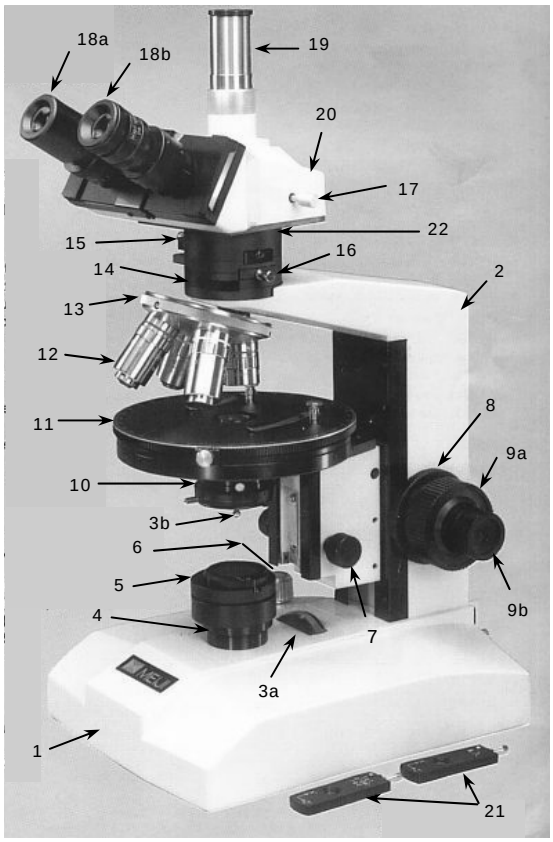


1 Microscope base
2 Microscope limb
3 Iris control (a) field (b) aperture
4 Koehler type illuminator
5 Polarizer, rotatable swing-out
6 Light intensity control knob
7 Substage focus control
8 Tension control knob
9 Focus (a) coarse (b) fine
10 Substage condenser (N.A. 1.25)
11 Rotating stage
12 Objective lenses (4, 10, 40, 60X)
13 Objective revolving nosepiece
14 Compensator slot
15 Bertrand lens aperture
16 Analyzer slider
17 Beam splitter lever
18 10X eyepiece (a) wide field (b) focusing cross-line
19 Photo tube
20 Rotatable 360°/60° inclination
21 Compensator plates (red and ¼ wave-length)
22 Switch-over beam splitter

Parts not shown in Figure
Camera attached to photo tube
Computer for image processing
Wrenches for objective centering

**Figure 14. Polarized Light Microscope Used in this Project.**

Other elements of the microscope serve to improve the image quality. The iris diaphragm (3) and the condenser (10), a lens between the illuminator and specimen, are used to control the angle of the illumination cone that passes through optical train and improve the contrast. The circular stage (11) rotates through a full 360 degrees, with angular measurement ability, to facilitate orientation studies in polarized light. The objectives (12) are mounted in a rotatable ball bearing nosepiece (13) allowing easy swing of the required objective in the optical path. Objectives with 4X, 10X, 40X and 60X magnifying powers were utilized in this study. A 100X objective is also available but was not used. If the 100X objective is to be used, immersion oil must be applied to the specimen slide so when the objective is swung in, as the slide and the 100X objective

are in good and bubble-free contact. The beam splitter (22) is used to switch the image between the binocular eyepiece (18) and the digital camera photo tube (19).

The focusing knob (9) allows course and fine adjustment of the distance between the specimen and objective for sharper images. The compensator (or retardation) plate (21) is a crystal that is selectively placed between the sample and analyzer to introduce a known optical path length difference to the re-combined light ray components and shift the colors of the generated images. The plates are sliding in a slot (14) cut in the tube just above the objective nosepiece (13). The microscope visual images can be observed through the eyepieces (18) or more conveniently snapped on a computer using a camera attached to the phototube (19). A photo camera (Sony DKC-5000, serial 10322) was used to generate digital images on a computer employing Image-Pro Plus (version 4.5.1.22, serial 41N40000-13717, Media Cybernetics Inc.) for image processing and manipulation.

A preparatory step to PLM operation is the preparation of good specimen slides with uncrowded fields (few crystals with empty spaces). Crystals are best viewed mounted in their mother liquor or in some solvent which will not dissolve the crystals, e.g., paraffin oil. Mounting them in air causes a large change in refractive index at the air-crystal interface and reduces the image resolution. Samples from crystallization experiments are normally taken from the slurry (or flash) solution at the end of the run using a plastic pipette. A small drop of the slurry is placed at the center of a 3”×1” plain slide (Part 2947, Corning) and preheated to the slurry temperature (40-60ºC). Then the drop is covered with a 22 mm circular glass cover (Part 12-546-1, Fisher Scientific) to spread the sample drop over the cover area. To test dry crystals, a small drop of paraffin oil (HR3-411, Hampton Research) is placed on the slide and a small number of the dry

crystals are spread over the oil before they are covered with the circular glass. The circular cover should rest evenly on the slide without any air spaces or crystal stacking. Such flaws can be fixed by gentle tapping on the cover with a spatula or by mild movement of the glasses.

The microscope may require some initial adjustments before its use; the major ones are illumination setup and objective centering. They would lead to good focusing, overlapping, and centering of the specimen image in the field of view, either in the eyepiece or computer preview screen. Illumination setup normally should be performed on each objective upon the use of microscope. A detailed procedure for optical setup and illumination adjustment is provided in the Appendix B. Objective centering is required less frequently if the microscope is properly treated. However, it should be tested from time to time to ensure good centering of the image. Centering can be simply tested by observing a crystal sample in the eyepiece with cross-line (18b). If the focused image of the crystal strays from the center of the cross-line upon stage (11) rotation, then the objective is slightly off the optical axis. The objective (12) can be centered using two hexagon keys supplied with the microscope accessories according to the procedure summarized in Appendix B. The centering test must be performed for all the objectives attached to the nosepiece (13).

It should be noted that initial adjustments of the microscope while observing the crystal specimen through the binocular eyepiece (18) will also adjust the image in the computer display if the digital camera is well aligned with the optical path. The computer display is more convenient although the field of view is somewhat more limited than the binocular eyepiece especially at high magnifications. Size scales can be added to the

recorded images for crystal size analysis. However, this requires a size calibration for each magnification objective using a 2.5 mm stage micrometer slide graduated with precise grids of 25, 100, 500, and 1000 μm. This can be done by snapping an image of the scaled grids of the micrometer slide with each objective and use a grid of known length in the image to calibrate the length estimated by the Image-Pro Plus software. Details of the calibration procedure are provided in Appendix B.

For PLM characterization of the crystallization runs, a sample is taken from the slurry solution and mounted on a preheated slide as described before. The slide is preheated to the temperature of slurry to minimize formation of additional crystals on the slide by cooling; therefore, the slides should be tested immediately after preparation.

To characterize:

- Turn on the illuminator and pass some light by switching the intensity control knob (6);
- Turn on the digital camera button and start the Image-Plus Pro imaging software menu on the computer desktop;
- From the main menu select the Video/Digital icon on the tool bar or from *Acquire* → *Video/Digital* commands to activate the Preview Page for video capturing and image setup.;
- Start the live preview by pressing "Start Preview." The preview will look white if the analyzer (16) is out. Make sure the substage polarizer (5) is swung in and set at 0 degrees then slide the analyzer plate (16) in. The live preview

gets black because the polarizer and analyzer are crossed which prevents any light from passing through;

- Place the crystal slide on the rotatable stage (11) with the sample centered in the field of light and rotate the smallest objective, 4X, into position for focus. Crystal bodies should appear on the live preview;
- Modify the light intensity using the control knob (6) then focus down on the crystal slides with coarse and fine focus (9) until details can be seen. Most of the crystals in this study had a grey color with poor contrast so the red compensator (21) was used most of the time. The compensator turns the background into pink and improves the crystal coloring;
- Scan the whole crystal slide and study various crystals available in the sample. Crystal types can be identified from the shape and color of the crystals. Also rotate the stage about the axis of crystals and observe the change in colors and the extinction positions. These observations can be used to distinguish crystals which have similar shapes, e.g., sodium nitrate vs. sodium nitrite, sodium oxalate vs. sodium phosphate, etc.;
- Switch to higher power objectives by revolving the nosepiece (11) to enlarge crystal view and get more details. Switching between objectives requires re-adjustment of the lighting intensity and focusing;
- Desired PLM images can be recorded by pressing “Snap” from the Preview Page window. The recorded image will appear separately behind the live preview screen; and,

- Add a scale to the recorded image by pressing the Spatial Calibration icon (the vernier icon on the top right) on the tool bar or by selecting *Measure* → *Calibration* → *Spatial* sequence from the command Menu. A new small calibration window will open. From that window select the objective power from the drop menu list (4X, 10X, 40X, or 60X) then press "Mark" to write the desired scale, e.g. 100μ for the 10X images. The scale bar will appear on the image. Move it to the desired location on the image then right click to fix it there. The image is finally renamed and saved in the desired location. These steps are repeated for every recorded image from the slide.

Crystal identification is carried out by comparing the crystal images obtained from our crystallization runs with typical PLM image of crystals found in Hanford waste tanks. The typical images were provided on a CD.[2]

**2.1.5.3** Balances

Three different digital balances were used. Condensate mass was determined on a Mettler Toledo digital balance (PB1502-S, obtained from VWR) attached through DAQ board to a computer for continuous recording of the mass. Another Mettler Toledo digital balance (PG2002-S) was utilized for assorted measurements of beakers, chemicals, sieves, and experimental accessories. When extremely small masses were involved, a sensitive balance (Ohaus Analytical Plus, AP2500, serial M99315) was used; e.g., this balance was used for weighing small quantities of cesium nitrate in the preparation of simulant solutions.

[2] D. Herting, G. Cook, R,. Warrant, Document Number HNF-11585 "Identification of Solid Phases in Saltcake from Hanford Site Waste Tanks," Richland, Washington, 2002.

### 2.1.6 Chemicals

Chemicals used in this project were sodium hydroxide pellets (NaOH, ACS grade), potassium nitrate ($KNO_3$, ACS grade), sodium nitrate ground ($NaNO_3$, ACS grade), sodium sulfate anhydrous ($Na_2SO_4$, ACS grade), sodium chloride (NaCl, ACS grade), sodium carbonate anhydrous ($Na_2CO_3$, ACS grade), sodium oxalate ($Na_2C_2O_4$, ACS grade), and sodium dichromate dihydrate ($Na_2Cr_2O_7 \cdot 2H_2O$, ACS grade) all from EMD Chemicals Inc., and sodium aluminate anhydrous ($NaAlO_2$, technical grade), sodium nitrite ($NaNO_2$, 97 + % ACS reagent), sodium phosphate dodecahydrate ($Na_3PO_4 \cdot 12H_2O$, 98 + % ACS reagent), sodium fluoride (NaF, 99 + % ACS reagent), sodium acetate trihydrate ($NaC_2H_3O_2 \cdot 3H_2O$, ACS reagent) and cesium nitrate ($CsNO_3$, 99.99%) from Sigma-Aldrich. A polydimethylsiloxane heating fluid for the heater/circulator (Dow Corning 200, 5) was purchased from Ashland, Georgia.

## 2.2 CRYSTALLIZATION EXPERIMENTAL PROCEDURES

### 2.2.1 General Operations

There were two types of crystallization runs performed in the study: batch and semi-batch. Most of the early runs in Phase I were batch and, thus, involved adding a feed charge to the crystallizer prior to the start of the run and removal of product slurry after the requisite amount of vapor had been generated. Variables in such runs include the rate at which vapor is generated, operating temperature (pressure), and whether or not seed crystals are added.

Prior to the start of either a batch or a semi-batch run, water was boiled in the crystallizer to saturate dead spaces in the system with water. A known mass of deionized

water was charged to the crystallizer and boiled for at least 20 minutes. This procedure saturated dead spaces in the glassware with around 15 g of water (determined from a mass balance around the system). A batch or semi-batch crystallization could then be done with the apparatus, and closure of mass balances around the system was enhanced.

Several difficulties were encountered with batch operation that led to use of the alternative semi-batch procedure for the certification runs. The primary and overriding difficulty was the quantity of vapor that must be produced to obtain the desired yield of solute. This led to production of a slurry of much reduced volume in a crystallizer of fixed dimensions. For example, the agitator in the largest crystallizer was designed to provide good mixing when the active volume was around 1000 mL; after nearly 60% of the charge had been vaporized, the remaining fraction may very well fall at or below the impeller used to mix the slurry. In either case, the contents of the crystallizer were poorly mixed. Furthermore, as the level in the crystallizer fell, the exposed, wet walls of the crystallizer had a tendency for scale to form on them. This resulted in what was called accumulation in the system. An additional problem with using pure batch operation was that the amount of material recovered from the first stage of a two-stage process was too small to provide good operation in the second stage.

In the semi-batch procedure, an initial charge of the feed material was added to the crystallizer, and the conditions throughout the system were brought to their desired state: the pressure in the system was set, flow of cooling water through the jacket of the condenser started, mixing in the crystallizer begun, and all monitoring instrumentation started. At this point the flow of the heating fluid was started, and the temperature of the material in the crystallizer began to rise to a value that corresponded to the system

pressure. When vapor began to form and produce condensate that entered the receptacle on the balance, the temperature of the heating fluid was adjusted to set the rate at which vapor was generated.

As vapor was generated, the feed solution was added manually from the vessel atop the crystallizer so as to maintain the level in crystallizer. This was done carefully so that the vacuum in the system was not broken. Vapor generation continued until crystals were observed in the crystallizer. At this point the evaporation was stopped and additional feed, which was unsaturated, was added to dissolve all of the crystals in the system. From this point on, the rate of evaporation was much slower than had been the case in the earlier phases of the run. Figure 15 shows data from an early run in which this procedure was developed.

The approach was chosen so as to minimize run time by rapidly evaporating water while the solution was undersaturated, but then to eliminate all crystals that had been formed under such conditions; this was followed by slowly evaporating solvent to minimize nucleation in relationship to crystal growth.

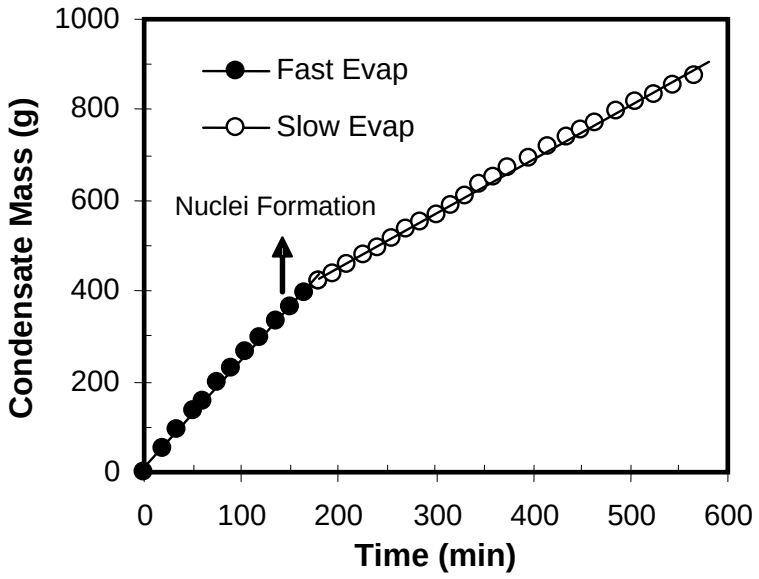


**Figure 15. Plot of Mass of Condensate Generated from an Early Semi-Batch Run in Which Rapid Evaporation to Saturation was Followed by Dissolution of Crystals and Subsequent Slow Evolution of Vapor.**

The vacuum in the system had to be adjusted during a run to control the temperature of slurry in the crystallizer. This was necessary because there was an increase in the concentrations of non-crystallizing species as solvent was evaporated. The concomitant decrease in vapor pressure required an increase in temperature or decrease in pressure to continue evaporation. The regulating valve on the vacuum pump was closed slightly to increase the vacuum drawn in the equipment. Unfortunately, this tended to increase violent boiling of the solution in the vessel, which often led to splashing of the slurry on the upper walls of the crystallizer. Gradual closing of the valve somewhat mitigated this problem.

When the desired amount of condensate had been collected (as determined by a condensate-to-feed ratio set by a corresponding simulation), the monitoring Labview

software was stopped and the final slurry was collected for subsequent treatment and characterization.

### 2.2.2 Washing and Filtration

The slurry was drained from the bottom opening of the crystallizer into a beaker, which had been heated to the temperature of the slurry, and transferred to the jacketed filter. In order to maintain a constant temperature, heating fluid at the crystallization temperature was pumped through the jacketed portion of the apparatus. As the slurry was transferred to the filter, a vacuum pump pulled a vacuum in the filtration flask in which the filtrate was collected. During filtration, the top half of the apparatus was disconnected from the filter, leaving the funnel open to the air.

The rate of slurry addition to the filter depended on the difficulty of filtration; this is generally a function of the size of the crystals, as fine crystals, especially when part of a broad distribution, have a tendency to plug the filter and slow the rate of filtration. When extreme problems of this kind were encountered (e.g., in the first stage of the DST Certification Run) the difficulty was mitigated by using three jacketed filters mounted in parallel so as to process the slurry as rapidly as possible. It was important to keep access to the slurry during the filtration step in order to mix it with a Teflon spatula. Such mixing sped filtration by alleviating filter plugging.

After the filtration step, the filtration flask was changed, the mass of unwashed solids determined, and the wet crystals returned to the filter. The top half of the apparatus was placed in position and sealed. At this time the upper valve was put in the closed position and the washing solution loaded into the funnel. The vacuum pump was turned

on to decrease the pressure inside the vessel and then the upper valve was opened to distribute the solution through the perforated plate.

### 2.2.3 Accumulation Removal

Accumulation of crystalline material on the walls of the crystallizer above the baffle cage was considered another major product from a run. Although attempts were made to minimize the amount of this material, it was almost always found after a run had been completed. Of course, it had to be collected at the end of a run and its mass determined for closure of mass balances.

In order to collect the accumulation, the condenser and agitator (with its motor) were removed from the apparatus and the vessel lid was removed. The solids that remained on the walls and baffles were collected carefully using a spatula; they were then weighed and stored in a sealed bottle for further analysis. Solids that could not be recovered contributed to non-closure of mass balances.

### 2.2.4 Preparation of Wash Solutions

All stages of the certification runs included a washing step that used an aqueous solution of sodium nitrate and sodium carbonate. Sodium hydroxide was also included in the wash solution for the DST run so that alkaline conditions were maintained and gel formation was avoided. In all cases, the wash solution was prepared in a beaker of known mass and the salts were added in measured quantities. Water was added slowly to the salt mixture and the beaker was placed on a hot plate stirrer, which turned a magnetic stir bar that had been placed in the beaker, and the solution was brought to the desired temperature. Once the solution reached the appropriate temperature, additional water was

added until all crystals had dissolved. Before using the wash solution, the full beaker was weighed to determine the amount of water added to the solution.

### 2.2.5 Stage Two Preparation

In a two-stage crystallization run, the filtrate from the first stage was the feed to Stage 2. A known amount of water was added to the filtrate to dissolve any crystals that had formed as the filtrate cooled. This also was necessary to preserve the integrity of samples of the filtrate; i.e., without dilution, the filtrate quickly became a two-phase mixture that would have been difficult to analyze. In any case, the diluted filtrate was used as feed for the second stage, and the ratio of pure filtrate to dilution water was used in mass balance calculations. All other procedures for operating the second stage were identical to those followed for the first stage.

### 2.2.6 Mass Balances and Loss Estimation

Continual improvement in procedures led to mass balance closures to within 3% for each stage of the certification runs. The tare weights of all beakers and flasks were determined before use and after they were filled with the designated process stream (slurry, accumulation, etc.). The beakers were also weighed after they have been emptied to determine the amount of residual mass remaining in the beaker. Other possible losses of mass came from (1) the crystallization vessel, (2) the filtration apparatus, and (3) the washing apparatus. In order to account for accumulations in each apparatus, they were each washed with a known amount of water, and the collected water was weighed to determine the amount that remained in the apparatus. In order to account for wash water that remained on the inner wall of the vessel or filters, a dry laboratory paper of measured

mass was used to collect this water. To close the mass balance further, all the accessories (Teflon and metal spatulas) used during the experiments were washed with a known amount of water. The addition of a trap before the vacuum pump reduced water loss through the pump during a run and collected water could be included in the overall mass balance.

The overall mass balance data are presented in tables similar to that shown in Table 3. These tables give the mass and species composition of each element and provide data in three columns: (1) *Input*, corresponding to the feed and wash solution, (2) *Output*, including the condensate water ("cond"), the washed solids (final crystals obtained after the washing step), the filtrate (liquid obtained at the end of the filtration step), the spent wash (liquid obtained at the end of the washing step) and the accumulation (solids remaining on the wall of the crystallizer at the end of the evaporation), and (3) *Loss,* which corresponds to the difference between the total input mass and the total output mass. Percentage loss is given as two values in the bottom two rows. The first corresponds to the overall closure percentage when no observable mass losses are accounted for. The second is the closure value deduced after all known losses are accounted for (following the procedures explained above). The mass balance data are also represented by a flow diagram summarizing the mass and flow patterns of all streams in addition to various processes and stages used in the experiment. Figure 16 gives an example of such a flow diagram.

**Table 3. Example of a Mass Balance Table.**

| | Input (g) | | Output (g) | | | | | Loss (g) |
|---|---|---|---|---|---|---|---|---|
| **Species** | **Feed** | **Wash** | **Cond** | **Washed Solids** | **Filtrate** | **Spent Wash** | **Accum. Solids** | |
| | 6479.97 | | | | | | | |
| **$H_2O$** | | 330.58 | 4482.99 | | | | | |
| **$Na_2CO_3$** | | 56.36 | | | | | | |
| **$NaNO_3$** | | 233.2 | | | | | | |
| **Solution** | | | | 469.25 | 1205.2 | 639.91 | 4.16 | |
| **Total** | 6479.97 | 620.14 | 4482.99 | 469.25 | 1205.2 | 639.91 | 4.16 | 298.6 |
| **Combined** | 7100.11 | | 6801.51 | | | | | 298.6 |
| | | | | | | **Loss (%)** | | 4.21% |
| | | | | | | **Corrected loss (%)** | | 3.5 % |

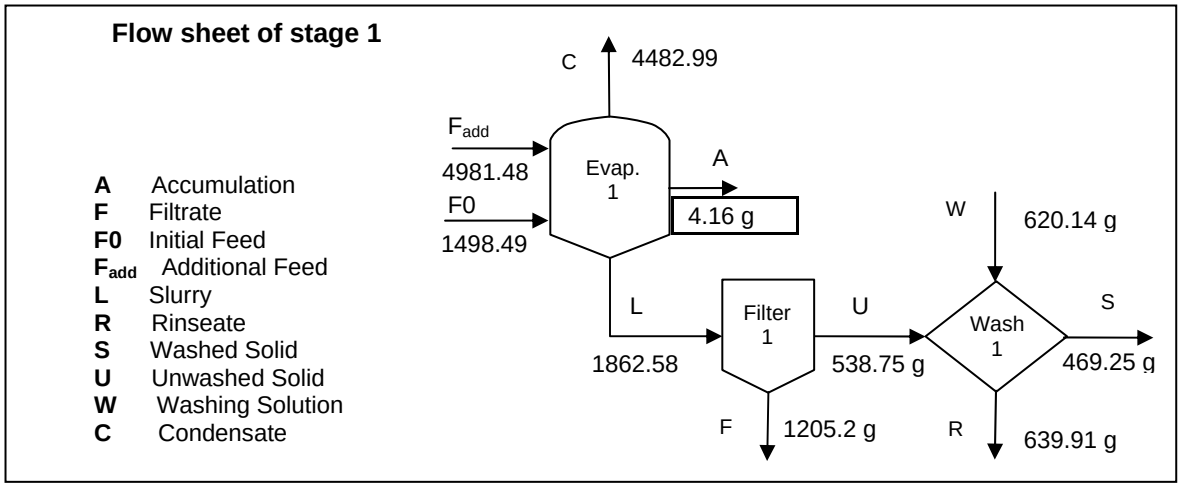


Amounts shown in grams.

**Figure 16. Example of Flow Diagram.**

### 2.2.7 Chemical Analysis

Chemical analysis was required in order to perform species mass balances and determine whether or not specifications given in the SOW had been met. For each stage in the certification runs the following samples were taken: feed solution, filtrate, spent wash, unwashed crystals, accumulation, and final crystals. These samples can be seen graphically in a two-stage schematic shown below in Figure 17. In order to ensure homogeneity in the samples and eliminate sampling uncertainties with two-phase mixtures, dilution water was added to the spent wash, filtrate, unwashed crystals, and accumulation. The amount of water added to each pure sample was recorded so mass balance calculations could be performed accurately. The only samples sent for analysis in solid form were the final crystals.

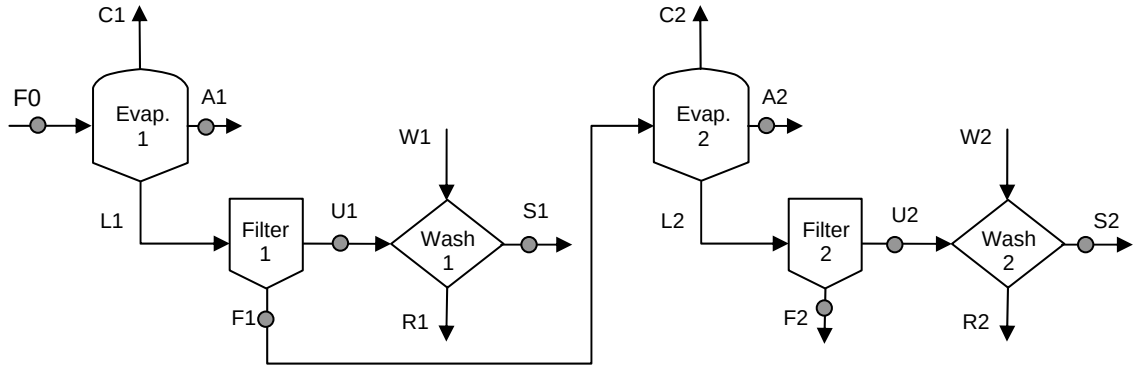


(Sample points marked with gray circles. The DST run also includes carbonation steps which are not shown here.)

**Figure 17. Schematic of the Two-Stage Certification Runs.**

### 2.2.8 Carbonation

The carbonation reaction was performed with DST feed prior to each of the crystallization stages. A schematic diagram of the apparatus used is shown in Figure 18. The first step in the procedure was to set the $CO_2$ to the desired flow rate. The input flow from the cylinder was regulated using two valves: a metering valve after the gas cylinder (coarse regulation) and a rotameter following the metering valve (fine regulation). The flow rate was measured (or calibrated) by switching the three-way valve to a bubble flow meter. The flow was verified by performing 10 measurements with an acceptable variance. When the input flow had been determined and regulated, the valve was switched to the vessel to allow measurement of the output flow. This was done to make sure the system was sealed. Agreement of the two flows showed that the apparatus was perfectly sealed.

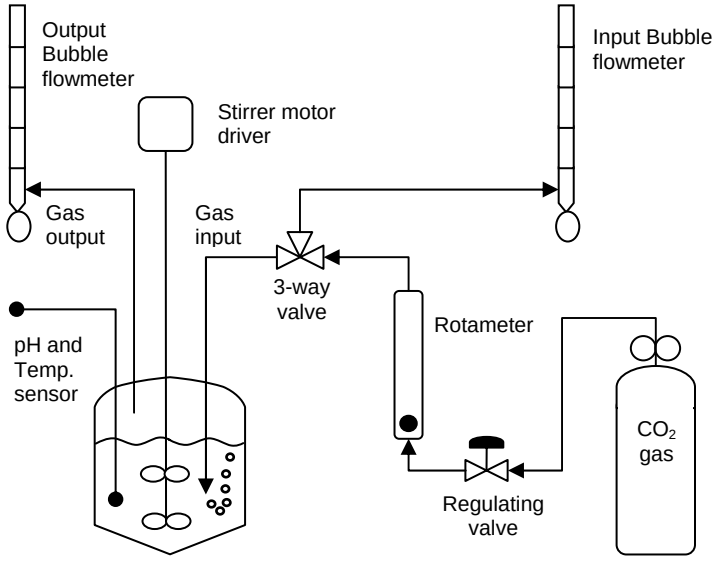


**Figure 18. Schematic Diagram of Apparatus Used.**

A known mass of DST simulant was then loaded into the 1000-mL vessel. The pH meter was calibrated with a buffer solution at pH 7 and with the simulant, which was set to a pH of 14. Once the pH meter was calibrated, the $CO_2$ was introduced and the time, pH, and temperature monitored (measurements taken every five minutes). The flow was continued until one of the three following conditions were met: (1) the desired amount of $CO_2$ had been added to the DST solution, (2) the pH began to decrease significantly and the temperature began to reach a plateau, and/or (3) the first gel appeared at the liquid surface.

The amount of $CO_2$ added to the DST was estimated using differences in volumetric flows into and out of the carbonation vessel, measurements of temperature and pressure, and the ideal gas law. When carbonation was terminated, the input tube was removed from the solution (to avoid any DST backflow into the tube), the gas cylinder was closed and mixing was increased (in order to dissolve the small amount of gel that may have formed). The DST simulant was then collected and weighed. The true amount of $CO_2$ added was then determined by comparing the initial and final masses of the solution.

### 2.2.9 Preliminary Runs

To become familiar with the experimental apparatus and prepare for certification runs, numerous runs were performed on simple salt solutions. A total of 31 runs (including the certification runs) were done in the laboratory. The simple salt solutions began with sodium nitrate and evolved to a more complicated mixture of sodium nitrate, sodium carbonate, and sodium sulfate and also included attempts at seeding (see

Appendix F). Initial runs were purely batch crystallizations where the heating bath was maintained at a constant temperature and pure water was used for crystal washing. During these runs experience was gained with the crystallization equipment, which led to the final apparatus design and crystallization procedure. The final procedure involved running semi-batch crystallizations at constant volume, varying the heating rate to promote crystal growth, and washing with a saturated solution to maximize the mass of final crystals. A listing of all 31 crystallization runs is given in Appendix D.

# CHAPTER 3: CARBONATION

As described in Section 1.0, carbonation is expected to minimize the possibility of gel formation during evaporation of DST solutions. It was also shown that to achieve the specified sodium recovery, carbonation may have to occur in stages. Carbonation involves the reaction of hydroxyl ions with carbon dioxide, as shown in the following equation:

$$CO_2 + 2\ OH^- \rightarrow CO_3^{2-} + H_2O \qquad (3\text{-}1)$$

Figure 19 illustrates the proposed method for DST treatment. This figure shows two cycles of carbonation, which consumes the hydroxyl ions, each of which is followed by evaporation. Throughout the carbonation and evaporation processes, gelation is avoided by remaining within the solubility curves of $NaAlO_2$ and $Al(OH)_3$. Figure 19 shows the initial step (represented by the dashed line) in which the DST simulant is carbonated; if gelation occurs as the solution conditions approach the $Al(OH)_3$ solubility curve, NaOH is to be added to re-dissolve the gel prior to initiating evaporation. During evaporation, crystals of sodium salts are generated and the concentration of aluminum increases, as illustrated by the solid line in Figure 19. This completes one stage in the process. The second cycle shown follows a strategy similar to the first, and is designed to increase the overall sodium recovery.

The kinetics of carbonation and gel formation are complex phenomena that need rationalization so that operating variables such as the total amount and the rate of $CO_2$ addition can be related to the onset of gel formation. In addition, the possibility of re-dissolving gel formed during carbonation by addition of sodium hydroxide must be

investigated. Such a possibility could have great utility should gel ever be formed in the processing of waste solutions.

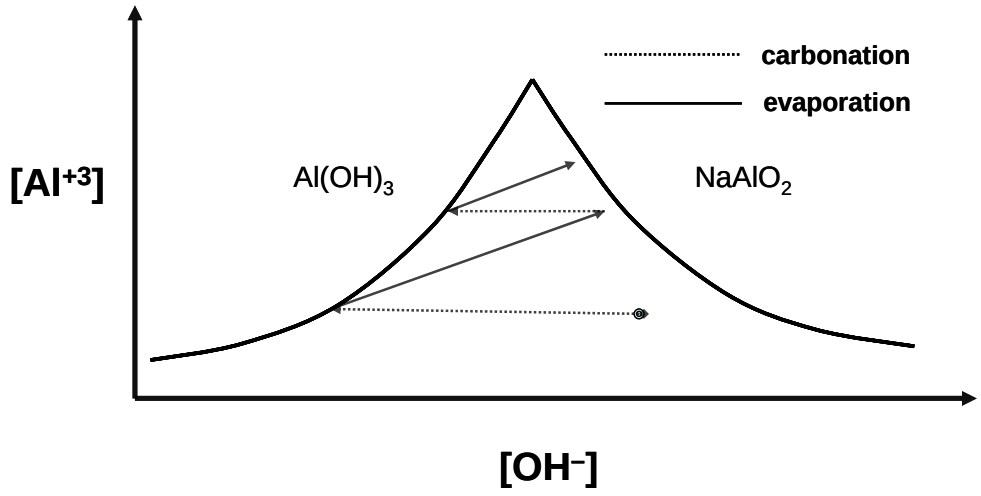


**Figure 19. DST Experimental Plan.**

## 3.1 PRELIMINARY CARBONATION EXPERIMENTS

Several carbonation experiments were performed in order to become familiar with the carbonation process and the gelation phenomenon related to carbonation. During these experiments the pH and temperature of the solution were monitored over time. Due to the fact that the actual pH of the DST solution was estimated to be greater than 15, pH was used as a qualitative measurement in these experiments. At the start of each carbonation run, the pH probe was calibrated with a buffer of pH 10 and the DST stimulant itself, which was set to a value of 14 (the maximum reading of the probe). Using this method, the pH readings taken during experiments were a relative measure of

pH, not an absolute measure. This method allowed comparisons to be made between the different experiments with regard to predictions on the gelation point.

The first carbonation experiment was performed to obtain a general idea of operating issues likely to be encountered during the carbonation process. The experiment was carried out in a 250 mL beaker by bubbling $CO_2$ through a DST solution that had been provided by CH2M Hill. $CO_2$ was introduced into the solution through a piece of perforated tubing immersed in the beaker. The experiment was conducted at ambient temperature and was open to the atmosphere. Mixing was performed by a magnetic stirrer and the $CO_2$ flow rate was very slow (bubble by bubble). The slow carbonation rate ensured that the total amount of $CO_2$ introduced was used in the carbonation process, as the bubbles were observed to disappear before reaching the surface. No solid precipitate was observed during this experiment; but a discontinuous gel phase formed at the surface after 215 minutes of carbonation. These bubbles spread from the center of the beaker and expanded until they covered the entire surface of the liquid, forming an impermeable gel layer. The gel then expanded downward from the surface, until it reached the bottom of the beaker.

Figure 20 shows how the pH and temperature of the solution changed with time near the end of the experiment. The figure is divided into two parts, the first of which is associated with carbonation and the second with gel formation. The carbonation phase ended after 215 minutes: i.e., when the first gel appeared. The decrease in pH with time was nearly linear until gel formation; after that point, there was a much more rapid decrease in pH. The addition of $CO_2$ and concomitant gel formation was continued for 10 minutes before proceeding to the addition of 1 M NaOH solution. Addition of the NaOH

solution was successful in completely dissolving the gel that had formed during carbonation.

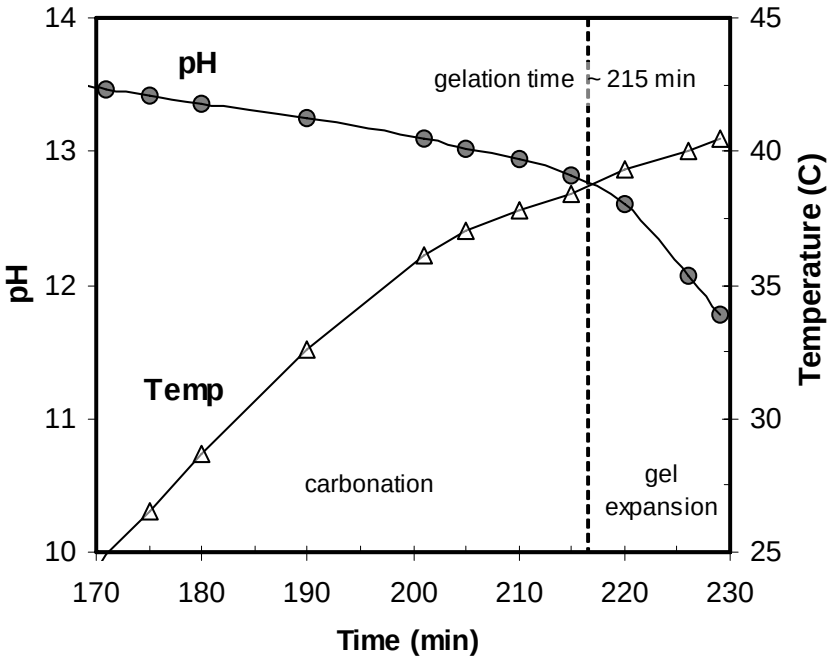


**Figure 20. Carbonation of DST in a Beaker at Ambient Conditions.**

A schematic diagram of the apparatus used for more refined carbonation experiments was introduced in Section 2.0, and is also shown in Figure 21. The $CO_2$ necessary for the reaction was provided by a gas cylinder and the flow was measured with a bubble flow meter. A three-way valve was used to allow the flow to be switched between the sealed 1-L crystallization vessel and the bubble flow meter. The pH and temperature were measured inside the vessel and the outflow of gas was measured using a switching valve connected to the bubble flow meter. Mixing was performed by a mechanical stirrer. Agitation was intended to improve the distribution of $CO_2$ by breaking the bubbles, thereby leading to a greater interfacial area between the gas and liquid phases.

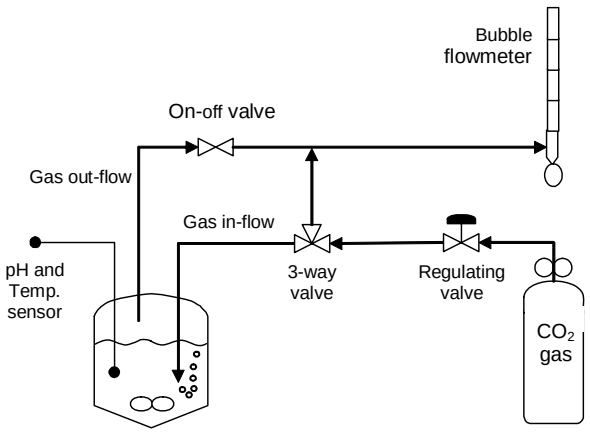


**Figure 21. Schematic of the Carbonation Setup.**

The first run using the apparatus shown in Figure 21 used 500 g of DST solution and had an input $CO_2$ flow rate of 54.2 mL/min. This flow rate was verified by comparing the input and output flows of the empty vessel with the bubble flow meter. Figure 22 shows how pH and temperature evolved during the run. Gel first appeared after 180 minutes of carbonation, at a pH value of 13.23. Following this point, the pH decreased rapidly and the temperature inside the vessel remained constant, evidently signifying the start of gel formation. Similar to the initial beaker experiment, the first gel appeared at the wall surface and then spread around the wall perimeter before bubbles of gel appeared. Due to improved mixing during this experiment the gel formed and spread inside the liquid instead of growing at the surface. As the density of the solution increased, the pH stabilized and the temperature began to increase once again. During the gel-spreading phase, the heterogeneous mixture of liquid and gel transitioned to a single gel phase. The experiment was stopped when pH measurement was made impossible due to the viscosity of the gel. Attempts to dissolve the gel with addition of 1 M NaOH

solution were unsuccessful because the available volume in the vessel was insufficient for base addition. For this reason, a more concentrated NaOH solution was used in the following experiments.

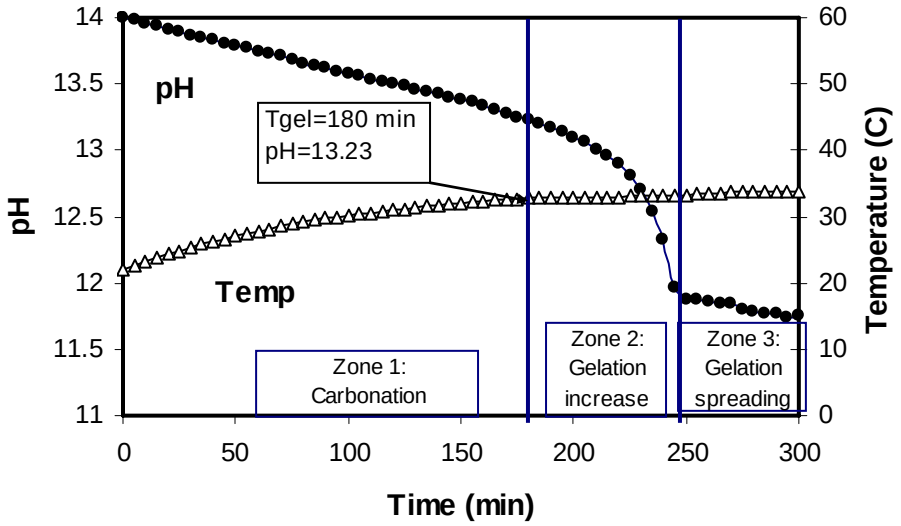


**Figure 22. Temperature and pH Evolution During Carbonation Experiment 2 ($CO_2$ Flow Rate of 54.2 mL/min).**

A third carbonation experiment was performed on 500 g of DST solution and used a $CO_2$ flow rate of 200 mL/min. Details of this experiment are shown in Figure 23. At this higher flow rate, gel formation occurred after 47 minutes of carbonation without any precipitated solids forming during the carbonation phase. After the gel had formed, an attempt was made to dissolve it through more intense mixing. It was determined that near the onset of gelation (when only a small amount of gel has formed) the gel could be dissolved by simple agitation. However, as soon as additional $CO_2$ was introduced, the gel formed spontaneously as if a saturation concentration in $CO_2$ were reached.

At the end of $CO_2$ addition, a gel had formed and the pH in the system was approximately 12.6. Figure 24 shows the measured pH in the system as 5 M NaOH was

added in an attempt to dissolve the gel. The gel did in fact dissolve after the addition of 60 mL of 5 M NaOH solution. It should be noted that at the point of gel dissolution the pH was nearly identical to the value observed at the point of gel formation during $CO_2$ addition. These points occurred at pH values of 13.19 and 13.18, respectively. In addition, the pH value observed at the onset of gel formation is comparable to the value of 13.23 obtained in the previous experiment. These experimental points demonstrate that the relative pH values may be useful as a prediction method for gelation during carbonation.

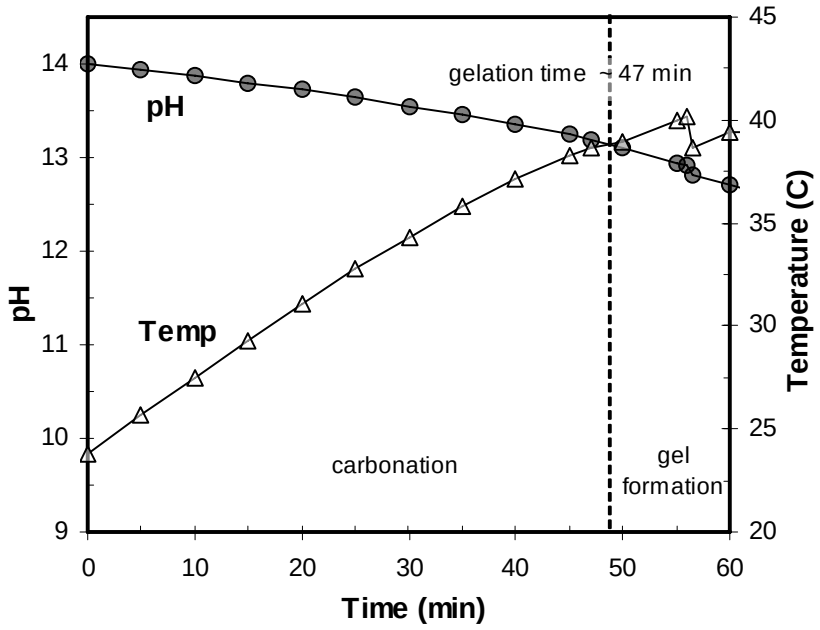


**Figure 23. pH and Temperature Evolution at the 200 mL/min Carbonation Rate.**

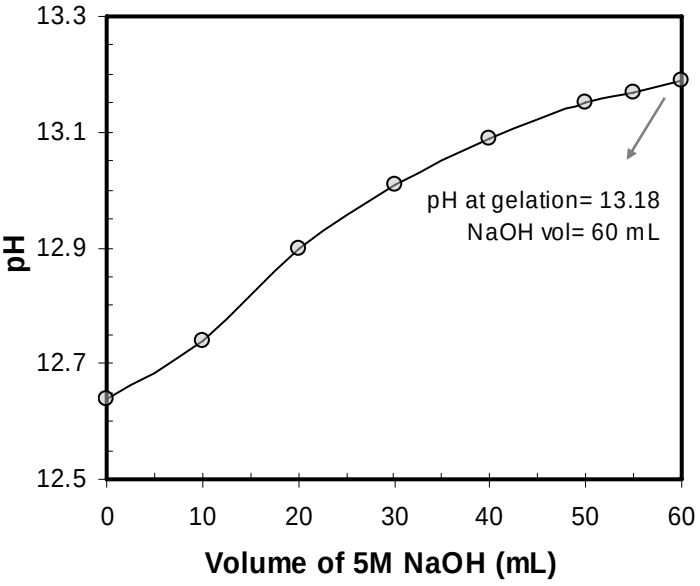


**Figure 24. pH Evolution During 5M NaOH Addition.**

## 3.2 DST CARBONATION FOR CRYSTALLIZATION

In preparation for crystallization experiments on DST Feed Solution, ten bottles of simulant were prepared and their contents were subjected to carbonation. The apparatus and procedures followed were described in Section 2.0. Details for each of the ten carbonation runs are shown in Table 4.

The first two bottles of carbonated DST were used in batch trial runs, which are described in Section 4.0. The third bottle of DST was carbonated with a ratio of about 30 g $CO_2$ per 1000 g DST simulant, resulting in the formation of a white precipitate after the solution was allowed to equilibrate overnight. The pH at the end of this run reached 12.56, by far the lowest value observed during any of the runs. This bottle was filtered in order to separate and study the precipitate. Separation of this precipitate was difficult, as it tended to plug the filter. The solid product obtained from filtration resembled a paste

and after oven drying it hardened into a substance thought to be gibbsite ($Al(OH)_3$). The basis for this assertion is that carbonation shifts the DST composition on the [$Al^{3+}$] vs. [$OH^-$] phase diagram toward the gibbsite region. The PLM image shown below confirmed the substance to be agglomerated gibbsite crystals.

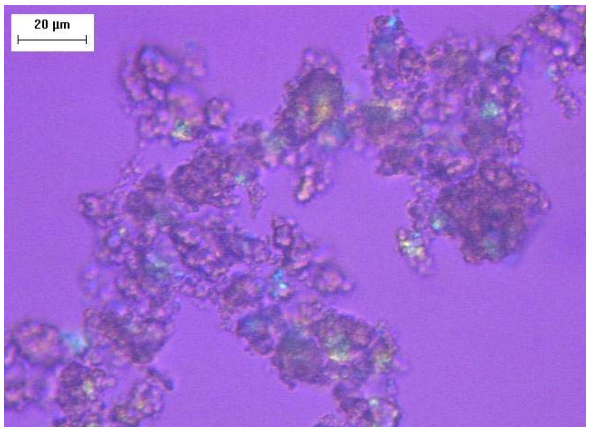


**Figure 25. Image of Gibbsite Precipitate Obtained After Carbonation of Bottle 3.**

**Table 4. Results from the Ten Carbonation Runs.**

| Bottle | Feed Mass (g) | $CO_2$[1] Added (g) | Carbonation Time (min) | Flow rate (mL/min) | Estimated[2] $CO_2$ Fed (g/1000g DST) | g $CO_2$ per 1000 g Feed | Initial pH | Final pH |
|---|---|---|---|---|---|---|---|---|
| 1 | 1000.0 | 26.1 | 144.0 | 116.0 | 30.3 | 26.1 | 14.02 | 13.21 |
| 2 | 1004.3 | 19.1 | 106.0 | 112.0 | 21.5 | 19.0 | 14.05 | 13.30 |
| 3 | 1000.2 | 29.7 | 225.0 | 111.0 | 45.4 | 29.7 | 14.00 | 12.56 |
| 4 | 1336.8 | 54.3 | 365.0 | 92.0 | 45.6 | 40.6 | 14.03 | 13.31 |
| 5 | 1292.6 | 39.6 | 203.0 | 119.0 | 34.0 | 30.6 | 13.94 | 13.25 |
| 6 | 1346.5 | 21.6 | 100.0 | 143.0 | 19.3 | 16.0 | 13.98 | 13.28 |
| 7 | 1318.3 | 30.7 | 125.0 | 143.0 | 24.6 | 23.3 | 13.94 | 13.22 |
| 8 | 1315.6 | 25.8 | 105.0 | 143.0 | 20.7 | 19.6 | 13.97 | 13.26 |
| 9 | 1330.1 | 41.9 | 170.0 | 139.5 | 32.4 | 31.5 | 14.00 | 13.41 |
| 10 | 1319.3 | 42.4 | 190.0 | 139.5 | 36.5 | 32.1 | 14.10 | 13.27 |

[1] Final Mass of Solution – Initial Mass of Solution

[2] Estimated From Volumetric Flow Rate and Ideal Gas Law

Bottles 1 through 3 were mixtures of solutions provided by CH2M HILL and prepared at Georgia Tech, Bottles 4 through 6 were solutions prepared at Georgia Tech, Bottles 7 and 8 were solutions provided by CH2M HILL, and Bottles 9 and 10 were prepared at Georgia Tech. The table shows the initial weight of DST in each bottle, the mass of $CO_2$ added, the run time, the

approximate volumetric flow rate of $CO_2$ to the solution being carbonated, the estimated amount of $CO_2$ fed to the system per 1000 g of solution, the actual amount of CO2 absorbed per 1000 g of solution, and the initial and final pH values of the carbonated solution. $CO_2$ is added to the system by a reaction with free hydroxide ions, as shown below:

$$CO_2 + 2\ OH^- \rightarrow CO_3^{2-} + H_2O \qquad (3\text{-}1)$$

The amount of $CO_2$ added for each run was determined by simply taking the weight of DST before and after the carbonation process.

As shown in Table 4, the amount of $CO_2$ absorbed and reacted in each of the bottles of feed solution differed. For example, 29.7 g $CO_2$ per 1000 g of feed solution were absorbed in carbonating the solution in Bottle 3. This is despite the fact that an estimated 45.4 g of $CO_2$ per 1000 g of feed solution were fed to the solution. In analyzing the data for this run, it was determined that the temperature of the solution rose to approximately 40 °C during the process. At that temperature, $CO_2$ solubility would be reduced, which explains the fact that significantly more $CO_2$ was fed to the system than was absorbed. As a corollary, when the solution temperature was not allowed to increase, the fraction of the fed $CO_2$ that was absorbed increased substantially. For example, the carbonation of Bottle 4 was performed in two steps; i.e. part of the way through the carbonation, the run was interrupted and the solution was allowed to cool to ambient temperature before carbonation was resumed. In that instance, the estimated amount of $CO_2$ fed was 45.6 g per 1000 g of solution, while the amount actually absorbed was 40.6 g per 1000 g of solution. The lessons taken from these runs include: using the pH alone to determine the amount of $CO_2$ absorbed is imprecise; reproducibility in the amount of $CO_2$

absorbed requires maintaining the temperature of the solution to which $CO_2$ is fed as near constant as possible.

An unexplained observation from the carbonation runs is that only carbonation of the solution in Bottle 3 led to formation of a precipitate, despite the fact that significantly more $CO_2$ was absorbed in the solution of Bottle 4. As pointed out above, the latter carbonation was performed in two different steps, with the second step occurring after the solution had remained overnight at ambient temperature.

# CHAPTER 4: PRELIMINARY DST CRYSTALLIZATION RUNS

In addition to carbonation experiments, preliminary DST crystallization runs were necessary to determine process difficulties associated with evaporation of DST solutions. A series of three batch crystallization runs were performed, which incorporated carbonation into the process in a progressive manner. The three DST solution experiments were planned as follows: 1) a two-stage crystallization of the DST solution without carbonation, 2) a two-stage crystallization, with carbonation applied before the first crystallization stage, and 3) a complete two-stage process, with carbonation applied before each crystallization stage.

## 4.1 INITIAL DST BATCH CRYSTALLIZATION

DST simulant crystallization was studied for the first time during Run 16. The main objective of this run was to determine any unique difficulties encountered with this simulant. One major concern during this DST run was that the vacuum system was not powerful enough to perform the run at the desired temperature of 60 °C. Under full vacuum, the operating temperature exceeded 75 °C during each stage. This issue was resolved in following runs by installing a more powerful vacuum pump.

Another issue encountered during Run 16 was gel formation of the product. After the first stage of evaporative crystallization, the slurry recovered was split into two equal amounts and submitted to two different filtration-washing procedures: 1) a two-step filtration and slurry washing and 2) a plug-flow equipment prototype test. The wash solution used during the experiment was saturated in sodium carbonate and sodium nitrate and prepared at 60 °C. The slurrying method (where the unwashed crystals are

combined with the wash solution in a beaker and agitated with a magnetic stir bar) led to gel formation during the washing (Figure 26), whereas using the prototype completely avoided this issue. In order to reduce the likelihood of gel formation during the wash steps in future runs, sodium hydroxide was added to the wash solution. This was done to maintain an alkaline environment during the washing step. In addition, the custom-designed washing apparatus derived from this prototype (detailed in Appendix A) was used for the DST Certification Run.

**Figure 26. Gel Formation During Slurrying Crystals in Wash Liquor.**

The crystal size distribution (CSD) obtained for the first stage of Run 16 is presented in Figure 27. To obtain the CSD the crystals were washed with acetone after the wash with saturated solution. The left side of the curve shows a narrow distribution centered near 100 μm. This can be explained by the fact that the experiment was conducted at elevated temperature and therefore nucleation did not occur until near the end of the run. The curve also presents a peak at the largest particle size (20 percent of

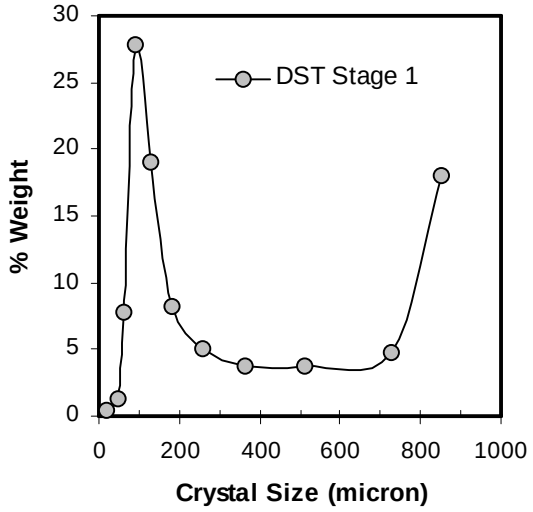


**Figure 27. Size Distribution of Crystals from the First Stage of Run 16.**

the crystal mass remained on the 850 μm sieve), which is explained by agglomeration of the small crystals and fines during filtration, washing, and drying. Due to the late nucleation of crystals in the first stage, only three grams of accumulation were collected from the crystallizer.

The main issue encountered in the second stage of Run 16 was gel formation inside the crystallizer. Although the gel formation caused problems in the downstream operations, it provided means to predict the onset of gelation in future runs. A decrease in the evaporation rate and the formation of sodium aluminate accumulation (shocks of wheat shaped crystals) on the walls of the vessel were the two main precursors to gel formation. These observations acted as warning signs for gelation in future runs. When gel was observed inside the crystallizer during the second stage, the slurry was immediately drained and sent to the filtration and washing steps. Unfortunately, the slurry

cooled and formed a gel; therefore a crystalline product was not obtained. Details of the mass balance for both stages of this run can be found in Appendix D.

Five main chemical species were identified from PLM images of DST Run 16: sodium nitrate, sodium nitrite, sodium carbonate monohydrate, sodium chloride and sodium oxalate. Along with these five species, the crystals shaped like shocks of wheat were observed on the walls of the crystallizer, which resembled sodium aluminate. Images obtained from Stage 1 (Figures 28A and B) showed large amounts of sodium nitrate and sodium nitrite, along with trace amounts of sodium carbonate monohydrate and sodium chloride. No burkeite crystals were observed during this run, although they were predicted. This could be linked to the fact that no accumulation was collected for PLM imaging during the first stage, since burkeite had been observed in the accumulation of previous runs. Figures 28C through 28E show crystals from the second stage; numerous crystals of sodium nitrate, sodium nitrite, and sodium chloride were observed (as seen in Figures 28D and 28E), but the second stage also included trace amounts of sodium oxalate crystals (Figure 28C).

**Figure 28. DST Images from the Slurry in the First Stage (A and B), Slurry in the Second Stage (C), and Accumulation from the Second Stage (D and E) of Run 16.**

## 4.2 DST BATCH CRYSTALLIZATION WITH CARBONATION

Batch crystallization runs were performed using Bottles 1 and 2 from the carbonation runs (described in Section 3.0) to determine at what point gel formation was likely to occur during the carbonated DST process. Run 28 was a two-stage operation following the simulation file DST1SIM2A(carbonation).xls. The simulation used a pre-carbonated feed with a ratio of 60 g $CO_2$ per 1000 g DST feed, while the actual feed for the run (Bottle 1) had a ratio of 26.1 g $CO_2$ per 1000 g feed. Although the feed composition was not identical to the one given in the simulation, the condensate-to-feed target ratio (of 0.45) was followed to determine if gelation would occur in the crystallizer when the evaporation target was exceeded. Results from this run showed that no gel formed during crystallization and that maintaining an isothermal process is extremely important to avoid gelation. Filtration for this run was not operated isothermally because the filter used was at room temperature instead of the desired 60 $^{o}$C. As the temperature of the slurry dropped, the solid product began to hold more water and show signs of gelation. This made solid-liquid separation less efficient than if it had been performed isothermally. 132.5 g of unwashed solids were collected from this run along with 86.2 g of accumulation. Mass balance results for both stages of Run 28 are given in Appendix D. Crystal washing was not necessary for Runs 28 and 29, so the final products shown in the mass balances are of the unwashed crystals.

The second stage of Run 28 used the diluted filtrate from the first stage and was operated at 40 $^{o}$C, following the simulation file provided by COGEMA. The calculated condensate-to-feed target ratio for the second stage was 0.69, while the actual ratio achieved during Stage 2 was 0.65. The evaporation was stopped early because the

contents of the crystallizer were starting to gel, as made evident by an apparent increase in viscosity, resulting in less efficient mixing by the impeller. Even though the evaporative crystallization stage was stopped short, there were gelation issues encountered during filtration. As had been observed during the first stage, the product seemed to hold an excess of water, which reduced separation efficiency. These results show that it is important to perform carbonation on the filtrate from the first stage before it is fed to the second stage.

Run 29 was a two-stage process that used a feed with a ratio of 19.1 g $CO_2$ per 1000 g DST (Bottle 2). The goals of this run were to use lower condensate-to-feed target ratios and apply two carbonation steps in order to try and avoid gel formation during the run. Run 29 used simulation files DST1SIM2A(carbonation).xls and DST1SIM3.xls to determine an appropriate condensate-to-feed target ratio. DST1SIM3.xls was a simulation done on a DST feed without carbonation and had a condensate-to-feed target ratio of 0.424. An intermediate condensate target of 0.435 was chosen for this stage since the feed was carbonated at a ratio falling between the two simulation files (0 g and 60 g per 1000 g feed). The first stage of the run was operated at 60 $^{o}$C and the second stage was operated at 40 °C, identical to Run 28 discussed above. Stage 1 was stopped at the desired condensate-to-feed ratio of 0.435 and showed no signs of gel during crystallization or filtration. The main issue with the first stage of the run was the amount of accumulation left on the walls of the crystallizer (more than 250 g were collected as accumulation). This accumulation was caused by the decreasing solution level during the batch process. Along with this accumulation, 188.1 g of unwashed solids and 84.6 g of filtrate were collected.

Due to the small amount of filtrate obtained from the first stage, the second stage was difficult to process and limited information was gathered for the DST Certification Run. For Stage 2 preparation, the filtrate from the first stage was diluted and carbonated with 0.7 g of $CO_2$, at which point of gelation appeared at the solution surface. The second crystallization step was stopped when the desired condensate-to-feed ratio of 0.81 was reached. At this point the vessel was drained, but the amount of slurry was so small that most of it remained in the vessel and had to be taken out manually. During this process the slurry began to cool and form a gel-like product. Due to this fact the slurry was weighed after it was collected from the vessel and was not subjected to the filtration process. Mass balance results for both stages of Run 29 are shown in Appendix D.

PLM images of Run 29 were taken of samples obtained from the slurry at the end of each stage and are shown in Figure 29. For the first stage, simulation file DST1SIM2A-(carbonation).xls predicted the formation of sodium carbonate monohydrate and aluminum hydroxide as major components, in addition to small quantities of trisodium fluoride sulfate, burkeite and sodium oxalate. Sodium carbonate monohydrate (rainbow colors and yellow/blue random shapes in Fig. 29A), trisodium fluoride sulfate (pyramid shape in Fig. 29B), burkeite (Fig, 29A) and sodium oxalate (blue/yellow needles in Fig. 29A) were observed as predicted. Sodium nitrate and sodium chloride (cube-like crystals in Fig. 29B) were also observed in this stage. Although aluminum hydroxide was predicted in large quantities, it was not observed in the PLM images. However, it may have formed and been confused with the trisodium fluoride sulfate crystals, which have similar low contrast shapes.

Sodium nitrite, sodium nitrate, sodium carbonate monohydrate, sodium chloride, potassium nitrate, sodium oxalate, and trisodium fluoride sulfate were expected from Stage 2. All of these crystals were identified in Stage 2 except potassium nitrate. Sodium nitrite crystals were clearly distinguished from sodium nitrate from their parallel extinction orientation and the appearance of rainbow patterns at their edges, e.g., as shown in Figure 29C. The content of sodium carbonate monohydrate was high in both the predicted simulation and the crystallization run. This is because during the carbonation process $CO_2$ reacts with free hydroxyl ions to produce carbonate anions, which in turn leads to more carbonate crystals in the final product.

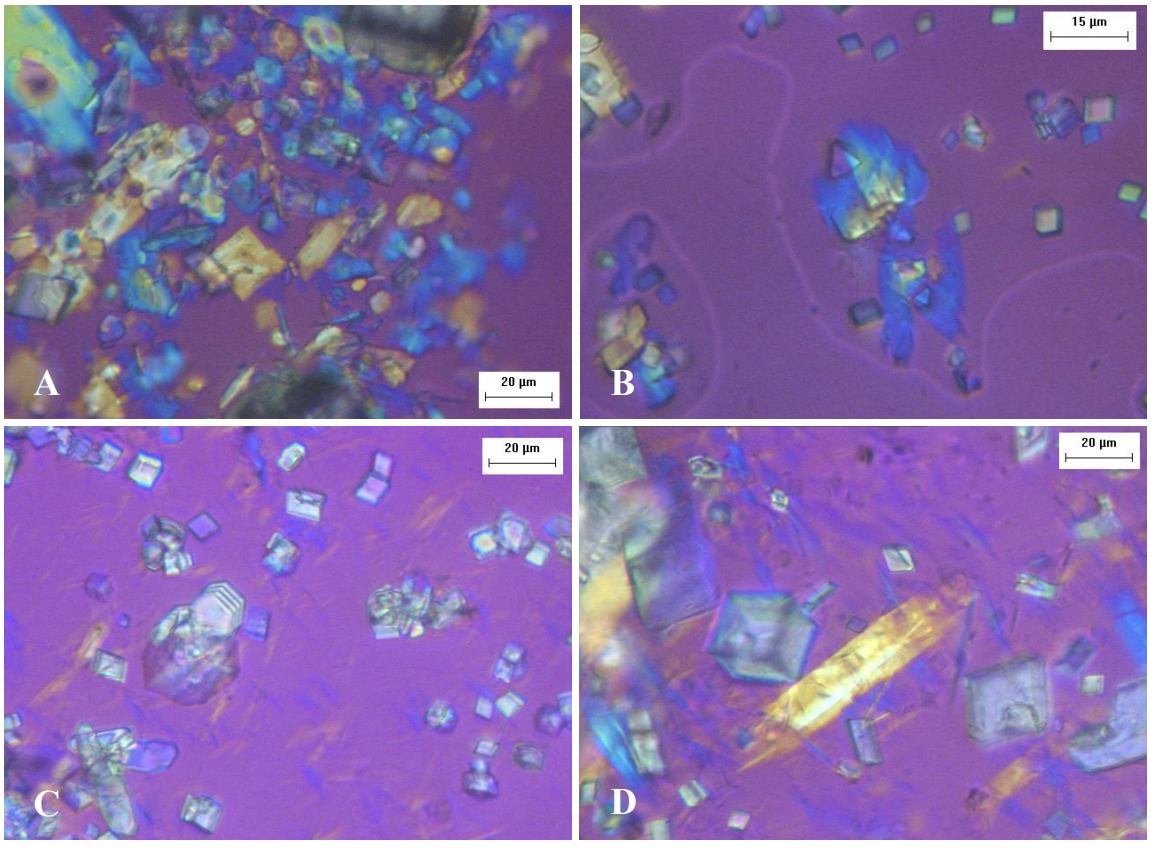


**Figure 29. PLM Images of the Carbonated DST Run 29. (A-B) from Stage 1 and (C-D) from Stage 2. All Samples were Obtained from the Slurry.**

# CHAPTER 5: DST CERTIFICATION RUN

The DST Certification Run was performed using a feed solution that had been prepared according to procedures provided by CH2M HILL[3]. The procedures led to formulation of a solution having the composition given in Table 5.

**Table 5. Composition of DST Feed Solution.**

| Chemical | MW | Intended Molarity |
|---|---|---|
| **$NaAlO_2 \cdot 2H_2O$** | **118.0** | **0.80** |
| **NaOH** | **40.0** | **2.80** |
| **$Na_2CO_3$** | **106.0** | **0.09** |
| **$Na_2C_2O_4$** | **134.0** | **0.004** |
| **$KNO_3$** | **101.1** | **0.27** |
| **$NaNO_3$** | **85.0** | **1.27** |
| **$NaNO_2$** | **69.0** | **1.60** |
| **$Na_2SO_4$** | **142.0** | **0.01** |
| **$Na_3PO_4 \cdot 12H_2O \cdot 0.25NaOH$** | **390.1** | **0.01** |
| **NaCl** | **58.4** | **0.16** |
| **$NaC_2H_3O_2 \cdot 3H_2O$** | **136.1** | **0.056** |
| **NaF** | **42.0** | **0.015** |
| **$Na_2Cr_2O_7 \cdot 2H_2O$** | **298.0** | **0.002** |
| **$CsNO_3$** | **194.9** | **0.0168 g/L** |

### 5.1.1 Operating Conditions

The two-stage crystallization was conducted using the 1-L crystallizer for Stage 1 and the 300-mL crystallizer for Stage 2. The procedures in performing the crystallizations followed the semi-batch approach outlined in Section 2.0. Each stage was operated under a variable evaporation-rate profile to reduce formation of fines, as shown in Figure 30. Carbonation was performed prior to each evaporation step to increase sodium recovery

[3] Communication CH2M-0403873 by Dan Herting to E. A. Nelson, December 10, 2004.

and to avoid the problem of gel formation described in the previous sections. Details of carbonation development and use are presented in Section 3.0.

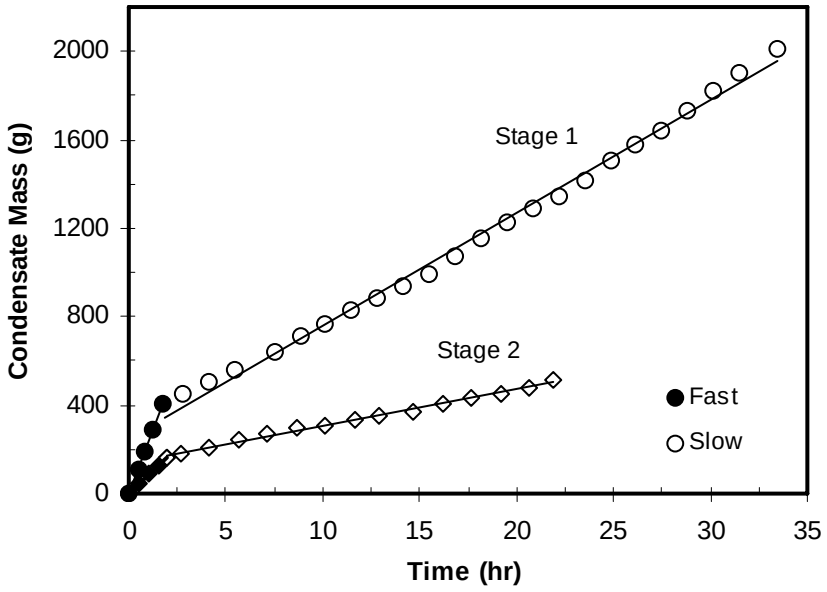


**Figure 30. Mass of Condensate Generated as a Function of Run Time for Stage 1 and Stage 2 of Run 31.**

The two carbonation steps were performed in the 1-L crystallization vessel using the experimental setup and procedures described in Sections 2.0 and 3.0. The initial carbonation was performed on four 1-L batches of DST solution (Bottles 7-10) and the four liters were mixed together to give a solution with an estimated 26.65 g $CO_2$ per 1000 g of pure DST feed. The second carbonation step involved adding 34.2 g of $CO_2$ to the diluted filtrate from Stage 1. The gas flow rates used during the two carbonation steps were 140 mL/min and 97 mL/min, respectively.

The evaporation rate during crystallization was controlled by varying the temperature difference between the heating medium and the slurry. This was done by adjusting the temperature of the heating fluid and the pressure inside the vessel. In the

more rapid evaporation step of Stage 1, vapor was generated at a rate of 230 g/h by adjusting the temperature of the heating fluid to 85 °C. The pressure in the crystallizer during this step was maintained around 110 mm Hg and the slurry temperature increased from 50 °C to 53 °C. This evaporation step lasted for 2.0 h, which is when crystals began appearing in the system. The addition of simulant feed returned the level in the crystallizer to its initial position and re-dissolved all crystals that had been formed. After this point, the evaporation rate was reduced to 50 g/h by reducing the temperature of the heating fluid to 65 °C. The temperature of the solution in the crystallizer was maintained near 60 °C by manipulating the regulating valve on the vacuum pump. Evaporation proceeded for over 31.4 h, at which time the slurry was drained from the crystallizer. The final slurry temperature was 58.4°C and the pressure was 75 mm Hg. The condensate-to-feed ratio for the first stage was 0.468, while the target ratio was 0.48 (Appendix C). The simulation files DST2SCC.xls and DST2SCC2.xls were provided by COGEMA and used as guidelines for this run.

The filtrate from the first stage was diluted with water and carbonated with 34.2 g of $CO_2$. The 300-mL crystallizer was used in the second stage crystallization since the volume of filtrate from the first stage was substantially less than that available for operation of the first stage. The target condensate-to-feed ratio obtained from the above-cited simulations was adjusted to 0.52 to account for the dilution water added to the filtrate. Because the volume of the second-stage crystallizer was 300 mL, only a fraction of the diluted filtrate (~50%) was required for its operation. The evaporation rate for Stage 2 followed the same pattern as was used for Stage 1; evaporation rates were 83 g/h and 16 g/h in the fast and slow regimes, respectively. The slurry temperature at the end of

the run was 59.7 ºC, the pressure was 93 mm Hg, and the actual condensate-to-feed ratio achieved was 0.427. Evaporation was terminated early due to the fact that the slurry viscosity appeared to be increasing, which was identified in Section 4.0 as a warning sign for gel formation.

### 5.1.2 Balances on Total Mass

The means used to satisfy mass balances were described in Section 2.0. The objectives of this process are (1) to determine the fate of species entering the process and (2) to use mass balances to identify potential problems with the operating procedures.

The schematic diagram in Figure 31 illustrates an overall mass balance around Stage 1 of Run 31. Included in the figure are definitions of quantities used in closing mass balances around each of the units in the stage. As shown in Table 6, the difference between input and output for each of these units was as follows: evaporation, 0.32%; filtration, 2.24%; washing, 3.24%.

*Stage 1.* Evaporative crystallization in Stage 1 is represented schematically in Figure 31. The figure shows the masses of vapor generated and either recovered in the condensate receiver or the cold trap protecting the vacuum pump, crystals that accumulated on the walls of the vessel, material that adhered to the vessel and was lost in the transfer process, and the recovered slurry.

The slurry recovered from the evaporative crystallization was filtered as shown schematically in Figure 31. The unwashed crystals leaving the filter correspond to the mass of solids recovered at the end of the filtration. The filtrate was collected inside the vacuum flask, and the funnel loss corresponds to the loss recovered after filtration by

washing the filtration funnel with a known amount of water and using a dry paper of known mass to collect the water accumulated on the wall of the apparatus. The slurry beaker loss for the DST run was excessive because the slurry began to form a gel after it was removed from the crystallizer and started to cool.

The unwashed crystals were washed as shown schematically in Figure 31. The mass of unwashed crystals entering the washing step corresponds to the mass coming from the filtration step, after subtracting the amount lost in the intermediary beaker and the amount removed as a sample. The beaker loss was small because the solids recovered from the filtration step are relatively dry and do not stick to the walls of the beaker. The crystals leaving the washing step are the product from Stage 1, while the other streams leaving are as previously defined.

*Stage 2.* Figure 32 is a schematic diagram for Stage 2 of Run 31. Each process unit functioned as described in the discussion of Stage 1, and the methods of closing total mass balances also were the same. The results of these analyses are shown in Table 23.

**Table 6. Mass Balances Around Process Units of Run 31.**

| Unit | Input (g) | Output(g) | Difference (g) | % Closure of Mass Balance |
|---|---|---|---|---|
| **Evaporator 1** | **4290.2** | **4276.55** | **13.65** | **0.32** |
| **Filtration 1** | **2173.82** | **2125.2** | **48.62** | **2.24** |
| **Washing 1** | **1167.83** | **1129.96** | **37.87** | **3.24** |
| **Evaporator 2** | **1198.14** | **1192.01** | **6.13** | **0.51** |
| **Filtration 2** | **657.03** | **629.23** | **27.8** | **4.23** |
| **Washing 2** | **217.61** | **211.45** | **6.16** | **2.83** |

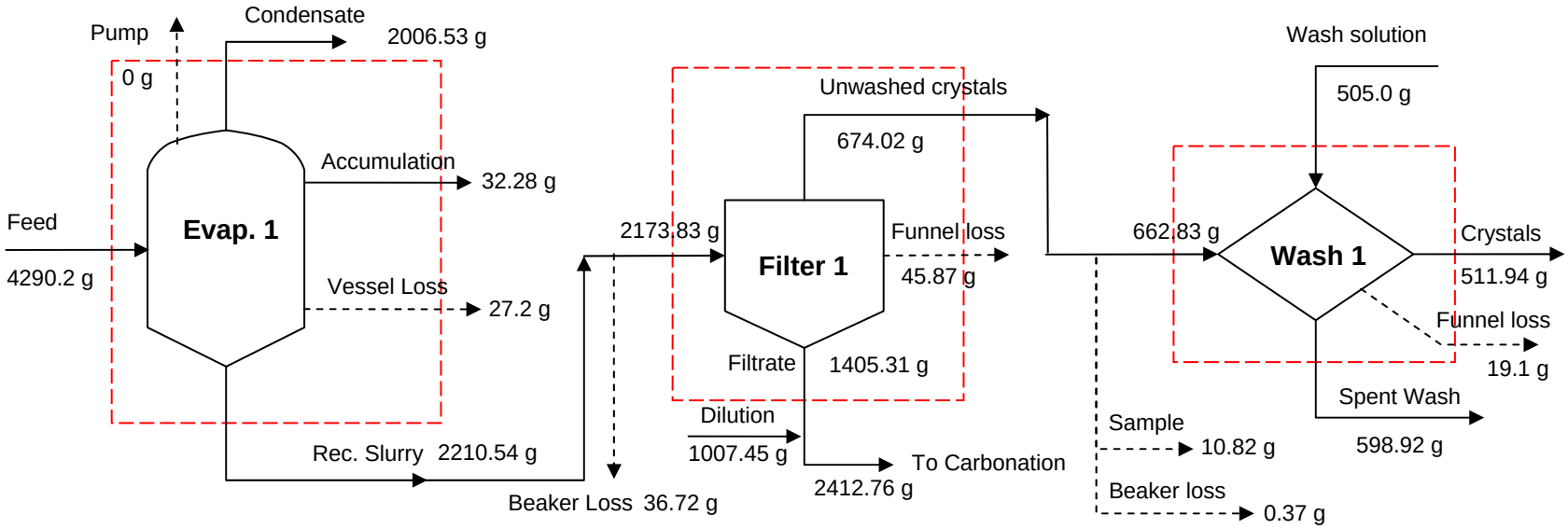


| | |
|---|---|
| **Pump** | Mass of the condensate collected in the cold trap protecting the vacuum pump. |
| **Rec. Slurry** | Mass of slurry recovered from the crystallizer. |
| **Vessel Loss** | Mass recovered by washing the vessel with a known amount of water. |
| **Dilution** | Water added to the filtrate to dissolve any precipitated crystals. |
| **Funnel Loss** | Mass recovered by washing the funnel with a known amount of water and then drying with paper of a known weight. Performed after the filtration and washing operations. |
| **Beaker Loss** | Mass of slurry lost in the several beakers necessary for the transfer from the vessel to the filter. |
| **Sample** | Mass collected from the un-washed crystals for chemical analysis. |

Solid arrows are the process streams and the dotted arrows represent the quantified losses. Closure on a total mass balance was performed for each dashed box around a process unit.

**Figure 31. Overall Mass Balance in Stage 1 of DST Feed Solution Run 31.**

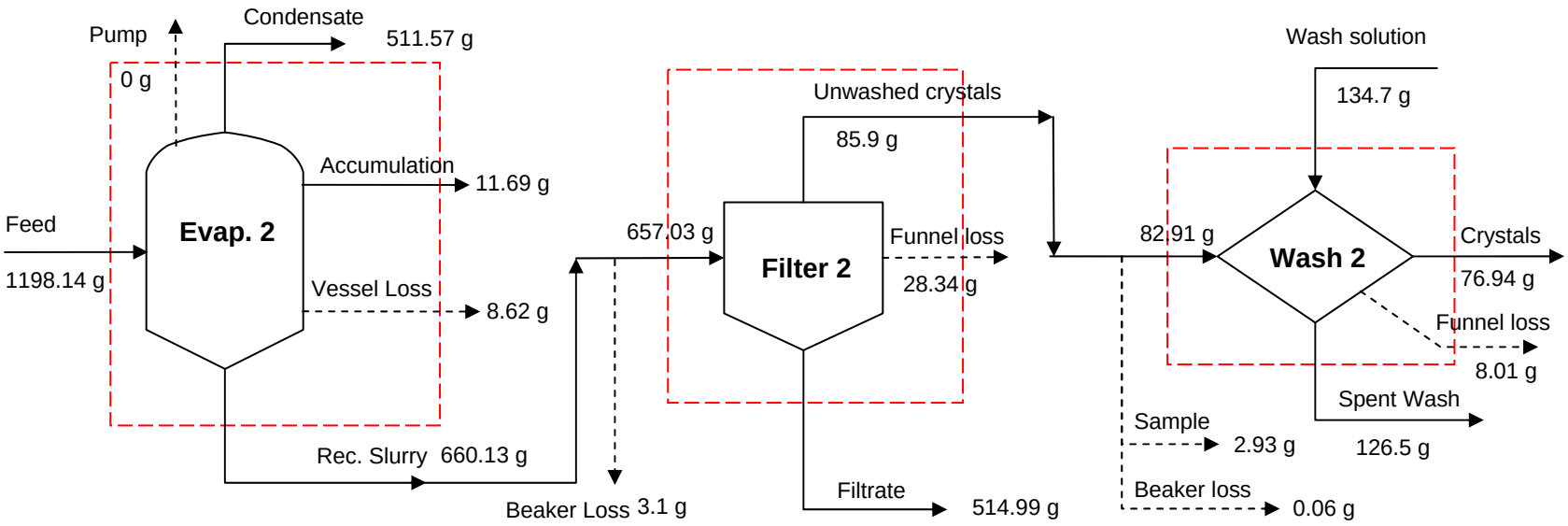


| | |
|---|---|
| **Pump** | Mass of the condensate collected in the cold trap protecting the vacuum pump. |
| **Rec. Slurry** | Mass of slurry recovered from the crystallizer. |
| **Vessel Loss** | Mass recovered by washing the vessel with a known amount of water. |
| **Funnel Loss** | Mass recovered by washing the funnel with a known amount of water and then drying with paper of a known weight. Performed after the filtration and washing operations. |
| **Beaker Loss** | Mass of slurry lost in the several beakers necessary for the transfer from the vessel to the filter. |
| **Sample** | Mass collected from the un-washed crystals for chemical analysis. |

Solid arrows are the process streams and the dotted arrows represent the losses. Closure on a total mass balance was performed for each dashed box around a process unit.

**Figure 32. Overall Mass Balance in Stage 2 of DST Feed Solution Run 31.**

### 5.1.3 Characterization of Crystal Products

*Polarized Light Microscopy.* Samples of crystals removed from the slurry produced in each stage were examined using polarized light microscopy (PLM). Images obtained from the examinations are given in Figure 33. The major crystals expected from the first stage were sodium carbonate monohydrate, sodium nitrate, and sodium nitrite, while trisodium fluoride sulfate and sodium oxalate were expected in trace amounts (as predicted by simulation files DST2SCC.xls and DST2SCC2.xls). Sodium carbonate monohydrate (rainbow patterns and yellow/blue random shapes in Figures 33A-D), sodium nitrate (Figure 33A), and sodium nitrite (crystals with shadow edges like that superimposed on the sodium carbonate monohydrate in Figure 33C) were observed in this stage as expected. Sodium oxalate (yellow needles in Figure 33D) was also observed as predicted, but the common six-sided habit of trisodium fluoride sulfate was not seen in these images. However, a different shape likely belonging to this crystal was noticed as a twinned plate (upper right of Figure 33A). Additional crystals that were observed include aluminum hydroxide (low contrast needles and particles in Figure 33D) and burkeite (cluster of small crystals in Figure 33D).

The major crystals expected from the second stage were sodium nitrite, sodium nitrate and sodium carbonate monohydrate, while potassium nitrate and trisodium fluoride sulfate were expected in smaller quantities. The three major crystal types were seen during PLM imaging and sodium nitrite crystals were clearly distinguished from sodium nitrate from the appearance of rainbow patterns at their edges (Figure 33E vs. Figure 33F). Trisodium fluoride sulfate was not explicitly seen and potassium nitrate could not be identified. The only other crystal type identified from the second stage was sodium oxalate (blue/yellow needles in Figure 33E).

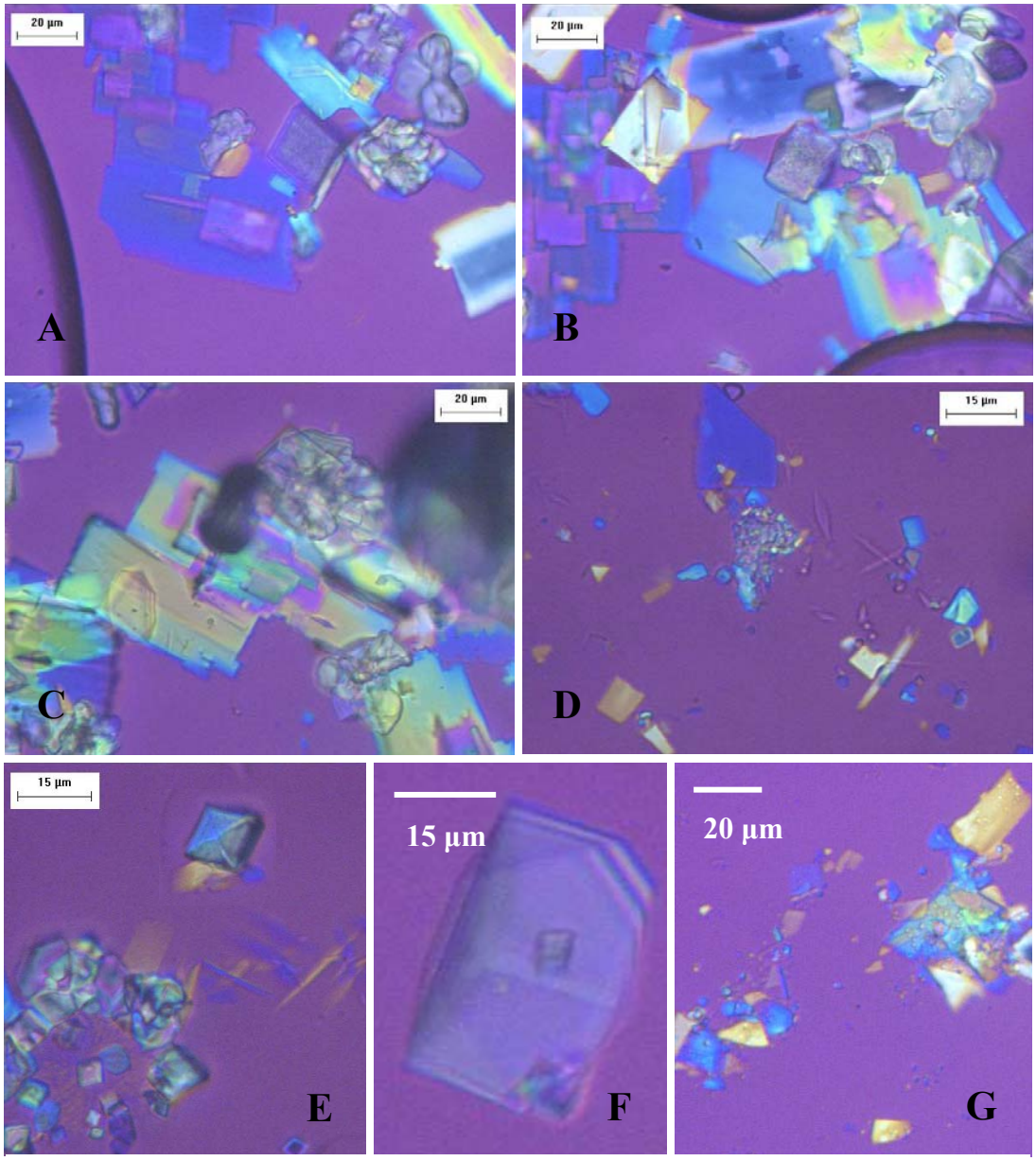


Images A through D were obtained from Stage 1 and Images E through G were obtained from Stage 2.

**Figure 33. PLM images of crystals obtained from DST Solution Certification Run 31.**

*Sieve Analyses.* A fraction of crystals obtained at the end of each stage of Run 31 was washed with acetone and allowed to air dry overnight. A 15-20 g sample from each stage was sieved as outlined in Section 2.0. Sieve results obtained on crystals from both stages are presented as histograms in Figures 34 and 35.

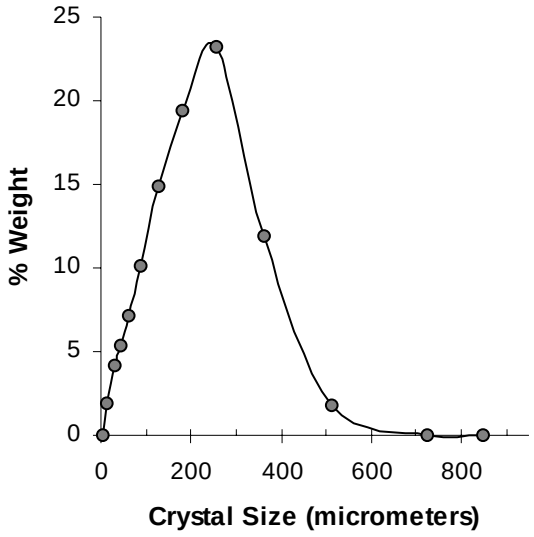


**Figure 34. Crystal Size Distribution of DST Run Stage 1.**

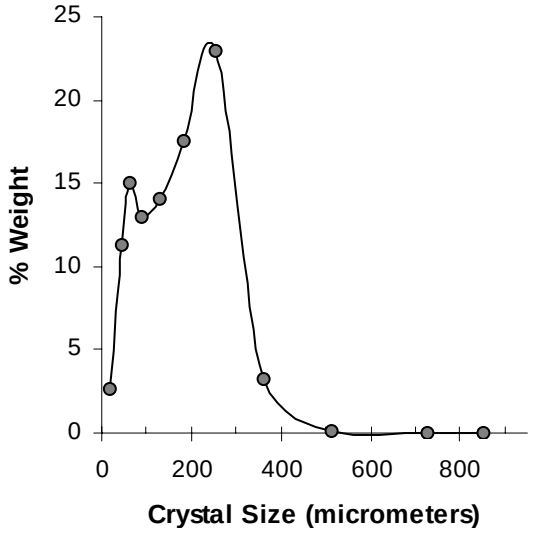


**Figure 35. Crystal Size Distribution of DST Run Stage 2.**

The distribution curve for the first stage of Run 31 is shown in Figure 34. Since gel had formed during the filtration process it is necessary to examine the washed product and determine how the gelation affected the crystals. If proven that the product is composed of single crystals, then the mode size (at 250 μm) is expected to correspond to sodium nitrate and sodium nitrite. Sodium carbonate monohydrate, sodium oxalate and trisodium fluoride sulfate are expected at the lower size range (20 to 100 μm).

In the same manner, the effect of gel formation has to be verified for the product obtained from Stage 2. The CSD obtained for the second stage product is shown in Figure 35. It displays a bimodal curve with the first mode size near 250 μm and the second near 65 μm. This curve is in good agreement with expectations since the simulation predicts three main crystal types for the carbonated DST run: 1) sodium nitrate 2) sodium nitrite and 3) sodium carbonate monohydrate. From these facts it was hypothesized that the mode size at 250 μm corresponded to nitrate and nitrite crystals while the mode at 65 μm corresponded to mostly carbonate crystals.

*Species Distribution*. The sieved crystalline products were used to analyze the distribution of chemical species within different size ranges and also to determine the effect of gelation on the crystals. Figures 36 and 37 show PLM images of crystals from Stages 1 and 2 of Run 31.

The PLM images taken from the sieved crystals of Stage 1 are presented in Figure 36. The mode is composed of a mixture of sodium nitrate or sodium nitrite, but which cannot be determined from the image in Figure 36A. The photomicrographs clearly illustrate that the crystals have been affected by the gel formation; only the size and shape of the crystals provide any evidence as to their identity. Three other types of crystals also have been observed at different size ranges. Sodium carbonate monohydrate (Figure 36B) and what is believed to be

either a trisodium fluoride sulfate affected by gel formation or a sodium nitrate crystal affected by the gel (Figure 36C). Some needle shapes (sodium oxalate) were also present. The gel formation during filtration has apparently affected crystal structure, bringing the CSD into question.

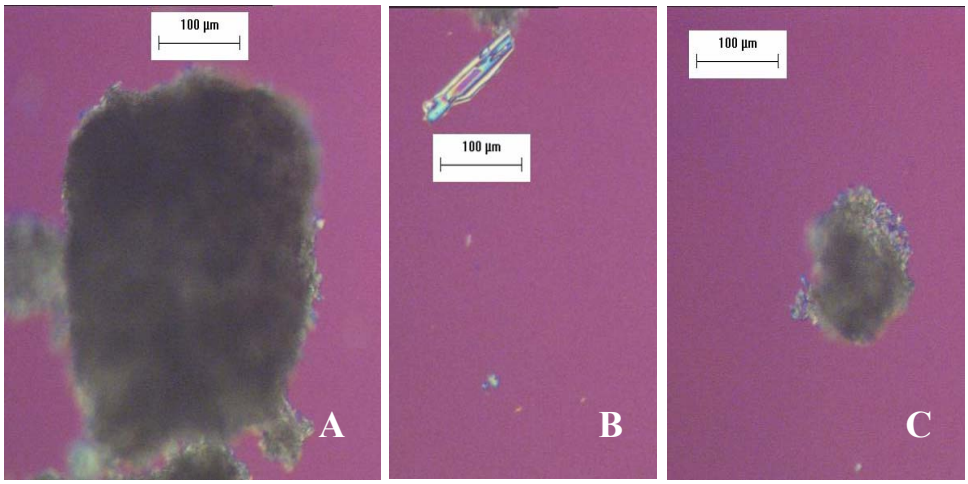


**Figure 36. PLM Images of Sieved Crystals from DST Feed Solution Run 31 Stage 1.**

The PLM images taken of the sieved product from Stage 2 are shown in Figure 37. These images confirm the expectations regarding the crystal types corresponding to each mode size. On the 53-µm sieve (corresponding to the first mode) sodium carbonate monohydrate crystals were observed almost exclusively. However, these crystals (Panel A) have been altered by the gel formed during the filtration process. Figure 37A displays an example of the oblong shape typical of sodium carbonate monohydrate. The crystal displays blue and yellow colors and a surface covered by an amorphous gel. At the second mode (212-µm sieve) the majority of the crystals appeared to have the shape of sodium nitrate with gel on the surface (Figure 37B). Some needle-shaped crystals were also observed on this sieve in minor quantities (Figure 37C). They have been identified as sodium phosphate based on (1) the knowledge of the species likely to

crystallize from the Hanford waste, (2) the size of the needle (close to 200 µm) and (3) the yellow color of the needle at the given orientation.

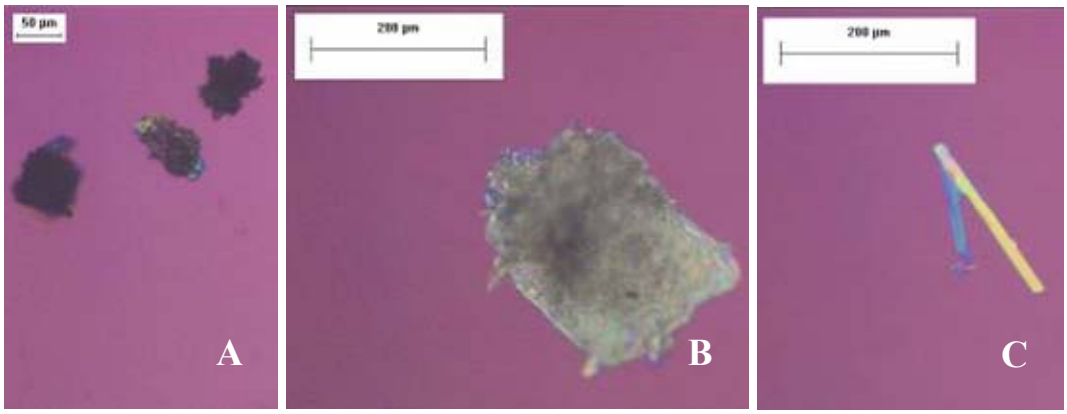


**Figure 37. PLM Images of Sieved Crystals from DST Feed Solution Run 31 Stage 2.**

### 5.1.4 Species Analyses and Balances

Figures 31 and 32 illustrate the accounting associated with the total mass entering and leaving Stage 1 and Stage 2 of Run 31. These have been used as the basis for balances on total mass that are illustrated in Figure 38 for Run 31, which is the Certification Run for DST Feed Solution. Table 7 shows the stream values, and it also identifies the amount of sodium nitrate, sodium hydroxide, and sodium carbonate that entered the system with the wash solution. (Recall that this solution was saturated with respect to sodium nitrate and sodium carbonate so as to reduce the dissolution of crystals in the filter cake. This was justified by recognizing that it more closely represented a continuous operation. Sodium hydroxide was added to the wash solution for the DST run to maintain alkaline conditions during the washing procedure.)

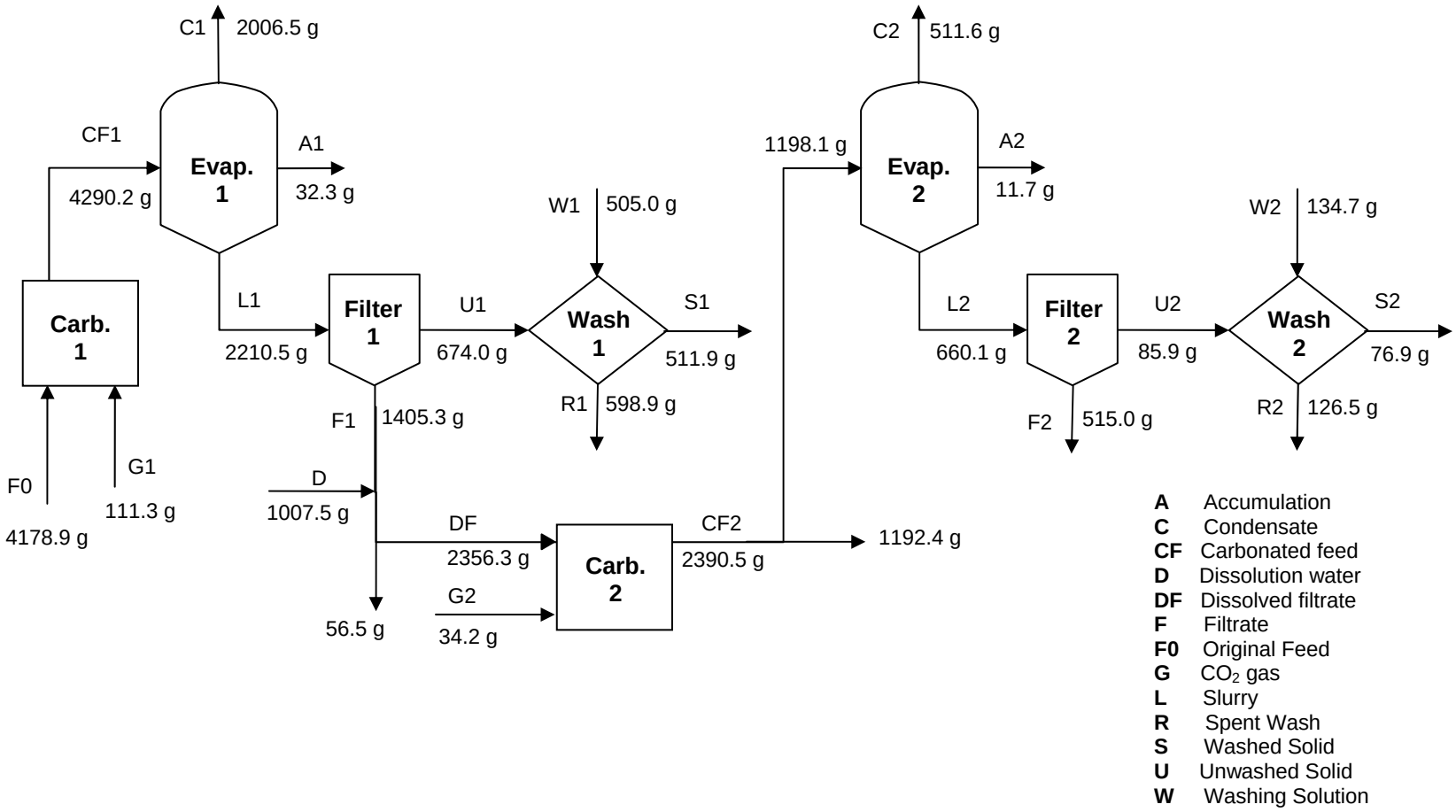


**Figure 38. Flowsheet for the Crystallization of DST Feed Solution Run 31.**

**Table 7. Overall Mass Balance of DST Feed Run 31.**

| Stage 1 | Input (g) | | Output (g) | | | | | Loss (g) |
|---|---|---|---|---|---|---|---|---|
| Species | Feed | Wash | Condensate | Washed Solids | Filtrate | Spent Wash | Accum. | |
| DST | 4178.9 | | | | | | | |
| $CO_2$ | 111.3 | | | | | | | |
| $H_2O$ | | 328.7 | 2006.5 | | | | | |
| $Na_2CO_3$ | | 27.9 | | | | | | |
| $NaNO_3$ | | 76.9 | | | | | | |
| NaOH | | 71.5 | | | | | | |
| Solution | | | | 511.9 | 1405.3 | 598.9 | 32.3 | |
| Total | 4290.2 | 505.0 | 2006.5 | 511.9 | 1405.3 | 598.9 | 32.3 | 240.3 |
| Combined | 4795.2 | | 4554.9 | | | | | 240.3 |
| | | | | | | % Loss | | 5.0% |
| | | | | | | Accounted loss (g) | | 140.1 |
| | | | | | | % Corrected Loss | | 2.1% |

| Stage 2 | Input (g) | | Output (g) | | | | | Loss (g) |
|---|---|---|---|---|---|---|---|---|
| Species | Feed | Wash | Condensate | Washed Solids | Filtrate | Spent Wash | Accum. | |
| Stg 1 Filtrate | 687.9 | | | | | | | |
| $CO_2$ | 17.1 | | | | | | | |
| $H_2O$ | 493.1 | 86.9 | 511.6 | | | | | |
| $Na_2CO_3$ | | 6.6 | | | | | | |
| $NaNO_3$ | | 21.3 | | | | | | |
| NaOH | | 19.9 | | | | | | |
| Solution | | | | 76.9 | 515.0 | 126.5 | 11.7 | |
| Total | 1198.1 | 134.7 | 511.6 | 76.9 | 515.0 | 126.5 | 11.7 | 91.2 |
| Combined | 1332.8 | | 1241.7 | | | | | 91.2 |
| | | | | | | % Loss | | 6.8% |
| | | | | | | Accounted loss (g) | | 51.1 |
| | | | | | | % Corrected Loss | | 3.0% |

The results of the balances on total mass show that 240.3 g were lost in Stage 1, but that 140.1 g could be accounted for using the methods described in Section 2.0. This means that the unaccounted loss was estimated to be 100.2 g; another way of saying this is that the balance on total mass was closed to within 2.1%. Addressing Stage 2, there was a loss of 91.2 g, of which 51.1 g were accounted for; in other words the total mass balance closed to within 3.0%.

Samples of each stream were obtained and sent to Galbraith Laboratories for chemical analyses (results of which are presented in Appendix E). The samples were of the feed solution, filtrate, spent wash, unwashed crystals, washed crystals, and accumulation. In addition, a sample was taken of the carbonated filtrate from Stage 1, which was used as the feed for Stage 2. All samples except for the final crystals were sent for analysis in liquid form in order to give a homogeneous sample. Results obtained from Galbraith were tabulated in a spreadsheet and the mass of each ionic species was calculated at each sample point in the process.

Table 8 gives inputs, outputs, and closures of mass balances around the entire process for each species. Details of the stage-wise species mass balances are given in Tables 9 and 10. For species analysis it was assumed that the total amount of filtrate from Stage 1 was used as feed for Stage 2. In reality, only a portion of the filtrate from Stage 1 was used as the feed for Stage 2, so the output streams from Stage 2 were scaled accordingly. It was also assumed that the relative amounts of each output stream in Stage 2 would remain constant when using the total filtrate from Stage 1.

DST Feed Solution Run 31 included two carbonation steps and dilution of the filtrate from Stage 1. In order to account for the second carbonation step in the overall species balances, the following chemical equation was used:

$$CO_2 + 2OH^- \rightarrow CO_3^{2-} + H_2O \quad (5\text{-}1)$$

The amount of $CO_2$ added to the solution was scaled to account for the total filtrate from the first stage. From the calculated moles of $CO_2$ added to the solution, the corresponding changes in moles (and mass) for the species $OH^-$, $CO_3^{2-}$, and $H_2O$ were estimated based on the above equation. The species mass balance for Stage 2 did not use these calculations for the input stream since a sample of the carbonated feed was taken directly.

**Table 8. Species Mass Balances for DST Feed Solution Run 31.**

| Species | Input (g) | Output (g) | Closure (%) |
|---|---|---|---|
| $Cs^+$ | 4.79E-02 | 3.97E-02 | 17.2 |
| $Na^+$ | 629.03 | 568.59 | 9.6 |
| $Al^{3+}$ | 86.69 | 75.45 | 13.0 |
| $CrO_4^{2-}$ | 1.32 | 1.16 | 12.1 |
| $F^-$ | 0.09 | 0.20 | -117.8 |
| $NO_2^-$ | 261.95 | 211.95 | 19.1 |
| $NO_3^-$ | 402.33 | 347.28 | 13.7 |
| $PO_4^{3-}$ | 2.16 | 1.82 | 15.8 |
| $SO_4^{2-}$ | 3.02 | 2.77 | 8.4 |
| $C_2O_4^{2-}$ | 1.05 | 1.08 | -3.1 |
| $CO_3^{2-}$ | 233.22 | 243.81 | -4.5 |
| $H_2O$ | 4334.99 | 4106.15 | 5.3 |
| $OH^-$ | 156.96 | 126.10 | 19.7 |

**Table 9. Species Mass Balances for DST Feed Solution Stage 1.**

| Stage 1 | Input (g) | | Output (g) | | | | | Closure |
|---|---|---|---|---|---|---|---|---|
| Species | Feed | Wash | Condensate | Filtrate | Spent Wash | Crystals | Accumulation | % |
| $Cs^{+}$ | 4.79E-02 | 0 | 0 | 3.79E-02 | 5.24E-03 | 1.45E-03 | 3.70E-04 | 6.1 |
| $Na^{+}$ | 514.07 | 74.01 | 0 | 295.77 | 99.22 | 164.05 | 7.21 | 3.7 |
| $Al^{3+}$ | 86.69 | 0 | 0 | 65.98 | 9.78 | 2.31 | 0.70 | 9.1 |
| $CrO_4^{2-}$ | 1.32 | 0 | 0 | 1.07 | 0.15 | 0.04 | 0.01 | 3.3 |
| $F^{-}$ | 0.091 | 0 | 0 | 0.018 | 0.009 | 0.164 | 0.004 | -112.9 |
| $NO_2^{-}$ | 261.95 | 0 | 0 | 193.54 | 27.94 | 7.83 | 2.01 | 11.7 |
| $NO_3^{-}$ | 314.48 | 56.09 | 0 | 201.52 | 95.41 | 32.16 | 2.49 | 10.5 |
| $PO_4^{3-}$ | 2.16 | 0 | 0 | 1.55 | 0.27 | 0.16 | 0.12 | 2.8 |
| $SO_4^{2-}$ | 3.02 | 0 | 0 | 0.76 | 0.58 | 1.43 | 0.12 | 4.4 |
| $C_2O_4^{2-}$ | 1.05 | 0 | 0 | 0.51 | 0.17 | 0.44 | 0.08 | -13.4 |
| $CO_3^{2-}$ | 162.06 | 15.81 | 0 | 3.54 | 5.95 | 168.89 | 5.91 | -3.6 |
| $H_2O$ | 2806.90 | 328.70 | 2006.53 | 538.63 | 324.48 | 120.38 | 12.71 | 4.2 |
| $OH^{-}$ | 136.36 | 30.39 | 0 | 102.38 | 34.94 | 14.04 | 0.95 | 8.7 |

**Table 10. Species Mass Balances for DST Feed Solution Stage 2.**

| Stage 2 | Input (g) | | Output (g) | | | | | Closure |
|---|---|---|---|---|---|---|---|---|
| Species | Carbonated Filtrate (Diluted) | Wash | Condensate | Filtrate | Spent Wash | Crystals | Accumulation | % |
| $Cs^{+}$ | 3.56E-02 | 0 | 0 | 3.04E-02 | 9.93E-04 | 8.62E-04 | 3.91E-04 | 8.2 |
| $Na^{+}$ | 294.65 | 40.95 | 0 | 203.78 | 39.73 | 49.50 | 5.11 | 11.2 |
| $Al^{3+}$ | 68.08 | 0 | 0 | 58.45 | 1.84 | 1.62 | 0.75 | 8.0 |
| $CrO_4^{2-}$ | 1.05 | 0 | 0 | 0.89 | 0.03 | 0.02 | 0.01 | 9.4 |
| $F^{-}$ | 0.02 | 0 | 0 | 0.007 | 0.001 | 0.013 | 0.001 | -24.8 |
| $NO_2^{-}$ | 189.46 | 0 | 0 | 161.51 | 5.73 | 4.77 | 2.16 | 8.1 |
| $NO_3^{-}$ | 203.61 | 31.76 | 0 | 174.15 | 31.64 | 9.13 | 2.29 | 7.7 |
| $PO_4^{3-}$ | 1.45 | 0 | 0 | 1.05 | 0.10 | 0.05 | 0.07 | 12.3 |
| $SO_4^{2-}$ | 0.76 | 0 | 0 | 0.42 | 0.10 | 0.05 | 0.07 | 16.1 |
| $C_2O_4^{2-}$ | 0.51 | 0 | 0 | 0.27 | 0.06 | 0.02 | 0.05 | 21.9 |
| $CO_3^{2-}$ | 69.85 | 7.60 | 0 | 4.83 | 5.90 | 49.00 | 3.34 | 18.6 |
| $H_2O$ | 1553.28 | 177.62 | 1045.13 | 391.87 | 158.22 | 37.59 | 9.24 | 5.1 |
| $OH^{-}$ | 65.03 | 17.27 | 0 | 54.88 | 15.09 | 5.42 | 0.79 | 7.4 |

### 5.1.5 Comparison to Minimum and Desired Targets

As described in Section 2.0, Stage 2 was operated using only a fraction of the total filtrate produced in Stage 1. In the calculations to evaluate the approach to the process criteria, the mass balances shown in Tables 8, 9, and 10 were scaled as if all of the filtrate had been used in the process. This is a standard approach for scaling up or scaling down process flowsheets.[4] Specifically, the sodium balance for Stage 2 sodium was scaled according to the amount of filtrate from Stage 1 that was used to feed Stage 2. It was also assumed that the sodium collected in the accumulation from each stage would be found as crystal mass in an ideal process. Results of these calculations are given in Table 11 and show that the sodium recovery was 43.9%, which falls short of the minimum target.

**Table 11. Sodium Balance and Recovery for DST Feed Solution Run 31.**

| Stream | Unit Value (g) | Totals (g) |
|---|---|---|
| **Input** | | **514.07** |
| **Crystals/Stage 1** | **164.05** | |
| **Accum/Stage 1** | **7.21** | |
| **Crystals/Stage 2** | **49.50** | |
| **Accum/Stage 2** | **5.11** | |
| **Output** | | **225.87** |
| **Recovery** | | **43.9%** |

The DF relating to cesium activity was calculated from the chemical analyses (performed by Galbraith Laboratories) of the washed crystals obtained from Stages 1 and 2 and also from the feed solution. Table 12 shows the analytical results for sodium and cesium and the calculated decontamination factors expected for dissolution of each of the filter cakes and for the combined

[4] R. M. Felder and R. W. Rousseau, *Elementary Principles of Chemical Processes*, 3rd Ed., John Wiley & Sons, Inc., New York, p. 94.

filter cakes. The calculations were based on the mass of cesium in each stream after dilution to 5 M sodium. As shown, the value for the combined solids exceeds the minimum requirement of 7.0 for the DST solution, but is well below the desired requirement of 292.

**Table 12. Compositions of Washed Crystals from DST Feed Solution Run 31 with Estimated Activities and Decontamination Factors.**

| | mass (g) | wt % Na | ppm Cs | Ci/L | DF |
|---|---|---|---|---|---|
| Carbonated Feed (1L) | 1331 | 11.8 | 11 | | |
| Stage 1 Crystals | 511.90 | 30.5 | 2.7 | 0.044 | 10.5 |
| Stage 2 Crystals | 157.19 | 29.3 | 5.1 | 0.087 | 5.4 |
| Combined Crystals | 669.09 | 30.22 | 3.3 | 0.054 | 8.6 |

The sulfate-to-sodium molar ratio in the filtrate streams from Stages 1 and 2 were calculated using the relative amounts of the two ions in the filtrate streams as determined by Galbraith Laboratories. The results given in Table 13 show that the combined filtrates from Run 31 exceed both the minimum requirement of 0.01 and the desired target of 0.0022 moles of sulfate ion per mole sodium ion.

**Table 13. Compositions of Filtrate Streams from DST Feed Solution Run 31 and Associated Sulfate-to-Sodium Molar Ratio.**

| | wt % Na | wt% SO4 | molar ratio sulfate:sodium |
|---|---|---|---|
| **Stage 1** | **21.05** | **0.054** | **0.0006** |
| **Stage 2** | **19.37** | **0.040** | **0.0005** |
| **Combined** | **20.33** | **0.048** | **0.00056** |

## 5.2 COMPARISON OF LAB RESULTS TO FLOWSHEET PREDICTIONS

Table 14 gives a comparison between the predicted and analyzed compositions of the final crystals for the DST Certification Run. The predicted values were calculated from the corresponding simulation file provided by COGEMA and the chemical analysis was performed by Galbraith Laboratories. Values in italics indicate that the exact chemical composition could not be determined due to sensitivity limitations of the analysis equipment.

Due to the fact that the DST simulation did not include final crystal compositions, the simulation values displayed in the table correspond to the crystals predicted in the slurry. As seen in the table, several cells contain zeroes. This is because the simulation divided the slurry up into solid and liquid streams, so the solid stream does not include the mother liquor adhering to the crystal surface.

**Table 14. Chemical Composition of Final Crystals.**

| | | $Cs^+$ | $Na^+$ | $Al^{3+}$ | $CrO_4^{2-}$ | $F^-$ | $NO_2^-$ | $NO_3^-$ | $PO_4^{3-}$ | $SO_4^{2-}$ | $C_2O_4^{2-}$ | $CO_3^{2-}$ | $H_2O$ | $OH^-$ |
|---|---|---|---|---|---|---|---|---|---|---|---|---|---|---|
| DST Stage 1 | Simulation | 0% | 34.4% | 0% | 0% | 0.05% | 15.9% | 12.6% | 0% | 0.24% | 0.17% | 28.1% | 8.4% | 0% |
| | Galbraith | 2.70E-06 | 30.50% | 0.43% | 0.01% | 0.03% | 1.46% | 5.98% | *0.03%* | 0.27% | 0.08% | 31.40% | 22.38% | 2.61% |
| DST Stage 2 | Simulation | 0% | 31.8% | 0% | 0% | 0.04% | 12.2% | 23.4% | 0% | 0.19% | 0% | 23.5% | 7.0% | 0% |
| | Galbraith | 5.10E-06 | 29.30% | 0.96% | 0.01% | 0.01% | 2.82% | 5.40% | 0.03% | *0.03%* | *0.01%* | 29.00% | 22.25% | 3.21% |

DST Simulation File – DST2SCC2.xls

One major difference between the predicted and actual values is the water content of the DST products. This likely arises from the gelation problems encountered during the filtration steps, which effectively trapped water in the product. The second main difference is the amount of carbonate in the crystal product. The amount of carbonate is supposed to be high, but the surprising point is that the percentage of carbonate is higher than that predicted by the simulation file. This is odd because the simulation shown here carbonated the original feed at a rate of 30 g of $CO_2$ per 1000 g DST, while the experiment only used 26 g of $CO_2$ per 1000 g DST feed. While the relative amounts of carbonate and water were higher than predicted, the amounts of nitrite and nitrate were significantly less than in the simulation file.

## 5.3 COMPARISON OF RESULTS TO PROCESS REQUIREMENTS

How the DST Certification Run was conducted and the details of the outcomes were provided above. Table 15 summarizes comparisons of the process criteria with experimentally determined (actual) values. There are two types of criteria to be met by the process: one type has to do with the exclusion of species (i.e., Cs) from the crystals produced while the other is related to the fractions of sodium and sulfate in the feed solutions that are removed in the crystalline product. In essence, the Cs is supposed to go with the filtrates from each stage, while the sodium and sulfate go with the crystals. Hence, the cesium requirement is based on crystal purity while the sodium and sulfate requirements are based on yield.

**Table 15. Comparison of Required and Desired Outcomes to Experimental Results.**

| DST Feed | Stage | Required | Actual | Desired |
|---|---|---|---|---|
| Cs Decon Factor | 1 | 7 | 10.5 | 292 |
| | 2 | 7 | 5.4 | 292 |
| | Total | 7 | 8.6 | 292 |
| Sodium Recovery | Total | 50% | 43.9% | 90% |
| Sulfate-to-Sodium | 1 | 0.01 | 0.0006 | 0.0022 |
| | 2 | 0.01 | 0.0005 | 0.0022 |
| | Total | 0.01 | 0.00056 | 0.0022 |

The mechanisms by which Cs could become part of the crystalline product include the formation of inclusions through overgrowth of mother liquor by the crystal surface, entrapment of mother liquor in either the irregularities of individual crystals or in the crystal cake, or lattice substitution. Because cesium has such a high solubility in the feed solutions, it is unlikely that it would be captured by lattice substitution, which leaves the possibility of inclusions and entrapment.

Inclusions typically are formed when crystal growth occurs at high supersaturations. In the DST Certification Run, attempts were made to control the supersaturation at which nucleation and growth occurred, but it is highly likely that some inclusions were formed. Should future work identify inclusions as a difficulty in batch operations, seeding could be used to do a better job of maintaining low supersaturation and good crystal growth. Moreover, it is important to add that the operation of a continuous crystallizer would undoubtedly maintain a significantly lower system supersaturation, and there should be less possibility of forming inclusions.

Entrapment of mother liquor in the irregularities of individual crystals or in the void spaces of multi-crystal agglomerates or cakes formed during filtration present problems quite different from inclusions. In principle, mother liquor can be flushed from crystal surfaces provided wash liquid flows through all void spaces. An excellent example of the effect of washing was provided in the experiments described in Appendix G. In that work, crystals produced from an SST Early Feed Solution were subjected to a series of washing steps and the color of the crystals was used as a measure of how well the washing had been performed. The yellowish color of the freshly produced crystals, which was attributed to the presence of chromium, was gradually eliminated each successive wash until after four washing stages the crystals were white. The washing done in this experiment involved mixing the crystals in a saturated wash liquid, so that there was no issue of flow through a filter cake, and filtering the resulting slurry.

It is unlikely that an operation like that described in the preceding paragraph would be possible in a full-scale unit, and that is why so much effort went into developing the washing-filtration apparatus described in detail in Appendix A. The objective of this device was to induce plug flow of the wash liquid through the filter cake. In addition, as with all instances of flow

through packed beds, an objective of the design was to provide uniform distribution of the wash liquid across the top of the filter cake.

There was no evidence of significant agglomeration of crystals during crystallization; both visual observations of the vessel contents and PLM images of crystal samples taken from the slurry were nearly free of agglomerates. Some agglomeration occurred during washing and filtration, as was noted in preparing samples for sieving and in some of the PLM images of sieved crystals. In any case, agglomeration does not seem to be a significant detriment to obtaining the desired crystal purity.

The formation of encrustations on the walls of the crystallizer was an issue in almost all of the crystallization runs performed as part of this research. It is related to agglomeration and is likely to present a future problem. This accumulation could only be removed by scraping it away from the surfaces to which it adhered, and it was not considered in reporting product purity.

Although substantial effort was made to reduce encrustations during crystallization (e.g., by reducing the evaporation rate and trying to wash the surfaces with feed solution), little success resulted. It is thought that part of the problem with encrustations is due to the way heat was supplied to the evaporating solution: namely, through the walls of the crystallizer. The salts in the system that exhibit reduced solubility at elevated temperature would be more likely to crystallize on the walls and there is a tendency to evaporate to dryness any solution that splashed onto regions of the wall that are not regularly irrigated. In continuous operations, the enhanced heat-transfer coefficients that result from forced circulation should reduce wall temperatures at the heat source and thereby reduce the formation of encrustations from both of these possible mechanisms.

As pointed out earlier, the crystal size distribution plays a very significant role in determining how easily solid-liquid separation occurs. It also greatly impacts washing and all other downstream operations. In the present work, attempts to produce crystals that were as large as possible were limited to reduced evaporation rates to minimize primary nucleation and good mixing to reduce possibilities of agglomeration and regions of excessive supersaturation. The use of seed crystals was explored briefly, as is described in Appendix F, but there was inadequate time to fully examine the impact of this processing step. Furthermore, as has been described elsewhere, seeding typically is useful only in batch operations, not in the continuous mode envisioned for the fully scaled version of the present process.

The sodium recovery and the sulfate-to-sodium ratio are directly related to the yield that can be obtained in the crystallization stages. The yield achieved is strongly influenced by the fraction of water that can be evaporated from a feed solution and the operating temperature of the crystallizer. In the extreme, for example, the feed could be evaporated to dryness and 100% of the sodium would be in the resulting solid mass, but none of the other process criteria would be satisfied. Another complicating factor is that some of the sodium salts (e.g., sodium nitrate) have solubilities that increase with increasing temperature, while others (e.g., burkeite) exhibit the opposite behavior. So, in large measure, the reason the desired targets on sodium recovery were not achieved is that insufficient water was evaporated from the feeds and/or the operating temperature was not at an optimal value.

The DST feed solutions present special problems in addressing the process criteria. Both purity and yield of crystals are greatly impacted by the tendency to form gels. The primary means of increasing the cesium decontamination concerns avoiding gelation that occurs during the filtration step due to the cooling of the slurry. Gelation also impacts the sodium recovery

from the DST Feed Solution, as evaporation must be stopped short if signs of gel formation arise. Improvement on these criteria requires better understanding and utilization of carbonation or a similar procedure to address the gelation issues.

# CHAPTER 6: CONCLUSIONS

The results obtained in performing the DST Certification Run and in the supporting activities leading up to this run provide guidance on important activities that should be performed in support of future research on FC from the Hanford wastes covered by this study. The purpose is to support the development of process flowsheets and the design of an operation that can be used to accelerate the treatment of Hanford waste.

As shown in Section 5.0, the required outcomes related to the purity of the crystals (i.e., Cs decontamination factor) and the sulfate-to-sodium ratio were satisfied in the DST Certification Run. However, the sodium recovery in the crystal product fell slightly short of that required. These results are quite promising, and it is believed that with further work on the crystallization protocols, FC can come significantly closer, if not achieve, the desired outcomes. Accordingly, the Georgia Tech team recommends that one of its avenues of additional research in Phase II address factors that would contribute to meeting the desired outcomes.

Increasing the cesium decontamination factor requires reducing inclusions in product crystals through better control of crystal growth. The two avenues to be investigated include control of evaporation rate and seeding. Figure 30 shows evaporation rates that were used in Stages 1 and 2 of the DST Feed Solution Certification Run. In both cases the evaporation rates were constant. The run times were determined by evaporating water from the feed solution until the specified condensate-to-feed ratio was attained. Even though this resulted in lengthy run times, we propose extending them even further; i.e. using even lower evaporation rates. By extending the run times, the quality of crystal growth should improve and the probability of inclusions forming should be minimized.

The introduction of seed crystals to a batch run is often done to control nucleation rates. This can have a very positive impact on the crystal size distribution, which makes the slurry easier to filter and wash. However, done properly, the introduction of a sufficient mass of seed crystals can result in control of crystal growth; in the extreme, there is no nucleation and the number of crystals in the product is the same as the number in the mass of seed crystals. In such instances, the supersaturation can be carefully controlled through the slow deposition of solutes onto the seed crystals. Implementation of this strategy in fractional crystallization is complicated by the formation of crystals of several species. In other words, rather than seeding with a single species, it may be necessary to seed with all species. We propose to explore such strategies by careful analysis of product crystals from fractional crystallization to try to determine if crystals of specific species contribute more significantly to impurity capture by inclusions, and if so, to develop seeding strategies involving those species. If all species contribute to inclusion formation, attention will be on seeding with a crystal population involving all species.

As described earlier, poor washing of impurities external to the crystal contributes to the contamination of crystal products, and the size distribution is the single most important characteristic of the crystal product determining washing effectiveness. Variables such as evaporation rate and the use of seeding that were described above also affect crystal size distribution. However, predicting their actual impact on size distribution is again complicated by the fact that several crystal species are produced in FC.

Each species is characterized by a crystal size distribution determined by species-specific nucleation and growth kinetics *and* flow characteristics in the crystallization system that are species-independent. For example, in the first stage of a process to which DST Feed is introduced, crystals of sodium carbonate monohydrate, sodium nitrite, sodium nitrate, and other

sodium salts are produced and exhibit unique crystal size distributions. It is also anticipated that implementation of fines- and course-removal functions can be used to tailor the overall crystal size distribution to one that results in a mixture of crystals that can be easily separated from the residual mother liquor.

Considerable effort has gone into developing models for batch, semi-batch, and continuous crystallizers that have the removal functions imposed by classified-fines or coarse-product removal systems, but none of the work with which we are familiar has addressed systems involving multiple solutes. Quantitative analysis, leading to rational scale up requires that such models be developed and tested on the systems of relevance. We recommend continuation of work that would facilitate such model development and testing.

We believe that doing so would contribute greatly to the improvement of protocols being used in this research and provide great insight in the design and operation of a scaled up, continuous operation. In fact, it could provide the direct link among Phase I, Phase II, pilot studies, and full-scale operations. Given the nucleation kinetics and the solubilities of the key species being crystallized, the problems can be formulated as follows for the batch and continuous systems:

1. As water is evaporated at a specific rate and feed is introduced to maintain a constant level in the batch crystallizer, what is the progression of the crystal size distribution as different species come out of solution with increasing amounts of water being evaporated?

2. Given a steady-state continuous operation where the solids fraction in the product and the operating temperature are specified, what is the crystal size distribution

produced? If various removal functions are implemented, what is the impact on crystal size distribution and the fates of individual species?

Despite the qualitative relationships described from work in Phase I, additional effort is needed to relate the effect of supersaturation on nucleation and growth kinetics of individual species. To do this precisely would take much greater effort than can be accommodated in the project schedule, but further refinement of the present knowledge is essential.

Sodium recovery is the second process objective that needs work. As pointed out earlier in this section, sodium recovery is tied directly to the fraction of water that is evaporated. In the batch and semi-batch operations, this means that higher yield requires increasing the solids content of the product slurry. This should be possible in the second stage of the batch operations, but further experimentation will be needed to confirm that prospect.

To obtain the required yield of sodium from DST solutions, the concentration of aluminum ions is increased during evaporation to levels that have been shown to lead to gel formation. This problem was recognized prior to the initiation of Phase I, and led to the treatment of DST solutions with carbon dioxide, which had adjustment of the hydroxide ion concentration in solution as its objective. With this treatment, solubility limits of gibbsite, $Al(OH)_3$, and sodium aluminate, $NaAlO_2$, could be adjusted and problems of gel formation mitigated. The promise of this step was verified in Phase I, but relatively little is known about the robustness of the operation and about means of recovery when gel limits have been exceeded and a gel has formed in the system.

Before proceeding with Phase II (radioactive) testing of DST waste, it is recommended that more effort be applied in simulant testing to map the variables that:

a. Enhance sodium yield;

b. Minimize problems with gel formation;

c. Quantify the relationship between the rates of addition and total amount of carbon dioxide added to the solution and sodium yield and gel formation; and,

d. Identify means to redissolve gel formed during either carbonation or evaporation.

# APPENDIX A

# CRYSTALLIZATION AND WASHING-FILTRATION APPARATUS

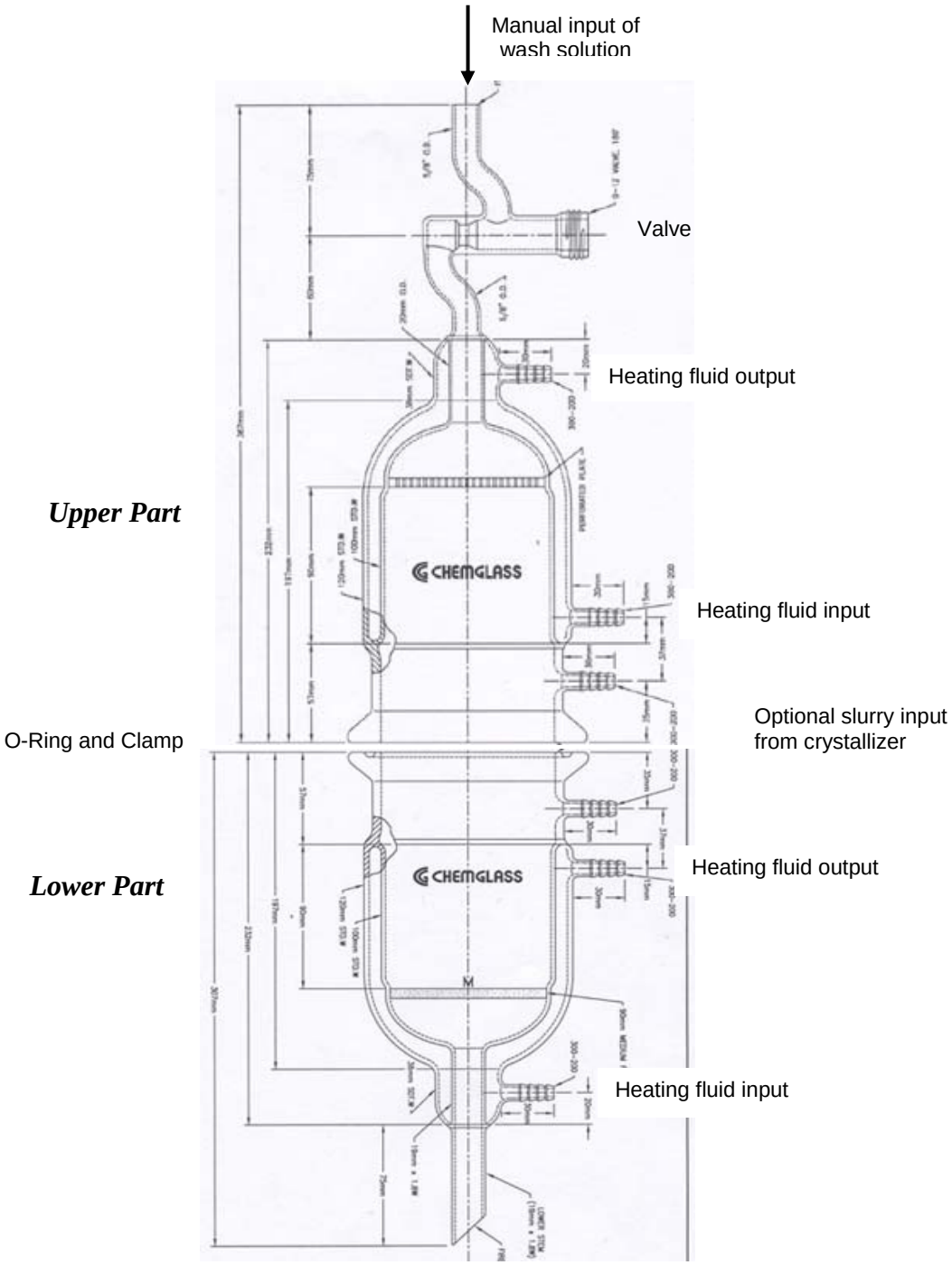


**Figure 39. Illustration of the Custom Designed Washing-Filtration Apparatus as per Chemglass Drawing.**

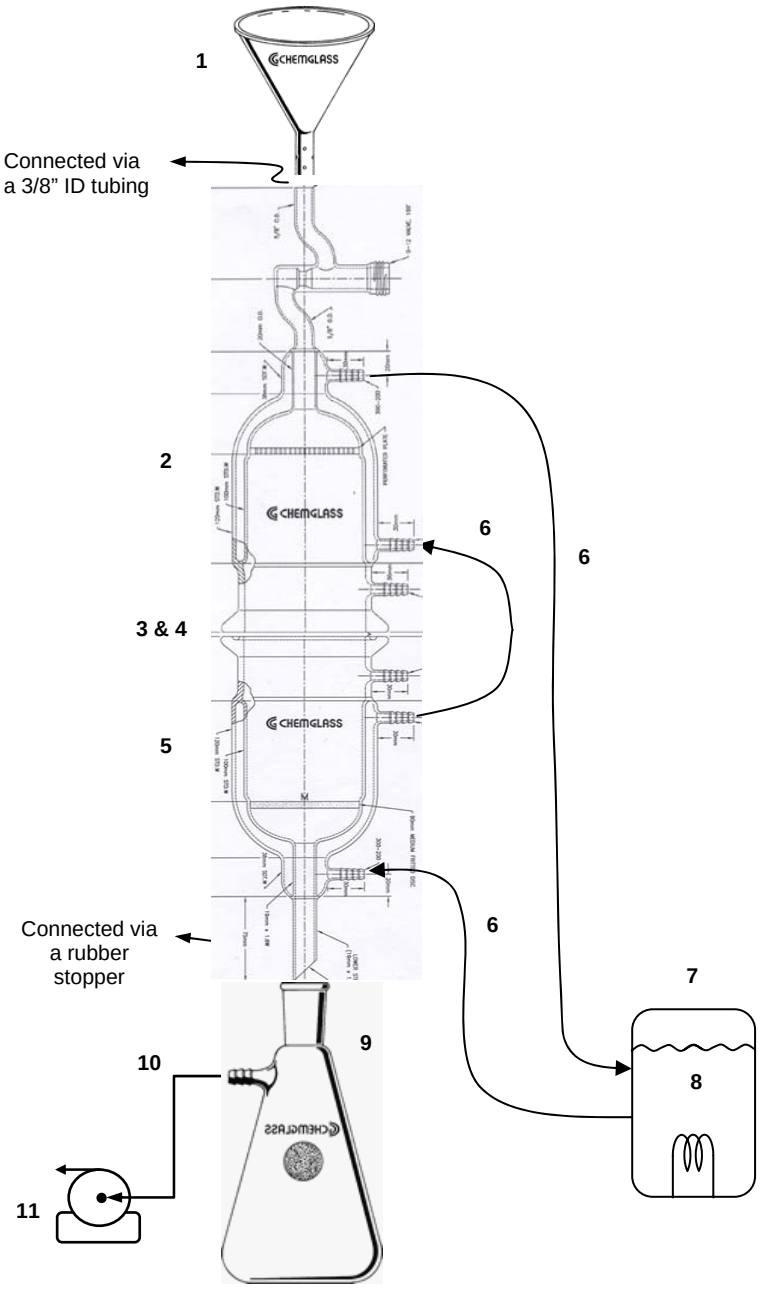


**Figure 40. Detailed Components of the Filtration and Washing Apparatus.**

**Table 16. Itemized List of Filtration/Washington Apparatus Components According to Figure 40.**

| Item | Description | Provider | Catalog No. | Notes |
|---|---|---|---|---|
| 1 | Funnel | GA Tech | | |
| 2 | Jacketed Buchner Funnel, 90mm Diameter Perforated Plate, 0-12mm Chem-Vac Valve on top, 100mm ID Schott Flat Flange on the bottom, 10mm OD Hose Connection@90° located between the Jacket and Flange per Chemglass Drawing | Chemglass | Special/GT-0507-011JS | Custom design |
| 3 | Clamp for Duran® reaction PER Quote# JS-16810 | Chemglass | CG-141-02 | |
| 4 | O-ring, Viton®, 100mm Flange | Chemglass | CG-147-21 | |
| 5 | Jacketed Buchner Funnel, 90mm Diameter Medium Frit, 100mm ID Schott Flat O-ring Flange on the top, 10mm OD Hose Connection@90° located between the Jacket and Flange, 3/4" OD Lower Drain, per Chemglass Drawing | Chemglass | Special/GT-0507-012JS | Custom design |
| 6 | Tygon Tubing, 1/2” OD x 3/8 ID, 10ft | GA Tech | | |
| 7 | VWR Heating bath 13l programmable 1157P | VWR | 13271-106 | |
| 8 | Heating fluid DC 200 5 cs | Ashland, GA | 3311089 600 | |
| 9 | Vacuum Filtration flask, 1000 mL | GA Tech | | |
| 10 | Vacuum tubing, 5/16" ID | Fisher | 14-175D | |
| 11 | Dry pressure/vacuum pump, Welch | Fisher | 01-051-1C | |

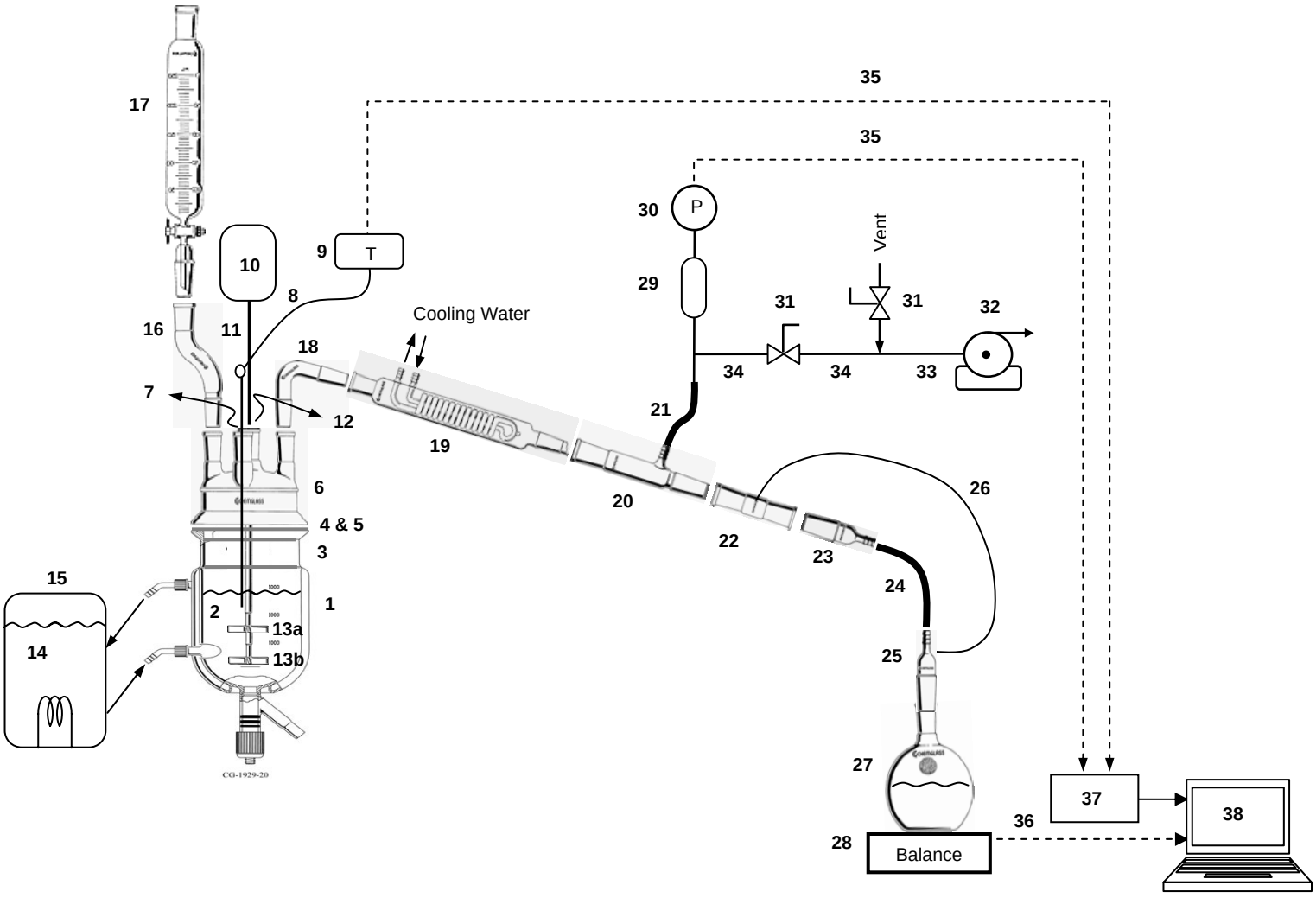


**Figure 41. Detailed Crystallizer Components.**

**Table 17. Itemized List of Crystallizer Components According to Figure 41.**

| Item | Description | Provider | Catalog No. | Notes |
|---|---|---|---|---|
| 1 | Jacketed Reaction Vessel, 1-Liter | Chemglass | CG-1929-14 | |
| | Jacketed Reaction Vessel, 300 mL | Chemglass | CG-1929-10 | |
| 2 | Baffles | GA Tech | | Home made |
| 3 | Clamp, 100mm | Chemglass | CG-141-02 | |
| 4 | Viton O-Ring, 100mm | Chemglass | CG-147-21 | |
| 5 | Support clamp, 100 mm | Chemglass | CG-1947-01 | |
| 6 | Reaction Vessel Lid, 4-necks, all 24/40 joints | Chemglass | CG-1941-01 | |
| 7 | Thermocouple, Hastalloy C-276, Type “T”, 1/8”, 12” long | Chemglass | CG-3498-302 | |
| 8 | Thermocouple Adapter, 24/40, 1/8" | Chemglass | CG-1042-E-01 | |
| 9 | Analog Temperature Controller/Display | Omega | CNi3253 | |
| 10 | Stirrer motor, IKA Model RW 16 | Fisher | 14-260-31 | |
| 11 | Stirrer Shaft, 555 mm | Chemglass | CG-2075-B-03 | |
| 12 | Stirrer Bearing, Chemvac™, Teflon®, 24/40, 10mm | Chemglass | CG-2077-G-01 | |
| 13a | Agitator, TFE, 10 mm Stir Shaft, 4 Blades, 45°, 75 mm Diameter | Chemglass | CG-2091-02 | |
| 13b | Agitator, TFE, 10 mm Stir Shaft, 4 Blades, 45°, 50 mm Diameter | Chemglass | CG-2091-01 | |
| 14 | Heating fluid DC 200 5 cs | Ashland, GA | 3311089 600 | |
| 15 | VWR Heating bath 13l programmable 1157P | VWR | 13271-106 | |
| 16 | Offset Adapter, 24/40 joint size | Chemglass | CG-1033-01 | |
| 17 | 250 mL Graduated separatory funnel, 2mm Teflon stopcock, 24/40 joint size | Chemglass | CG-1734-03 | |
| 18 | Adapter, Distillation, 75°, 24/40 | Chemglass | CG-1010-01 | |
| 19 | Reflux Condenser, 175mm Coil Length, 24/40 | Chemglass | CG-1213-L-21 | |
| 20 | Inlet adapter, straight, 24/20 joint, hose connection | Chemglass | CG-1062-01 | |
| 21 | TYGON Vacuum Tubing, 3/8"ID x 7/8"OD | Cole-Parmer | EW-06413-30 | |
| 22 | Adapter, 24/40 Outer Jt. to 24/40 Outer Jt. with a ¼”-28 Thread sealed in between the Jts., supplied complete with ¼”-28 Tefzel Union | Chemglass | GT-0505-061JS | Custom designed |
| 23 | Inner adapter, 24/40 Inner Joint, 86mm Height | Chemglass | CG-1012-01 | |
| 24 | Nalgen 980 Braided Clear PVC Tubing, 1/4" ID | Fisher | 14-169-10A | |
| 25 | Inlet Adapter, Top Hose Connection, Lower 24/40 Inner Jt. with a ¼”-28 Thread sealed in between the Jts., supplied complete with ¼”-28 Tefzel Union | Chemglass | GT-0505-062JS | Custom designed |
| 26 | Teflon Tubing, .062” ID x .125” OD, 10 ft. | Chemglass | CG-1164-02 | |

| Item | Description | Provider | Catalog No. | Notes |
|---|---|---|---|---|
| 27 | Flat Bottom Flask, 24/40, 1000 mL | Chemglass | CG-1500-07 | |
| 28 | Balance PB1502-S, Mettler Toledo | VWR | 11274-918 | |
| 29a | Pressure Transducer, 0-50 psia, Current Output) | Omega | PX305-050AI | |
| 29b | Snubber | Swagelok | SS-4-SA-EA | |
| 30 | Process Meter and Controller | Omega | DP25B-E | |
| 31 | Stainless 1-Piece Ball Valve, 1/4 in. Tube Fitting | Swagelok | SS-42S4 | |
| 32a | Two-stage Welch Vacuum Pump | Fisher | 01-129-4 | |
| 32b | Regulating Valve for Welch Pump | Fisher | NC9186594 | |
| 33 | PTFE Tubing,1/8" ID x 1/4" OD | Cole-Parmer | EW-06605-13 | |
| 34 | 316/316L Seamless Stainless Steel Tubing | Swagelok | SS-T4-S-035 | |
| 35 | Teflon Coated Cable, 10 ft | Omega | TECT10-11 | |
| 36 | RS-232 Serial Port | Measurement Computing | PCI-COM232/4-9 | |
| 37 | USB Based Data Acquisition Module | Measurement Computing | PMD-1208FS | |
| 38 | LabView software on a PC | | | |

# APPENDIX B

# OPTICAL SETUP AND ILLUMINATION ADJUSTMENT FOR THE PLM

## B.1 OPTICAL SETUP AND ILLUMINATION ADJUSTMENT FOR THE PLM

This procedure is supplementary to the description of the use of the PLM given in Section 2.0.

1. Turn on the illuminator and place the slide on the microscope stage (11) and fix it with the clamp. Slide out the analyzer (16) and compensator (21 placed in 14) plates from the light path then rotate the 10X objectives into position for focus.

2. Move the substage condenser up to its top position using the substage focusing control (7). Check to make sure that both the field iris (3a) and the aperture iris (3b) are fully open.

3. Focus down on the specimen slide (9) without bombing the objective into the slide until details can be seen in the eyepiece (18). Adjust the light brightness using the intensity control knob (6).

4. Adjust the distance between the two binocular eyepieces (18a and 18b) to fit the observer's eyes.

5. Fine focus (9b) to get a sharp image in the right eyepiece (18b) using your right eye.

6. Using your left eye, adjust the diopter adjustment collar on the left eyepiece (18a) (not the fine focus) to get the sharpest image.

7. Now turn the field iris adjustment ring (3a) until the field iris is seen.

8. Raise or lower the substage condenser (7) to focus the field iris sharp in the plane of the specimen. Then open out the field iris until it is just outside the field of view.

9. Remove one of the eyepieces (18) and reduce the intensity of the disc of light coming from the back of objective to about 75% using the aperture iris (3b).

10. Similar adjustments should be repeated for each objective.

* All numbers in parenthesis correspond to element numbers appearing in Figure 14.

## B.2 PLM OBJECTIVE CENTERING PROCEDURE

This procedure is supplementary to the description of the use of the PLM given in Section 2.0.

The objectives should be precisely seated in the optical axis. If it is even lightly off the axis the specimen image will stray from the center of view upon rotation of the stage. If this happens then the objective needs centering using two hexagon keys supplied with microscope as follows:

1. Remove the analyzer and compensator plates from the light path and swing in the 10X objective which is mounted in the non-centerable opening. All other objectives are mounted in floating centerable nosepiece holes.

2. Focus down on the specimen and memorize the pinpoint appearing on the eyepiece cross-line center (18b).

3. Turn the nosepiece (13) and bring the higher power objective to position and focus then see if the memorized specimen pinpoint is located at the cross mark. If not, insert the two centering screws into the key holes on the nosepiece ring above the objective and turn to move the pinpoint to the cross point.

4. Repeat the same procedure for the remaining objectives.

All numbers in parenthesis correspond to element numbers appearing in Figure 14.

## B.3 OBJECTIVE SCALE CALIBRATION

This procedure is supplementary to the description of the use of the PLM given in Section 2.0.

1. Turn on the illuminator and place the standard micrometer slide on the stage (11). Slide out the analyzer (16) and rotate desired objective, e.g., 10X, into position for focus. Turn on the Digital camera and start the Image-Pro Plus software and the live preview.

2. Focus down on the micrometer slide (9) and adjust the light intensity (6) until the graduated micro-ruler appears clearly on the live preview. Record the image of the micro-ruler by pressing "Snap."

3. On the Image-Pro Plus main menu, select *Measure* → *Calibration* → *Spatial* sequence where the Spatial Calibration window is displays. This window is linked to the active image of interest. Press "New" to create a new set of calibration value or to edit current ones. Edit the name to desired Objective power value, e.g., 10X, and then select the desired unit from the *Unit* list, preferably microns. This will be the unit of measurement that will appear on the graphs. On the "Pixels/Unit" group box press the "Image" button, where a scaling dialog box opens, and draw a straight horizontal line on the recorded micro-slide reference image between two grids of known length, e.g., 25 μm. Then write this value in the scaling dialog box and press OK to close the box and return the Spatial Calibration menu. Keep other values un-changed and press OK.

4. Repeat steps 1-3 for all other objectives to calibrate them.

All numbers in parenthesis correspond to element numbers appearing in Figure 14.

# APPENDIX C

# CONDENSATE-TO-FEED RATIO CALCULATIONS

## C.1 CONDENSATE-TO-FEED RATIO

Each certification run followed the corresponding simulation file provided by COGEMA (shown in parenthesis in the table) and the endpoint for the operation of each stage was determined by the amount of condensate collected. Table C1 gives the target condensate-to-feed ratios along with the actual experimental results. Since the laboratory experiments involved adding dilution water to the filtrate from the first stage, the target ratios had to be adjusted for the second stage of each run. The feed to the second stage of each run was a portion of the diluted filtrate from the first stage. An example of the adjusted target ratio calculations is given below.

Example calculation of the revised condensate-to-feed ratio for the DST Feed Solution Certification Run:

$$AdjustedRatio = \frac{(Filtrate \times OldRatio + DilutionWater)}{(Filtrate + DilutionWater)} \tag{C-1}$$

$$AdjustedRatio = \frac{(1405.31 \times 0.200 + 1007.45)}{(1405.31 + 1007.45)} = 0.534 \tag{C-2}$$

**Table 18. Condensate-to-Feed Ratio Calculations.**

| Experimental Stage | Experimental Value | DST (DST2SCC2.xls) | |
|---|---|---|---|
| | | **Simulation** | **Experimental** |
| Stage 1 | Feed (g) | 1030 | 4290.2 |
| | Condensate (g) | 501.9 | 2006.53 |
| | Condensate-to-Feed Ratio | **0.487** | **0.468** |
| | Filtrate from Stage 1 (g) | 343.82 | 1405.31 |
| | Dilution water to filtrate (g) | | 1007.45 |
| Stage 2 | Feed (g) | 343.82 | 1198.14 |
| | Condensate (g) | 68.8 | 511.57 |
| | Adjusted Target Ratio | | **0.534** |
| | Condensate-to-Feed Ratio | 0.200 | **0.427** |

## C.2 SAMPLE IDENTIFICATION FOR THE DST CERTIFICATION RUN

The following tables give the sampling information necessary to accurately calculate the species balances. Each table identifies the samples taken and gives the amounts of pure sample and water added to each sample container. As shown in the tables, the only samples sent in solid form were the final crystals from each stage.

**Table 19. Samples Taken from DST Certification Run, Stage 1.**

| Code | Name | Pure sample | Water added | Total mass | State |
|---|---|---|---|---|---|
| DST5-ST1-1 | filtrate | 32.88 | 23.59 | 56.47 | L |
| DST5-ST1-2 | spent wash | 103.45 | 19.64 | 123.09 | L |
| DST5-ST1-3 | final crystals | 15.22 | 0 | 15.22 | S |
| DST5-ST1-4 | accumulation | 8.41 | 93.69 | 102.1 | L |
| DST5-ST1-5 | unwashed solids | 10.82 | 94.64 | 105.46 | L |
| DST5-ST1-6 | carbonated feed | 67.07 | 0 | 67.07 | L |

**Table 20. Samples Taken from DST Certification Run, Stage 2.**

| Code | Name | Pure sample | Water added | Total mass | State |
|---|---|---|---|---|---|
| DST5-ST2-0 | carbonated filtrate | 97.72 | 0 | 97.72 | L |
| DST5-ST2-1 | filtrate | 96.06 | 57.49 | 153.55 | L |
| DST5-ST2-2 | spent wash | 110.30 | 19.93 | 130.23 | L |
| DST5-ST2-3 | final crystals | 9.01 | 0 | 9.01 | S |
| DST5-ST2-4 | unwashed solids | 2.93 | 29.92 | 32.85 | L |
| DST5-ST2-5 | accumulation | 5.86 | 50.18 | 56.04 | L |

## C.3 TEMPERATURE AND PRESSURE PROFILES FOR THE DST CERTIFICATION RUN

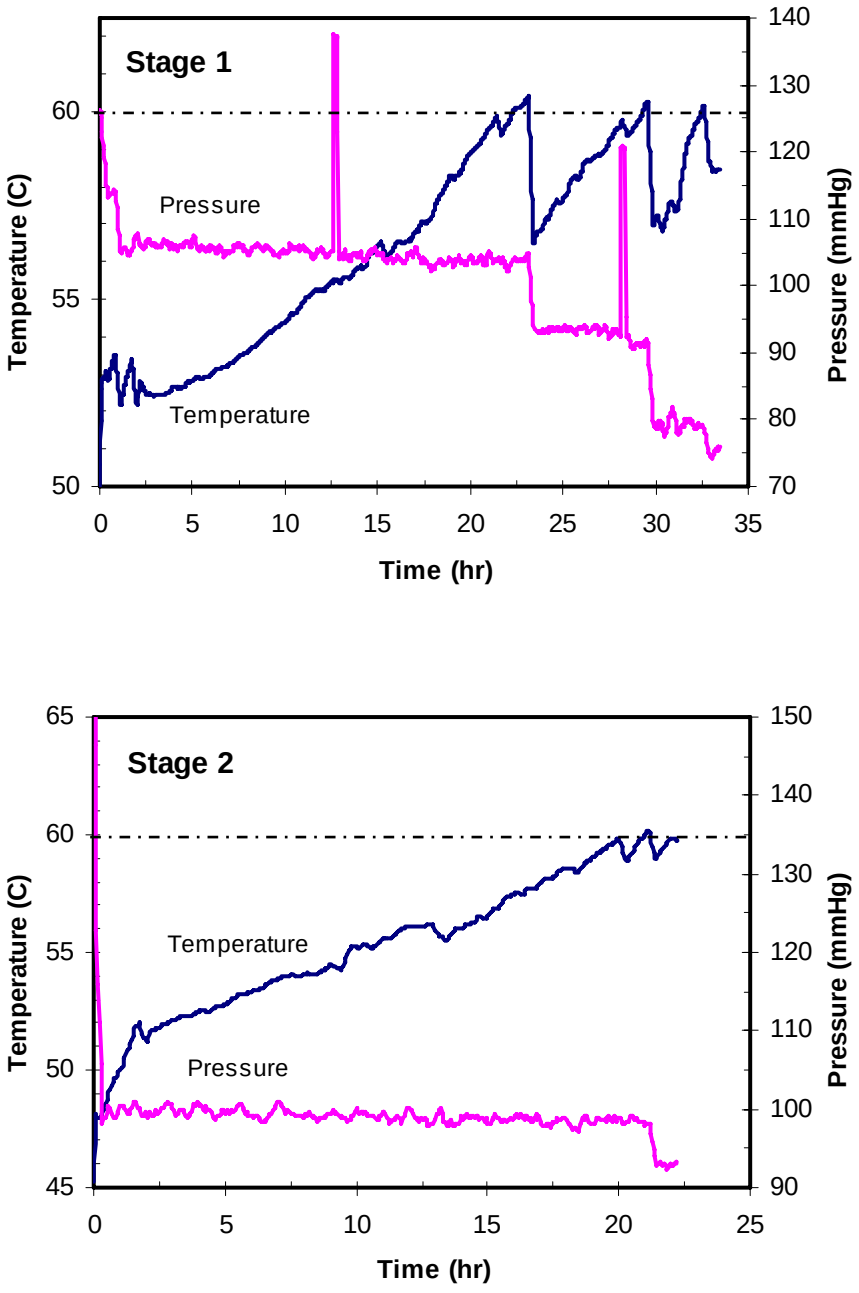


**Figure 42. Temperature and Pressure Profiles for the DST Feed Solution Certification Run. Dotted Lines Represent Target Temperatures.**

# APPENDIX D

# CRYSTALLIZATION RUNS AND MASS BALANCES

**Table 21. List of Crystallization Runs Performed.**

| Run # | Stages | Date | Solution | Comments |
|---|---|---|---|---|
| 1 | 1 | 3/24/2005 | NaNO3 | |
| 2 | 1 | 3/30/2005 | burkeite | |
| 3 | 1 | 4/5/2005 | NaNO3 | |
| 4 | 1 | 4/7/2005 | NaNO3 | |
| 5 | 1 | 4/12/2005 | burkeite | |
| 6 | 1 | 4/15/2005 | NaNO3 | |
| 7 | 1 | 4/22/2005 | NaNO3 | |
| 8 | 1 | 4/28/2005 | 3-salt | |
| 9 | 1 | 5/2/2005 | 3-salt | |
| 10 | 1 | 5/6/2005 | NaNO3 | |
| 11 | 1 | 5/11/2005 | NaNO3, CsNO3, NaOH | Used Cesium as a tracer |
| 12 | 1 | 5/12/2005 | 3-salt | try two stage experiment |
| | 2 | 5/13/2005 | 3-salt | |
| 13 | 1 | 5/17/2005 | Early Feed | initial examination of simulant |
| | 2 | 5/19/2005 | Early Feed | Sent samples for analysis |
| 14 | 1 | 5/24/2005 | 3-salt | |
| | 2 | 5/26/2005 | | |
| 15 | | 6/20/2005 | 3-salt | |
| 16 | 1 | 6/6/2005 | DST Feed | DST practice run |
| | 2 | 6/7/2005 | DST Feed | initial examination of simulant |
| 17 | 1 | 6/14/2005 | 3-salt | seeded with old burkeite run |
| 18 | 1 | 6/15/2005 | 3-salt | seeded with old burkeite run |
| 19 | 1 | 6/16/2005 | burkeite | try to grow new seeds |
| 20 | 1 | 6/21/2005 | 3-salt | use spray nozzle for tank washing |
| 21 | 1 | 6/22/2005 | 3-salt | semi-batch study |
| 22 | 1 | 6/27/2005 | Late Feed | get used to late feed simulant |
| | 2 | 6/28/2005 | Late Feed | |
| 23 | 1 | 7/1/2005 | 3-salt | constant level in 600mL, "continuous" feed |
| 24 | 1 | 7/8/2005 | Burkeite in crystallizer | grow seeds |
| 25 | 1 | 7/21/2005 | Late Feed #2 | try constant level cert. run |
| | 2 | 7/23/05 | Late Feed | |
| 26 | 1 | 7/26/05 | Early Feed | Early Feed certification run |
| | 2 | 7/28/05 | Early Feed | |
| 27 | 1 | 8/1/2005 | Late Feed #3 | Late Feed certification run |

| Run # | Stages | Date | Solution | Comments |
|---|---|---|---|---|
| 27 | 2 | 8/4/2005 | Late Feed | Slowed evaporation rate for both stages |
| | 2a | 8/11/2005 | Late Feed | |
| 28 | 1 | 8/7/2005 | DST Practice | carbonation on first stage |
| | 2 | 8/15/05 | | batch experiment |
| 29 | 1 | 8/17/2005 | DST Practice | carbonation on both stages |
| | 2 | 8/17/05 | | batch experiment |
| 30 | 1 | 8/23/05 | DST | cert. run trial |
| | 2 | 8/25/05 | | Gelling problems |
| 31 | 1 | 8/28/05 | DST | certification run |
| | 2 | 8/31/05 | | |

**Run 16 Stage 1**

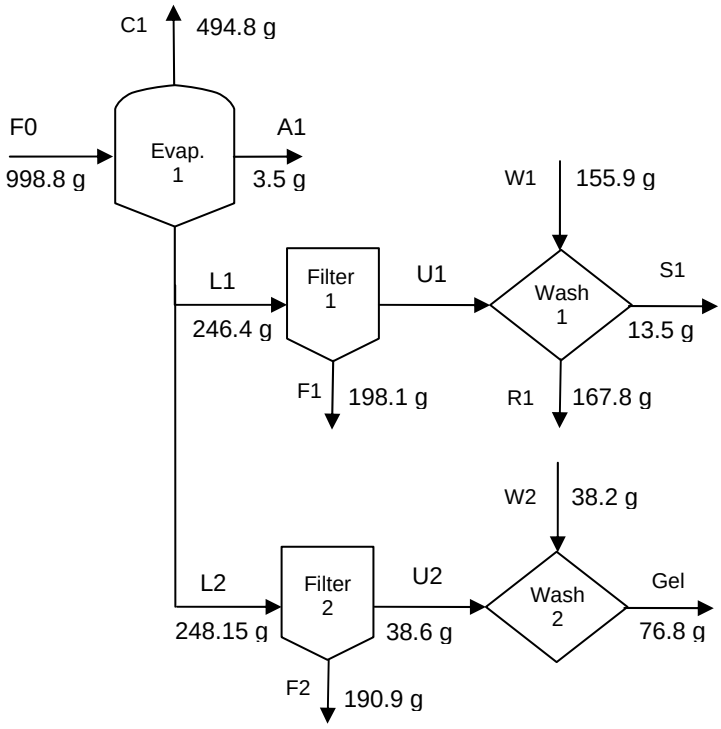


**A** Accumulation
**F** Filtrate
**F0** Feed
**L** Slurry
**R** Spent Wash
**S** Washed Solid
**U** Unwashed Solid
**W** Washing Solution

Mass Balance of Run 16 Stage 1

| | Input (g) | | Output (g) | | | | | | Loss (g) |
|---|---|---|---|---|---|---|---|---|---|
| **Species** | **Feed** | **Wash** | **Cond** | **Washed Solids** | **Gel Product** | **Filtrate** | **Spent Wash** | **Accum (g)** | |
| **$H_2O$** | | 82.3 | 494.8 | | | | | | |
| **DST Feed** | 998.8 | | | | | | | | |
| **$NaNO_3$** | | 90.0 | | | | | | | |
| **$Na_2CO_3$** | | 21.8 | | | | | | | |
| **Solution** | | | | 13.5 | 76.8 | 389.1 | | 3.5 | |
| **Total** | 998.8 | 194.1 | 494.8 | 13.5 | 76.8 | 389.1 | 167.8 | 3.5 | |
| **Combined** | 1192.9 | | 1145.4 | | | | | | 47.5 |
| | | | | | | | | | 4.0% |

| Source | Loss (g) |
|---|---|
| Filtration paper 1 | 2.44 |
| Filtration paper 2 | 2.54 |
| Slurry beaker 1 | 3.63 |
| Slurry beaker 2 | 1.28 |
| Microscope sample | 2.61 |
| **Total** | **12.5** |

We accounted for 12.5 grams of loss in transfers between beakers and filter paper accumulation; this leaves 2.9% unaccounted for.

**Figure 43. Flowsheet and Mass Balance for DST Practice Run 16, Stage 1.**

**Run 16 Stage 2**

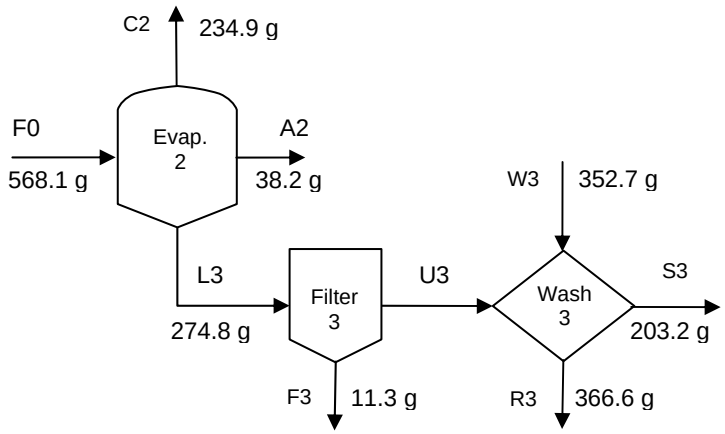


**A** Accumulation
**F** Filtrate
**F0** Feed
**L** Slurry
**R** Rinseate
**S** Washed Solid
**U** Unwashed Solid
**W** Washing Solution

Mass Balance of Run 16 Stage 2

| | Input (g) | | Output (g) | | | | | Loss (g) |
|---|---|---|---|---|---|---|---|---|
| **Species** | **Feed** | **Wash** | **Cond** | **Washed Solids** | **Filtrate** | **Spent Wash** | **Accum** | |
| **$H_2O$** | 179.0 | | 234.9 | | | | | |
| **$NaNO_3$** | | | | | | | | |
| **$Na_2CO_3$** | | | | | | | | |
| **Solution** | 389.1 | 352.7 | | 203.2 | 11.3 | 366.5 | 38.2 | |
| **Total** | 568.1 | 352.7 | 234.9 | 203.2 | 11.3 | 366.5 | 38.2 | |
| **Combined** | 920.8 | | 854.0 | | | | | 66.8 |
| | | | | | | | | 7.3% |

**Figure 44. Flowsheet and Mass Balance for DST Practice Run 16, Stage 2.**

**Run 28 Stage 1**

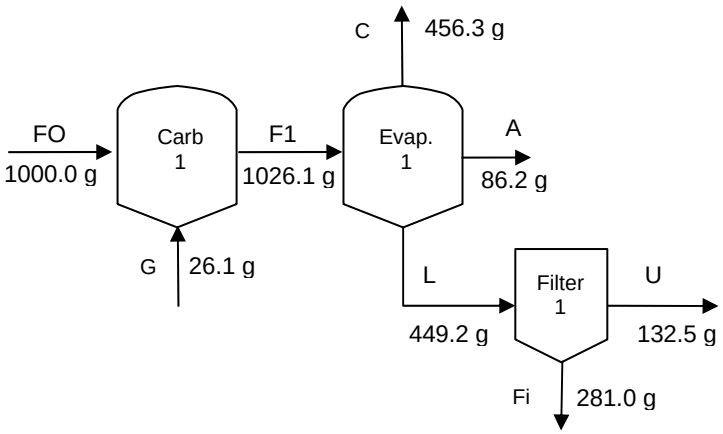


**A** Accumulation
**C** Condensate
**Fi** Filtrate
**F0** Feed
**F1** Carbonated Feed
**G** Gas Addition
**L** Slurry
**U** Unwashed Solid

**Mass Balance for Stage 1**

| | Input (g) | Output (g) | | | Accum (g) | Loss (g) |
|---|---|---|---|---|---|---|
| **Species** | **Feed** | **Cond** | **Unwashed Solids** | **Filtrate** | **Solids** | |
| **DST** | 1000.0 | | | | | |
| **$H_2O$** | | 456.3 | | | | |
| **$CO_2$** | 26.1 | | | | | |
| **Solution** | | | 132.5 | 281.0 | 86.2 | |
| **Total** | 1026.1 | 456.3 | 132.5 | 281.0 | 86.2 | 70.1 |
| **Combined** | 1026.1 | 956.0 | | | | 70.1 |
| | | | | | | 6.8% |

**Figure 45. Flowsheet and Mass Balance for DST Practice Run 28, Stage 1.**

**Run 28 Stage 2**

**A** Accumulation
**C** Condensate
**Fi** Filtrate
**F0** Feed
**R** Rinseate
**S** Washed Solid
**U** Unwashed Solid
**W** Washing Solution

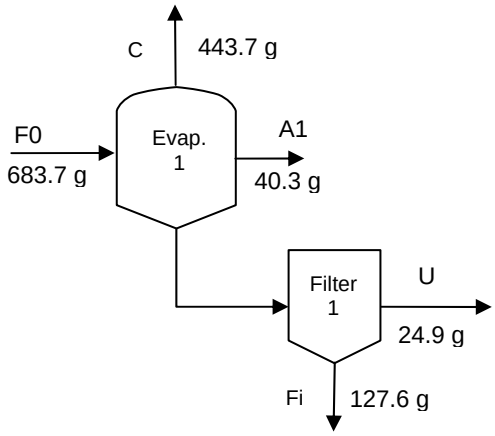


**Mass Balance for Stage 2**

| | Input (g) | Output (g) | | | Accum (g) | Loss (g) |
|---|---|---|---|---|---|---|
| **Species** | **Feed** | **Cond** | **Unwashed Solids** | **Filtrate** | **Solids** | |
| **Stage 1 Filtrate** | 281.0 | | | | | |
| **$H_2O$** | 402.7 | 443.7 | | | | |
| **Solution** | | | 24.9 | 127.6 | 40.3 | |
| **Total** | 683.7 | 443.7 | 24.9 | 127.6 | 40.3 | 47.3 |
| **Combined** | 683.7 | 636.4 | | | | 47.3 |
| | | | | | | 6.9% |

**Figure 46. Flowsheet and Mass Balance for DST Practice Run 28, Stage 2.**

**Run 29 Stage 1**

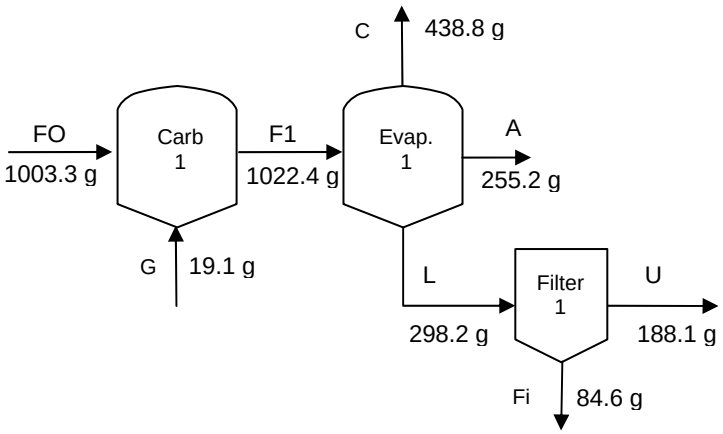


**A** Accumulation
**C** Condensate
**Fi** Filtrate
**F0** Feed
**F1** Carbonated Feed
**G** Gas Addition
**L** Slurry
**U** Unwashed Solid

**Mass Balance for Stage 1**

| | Input (g) | Output (g) | | | Accum (g) | Loss (g) |
|---|---|---|---|---|---|---|
| **Species** | **Feed** | **Cond** | **Unwashed Solids** | **Filtrate** | **Solids** | |
| **DST** | 1003.3 | | | | | |
| **$H_2O$** | | 438.8 | | | | |
| **$CO_2$** | 19.1 | | | | | |
| **Solution** | | | 188.1 | 84.6 | 255.2 | |
| **Total** | 1022.4 | 438.8 | 188.1 | 84.6 | 255.2 | 55.8 |
| **Combined** | 1022.4 | 966.6 | | | | 55.8 |
| | | | | | | 5.5% |

**Figure 47. Flowsheet and Mass Balance for DST Practice Run 29, Stage 1.**

**Run 29 Stage 2**

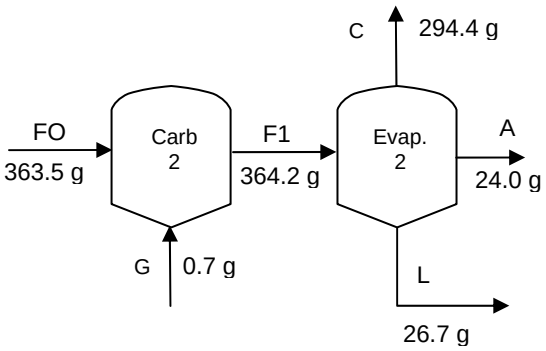


**A** Accumulation
**C** Condensate
**Fi** Filtrate
**F0** Feed
**F1** Carbonated Feed
**G** Gas Addition
**L** Slurry
**U** Unwashed Solid

**Mass Balance for Stage 2**

| | Input (g) | Output (g) | | Accum (g) | Loss (g) |
|---|---|---|---|---|---|
| **Species** | **Feed** | **Cond** | **Slurry** | **Solids** | |
| **Stage 1 Filtrate** | 84.6 | | | | |
| **$H_2O$** | 278.9 | 294.4 | | | |
| **$CO_2$** | 0.7 | | | | |
| **Solution** | | | 26.7 | 24.0 | |
| **Total** | 364.2 | 294.4 | 26.7 | 24.0 | 19.1 |
| **Combined** | 364.2 | 345.0 | | | 19.1 |
| | | | | | 5.3% |

**Figure 48. Flowsheet and Mass Balance for DST Practice Run 29, Stage 2.**

# APPENDIX E

# GALBRAITH LABORATORIES SAMPLE ANALYTICAL RESULTS

## E.1 CHEMICAL ANALYSES FROM GALBRAITH LABORATORIES

**Table 22. Identification of Samples from Crystallization from DST Feed Solution Certification Run 31 Sent to Galbraith Laboratories for Analysis.**

| Sample ID | Description | Condition |
|---|---|---|
| DST5-ST1-1 | Filtrate from Stage 1 | Liquid |
| DST5-ST1-2 | Spent wash from Stage 1 | Liquid |
| DST5-ST1-3 | Washed crystals from Stage 1 | Solid |
| DST5-ST1-4 | Accumulation from Stage 1 crystallizer | Liquid |
| DST5-ST1-5 | Unwashed crystals from Stage 1 | Liquid |
| DST5-ST2-6 | SST Early Feed Solution | Liquid |
| DST4-ST2-0 | Carbonated Feed Solution | Liquid |
| DST4-ST2-1 | Filtrate from Stage 2 | Liquid |
| DST4-ST2-2 | Spent wash from Stage 2 | Liquid |
| DST4-ST2-3 | Washed crystals from Stage 2 | Solid |
| DST4-ST2-4 | Accumulation from Stage 2 crystallizer | Liquid |
| DST4-ST2-5 | Unwashed crystals from Stage 2 | Liquid |

## LABORATORY REPORT

Dr Ronald W Rousseau
Georgia Institute of Technology
School of Chemical & Biomolecular Engineering
311 Ferst Drive
Atlanta GA 30332-0100

Reanalysis Request: 09/23/05
Previous Lab ID #: X-3191-3225, X-0051-62, X-3191-
Report Date: 09/23/05

E-mail Addresses: EANelson@cogema-eng.com
FRRenz@cogema-eng.com

| SAMPLE ID | LAB ID | ANALYSIS | RESULTS | | DUPLICATE RESULTS | MATRIX SPIKE RECOVERY |
|---|---|---|---|---|---|---|
| DST5-ST1-1 | X-1834 | Oxalate | <200 [a] | ppm | | |
| | | Sodium | 11.7 | % | | |
| | | Aluminum | 2.61 | % | | |
| | | Chromium | 190 | ppm | | |
| | | Cesium | 15 | ppm | | |
| | | Fluoride | <7 | ppm | | |
| | | Nitrate as Nitrogen | 1.80 | % | | |
| | | Nitrite as Nitrogen | 2.33 | % | | |
| | | Sulfate as Sulfur | <100 | ppm | | |
| | | Carbonate | 0.14 | % | | |
| | | Hydroxide | 4.05 | % | | |
| | | Karl Fischer Water | 61.19 | % | | |
| | | Phosphate as Phosphorus | 200 | ppm | | |
| | | Density | 1.333 | g/mL | | |
| | X-3191 | Loss on Drying | 55.34 | % | | |
| DST5-ST2-3 | X-1835 | Oxalate | <100 | ppm | | |
| | | Sodium | 29.3 | % | | |
| | | Aluminum | 0.957 | % | | |
| | | Chromium | 65 | ppm | | |
| | | Cesium | 5.1 | ppm | | |
| | | Fluoride | 76 | ppm | | |
| | | Nitrate as Nitrogen | 1.22 | % | | |
| | | Nitrite as Nitrogen | 0.859 | % | | |
| | | Sulfate as Sulfur | <100 | ppm | | |
| | | Carbonate | 29.0 | % | | |
| | | Hydroxide | 3.21 | % | | |
| | | Karl Fischer Water | 7.60 | % | | |
| | | Phosphate as Phosphorus | 105 | ppm | | |
| | X-3192 | Loss on Drying | 22.25 | % | | |

LABORATORY REPORT

Dr Ronald W Rousseau
Georgia Institute of Technology

Report Date: 09/23/05
Lab ID#: X-3191-3225

| SAMPLE ID | LAB ID | ANALYSIS | RESULTS | | DUPLICATE RESULTS | | MATRIX SPIKE RECOVERY |
|---|---|---|---|---|---|---|---|
| DST5-ST1-3 | X-1836 | Oxalate | 819 | ppm | | | |
| | | Sodium | 30.5 | % | | | |
| | | Aluminum | 0.429 | % | | | |
| | | Chromium | 36 | ppm | | | |
| | | Cesium | 2.7 | ppm | | | |
| | | Fluoride | 304 | ppm | | | |
| | | Nitrate as Nitrogen | 1.35 | % | | | |
| | | Nitrite as Nitrogen | 0.443 | % | | | |
| | | Sulfate as Sulfur | 885 | ppm | | | |
| | | Carbonate | 31.4 | % | | | |
| | | Hydroxide | 2.61 | % | | | |
| | | Karl Fischer Water | 41.59 | % | | | |
| | | Phosphate as Phosphorus | <100 | ppm | | | |
| | X-3193 | Loss on Drying | 22.38 | % | | | |
| DST5-ST1-2 | X-1837 | Oxalate | 234 | ppm | | | |
| | | Sodium | 14.0 | % | | | |
| | | Aluminum | 1.38 | % | | | |
| | | Chromium | 96 | ppm | | | |
| | | Cesium | 7.4 | ppm | | | |
| | | Fluoride | 13 | ppm | | | |
| | | Nitrate as Nitrogen | 3.04 | % | | | |
| | | Nitrite as Nitrogen | 1.20 | % | | | |
| | | Sulfate as Sulfur | 273 | ppm | | | |
| | | Carbonate | 0.84 | % | | | |
| | | Hydroxide | 4.93 | % | | | |
| | | Karl Fischer Water | 61.83 | % | | | |
| | | Phosphate as Phosphorus | 123 | ppm | | | |
| | | Density | 1.379 | g/mL | | | |
| | X-3194 | Loss on Drying | 46.01 | % | 46.29 | [a] % | |

LABORATORY REPORT

Dr Ronald W Rousseau
Georgia Institute of Technology

Report Date: 09/23/05
Lab ID#: X-3191-3225

| SAMPLE ID | LAB ID | ANALYSIS | RESULTS | | DUPLICATE RESULTS | | MATRIX SPIKE RECOVERY |
|---|---|---|---|---|---|---|---|
| DST5-ST1-4 | X-1838 | Oxalate | <200 [a] | ppm | | | |
| | | Sodium | 1.83 | % | | | |
| | | Aluminum | 0.177 | % | | | |
| | | Chromium | 13 | ppm | | | |
| | | Cesium | 0.94 | ppm | | | |
| | | Fluoride | 11 | ppm | | | |
| | | Nitrate as Nitrogen | 0.143 | % | | | |
| | | Nitrite as Nitrogen | 0.155 | % | | | |
| | | Sulfate as Sulfur | <100 | ppm | | | |
| | | Carbonate | 1.50 | % | | | |
| | | Hydroxide | 0.240 | % | | | |
| | | Karl Fischer Water | 96.29 | % | | | |
| | | Phosphate as Phosphorus | <100 | ppm | | | |
| | X-3195 | Loss on Drying | 94.59 | % | | | |
| DST5-ST1-5 | X-1839 | Oxalate | <200 [a] | ppm | | | |
| | | Sodium | 3.04 | % | | | |
| | | Aluminum | 0.202 | % | | | |
| | | Chromium | 2.9 | ppm | | | |
| | | Cesium | 1.1 | ppm | | | |
| | | Fluoride | 35 | ppm | | | |
| | | Nitrate as Nitrogen | 0.268 | % | | | |
| | | Nitrite as Nitrogen | 0.175 | % | | | |
| | | Sulfate as Sulfur | 105 | ppm | | | |
| | | Carbonate | 2.67 | % | | | |
| | | Hydroxide | 0.348 | % | 0.269 [b] | % | |
| | | Karl Fischer Water | 92.87 | % | | | |
| | | Phosphate as Phosphorus | <100 | ppm | | | |
| | X-3196 | Loss on Drying | 91.70 | % | | | |

## LABORATORY REPORT

Dr Ronald W Rousseau
Georgia Institute of Technology

Report Date: 09/23/05
Lab ID#: X-3191-3225

| SAMPLE ID | LAB ID | ANALYSIS | RESULTS | | DUPLICATE RESULTS | | MATRIX SPIKE RECOVERY |
|---|---|---|---|---|---|---|---|
| DST5-ST1-6 | X-1840 | Oxalate | 241 | ppm | | | |
| | | Sodium | 11.8 | % | | | |
| | | Aluminum | 1.99 | % | | | |
| | | Chromium | 136 | ppm | | | |
| | | Cesium | 11 | ppm | | | |
| | | Fluoride | 21 | ppm | | | |
| | | Nitrate as Nitrogen | 1.63 | % | | | |
| | | Nitrite as Nitrogen | 1.83 | % | | | |
| | | Sulfate as Sulfur | 231 | ppm | | | |
| | | Carbonate | 3.72 | % | | | |
| | | Hydroxide | 3.13 | % | 3.09 [b] | % | |
| | | Karl Fischer Water | 64.43 | % | | | |
| | | Phosphate as Phosphorus | 162 | ppm | | | |
| | | Density | 1.331 | g/mL | | | |
| | X-3197 | Loss on Drying | 46.89 | % | | | |
| DST5-ST2-0 | X-1841 | Oxalate | <200 [a] | ppm | | | |
| | | Sodium | 11.6 | % | | | |
| | | Aluminum | 2.68 | % | | | |
| | | Chromium | 186 | ppm | | | |
| | | Cesium | 14 | ppm | | | |
| | | Fluoride | <7 | ppm | | | |
| | | Nitrate as Nitrogen | 1.81 | % | | | |
| | | Nitrite as Nitrogen | 2.27 | % | | | |
| | | Sulfate as Sulfur | <100 | ppm | | | |
| | | Carbonate | 2.75 | % | | | |
| | | Hydroxide | 2.56 | % | | | |
| | | Karl Fischer Water | 61.15 | % | | | |
| | | Phosphate as Phosphorus | 186 | ppm | | | |
| | | Density | 1.335 | g/mL | | | |
| | X-3198 | Loss on Drying | 53.37 | % | | | |

LABORATORY REPORT

Dr Ronald W Rousseau
Georgia Institute of Technology

Report Date: 09/23/05
Lab ID#: X-3191-3225

| SAMPLE ID | LAB ID | ANALYSIS | RESULTS | | DUPLICATE RESULTS | | MATRIX SPIKE RECOVERY |
|---|---|---|---|---|---|---|---|
| DST5-ST2-1 | X-1842 | Oxalate | 151 | ppm | | | |
| | | Sodium | 11.4 | % | | | |
| | | Aluminum | 3.27 | % | | | |
| | | Chromium | 223 | ppm | | | |
| | | Cesium | 17 | ppm | | | |
| | | Fluoride | <4 | ppm | | | |
| | | Nitrate as Nitrogen | 2.20 | % | | | |
| | | Nitrite as Nitrogen | 2.75 | % | | | |
| | | Sulfate as Sulfur | 79 | ppm | | | |
| | | Carbonate | 0.27 | % | | | |
| | | Hydroxide | 3.07 | % | | | |
| | | Karl Fischer Water | 57.13 | % | | | |
| | | Phosphate as Phosphorus | 191 | ppm | | | |
| | | Density | 1.357 | g/mL | | | |
| | X-3199 | Loss on Drying | 57.15 | % | | | |
| DST5-ST2-2 | X-1843 | Oxalate | <200 | [a] ppm | | | |
| | | Sodium | 12.4 | % | | | |
| | | Aluminum | 0.575 | % | | | |
| | | Chromium | 41 | ppm | | | |
| | | Cesium | 3.1 | ppm | | | |
| | | Fluoride | 4 | ppm | | | |
| | | Nitrate as Nitrogen | 2.23 | % | | | |
| | | Nitrite as Nitrogen | 0.544 | % | | | |
| | | Sulfate as Sulfur | <100 | ppm | | | |
| | | Carbonate | 1.84 | % | | | |
| | | Hydroxide | 4.71 | % | | | |
| | | Karl Fischer Water | 74.05 | % | | | |
| | | Phosphate as Phosphorus | <100 | ppm | | | |
| | | Density | 1.299 | g/mL | 1.317 [b] | g/mL | |
| | X-3200 | Loss on Drying | 63.96 | % | | | |

## LABORATORY REPORT

Dr Ronald W Rousseau
Georgia Institute of Technology

Report Date: 09/23/05
Lab ID#: X-3191-3225

| SAMPLE ID | LAB ID | ANALYSIS | RESULTS | | DUPLICATE RESULTS | | MATRIX SPIKE RECOVERY | |
|---|---|---|---|---|---|---|---|---|
| DST5-ST2-4 | X-1844 | Oxalate | <200 [a] | ppm | | | 117 [b] | % |
| | | Sodium | 2.57 | % | | | | |
| | | Aluminum | 0.181 | % | | | | |
| | | Chromium | 121 | ppm | | | | |
| | | Cesium | 0.90 | ppm | | | | |
| | | Fluoride | <4 | ppm | | | | |
| | | Nitrate as Nitrogen | 0.137 | % | | | 105 [b] | % |
| | | Nitrite as Nitrogen | 0.177 | % | | | 101 [b] | % |
| | | Sulfate as Sulfur | <100 | ppm | | | 102 [b] | % |
| | | Carbonate | 2.58 | % | | | | |
| | | Hydroxide | 0.171 | % | | | | |
| | | Karl Fischer Water | 97.47 | % | | | | |
| | | Phosphate as Phosphorus | <100 | ppm | | | 108 [b] | % |
| | X-3201 | Loss on Drying | 92.49 | % | | | | |
| DST5-ST2-5 | X-1845 | Oxalate | <200 [a] | ppm | | | | |
| | | Sodium | 2.22 | % | 2.17 [b] | % | 100 [b] | % |
| | | Aluminum | 0.327 | % | 0.324 [b] | % | 101 [b] | % |
| | | Chromium | 23 | ppm | 22 [b] | ppm | 99 [b] | % |
| | | Cesium | 1.7 | ppm | 1.7 [b] | ppm | 95 [b] | % |
| | | Fluoride | <4 | ppm | | | | |
| | | Nitrate as Nitrogen | 0.225 | % | | | | |
| | | Nitrite as Nitrogen | 0.286 | % | | | | |
| | | Sulfate as Sulfur | <100 | ppm | | | | |
| | | Carbonate | 1.45 | % | | | | |
| | | Hydroxide | 0.344 | % | | | | |
| | | Karl Fischer Water | 95.49 | % | | | | |
| | | Phosphate as Phosphorus | <100 | ppm | | | | |
| | X-3202 | Loss on Drying | 92.86 | % | | | | |

# APPENDIX F

# SEEDING

## F.1 SEEDING OF BATCH RUNS

The addition of seed crystals is a well-accepted procedure for controlling nucleation and the resulting crystal size distribution produced in batch crystallization; on the other hand, seeding is unnecessary, except in special circumstances, when the operation is of a continuous nature. It is thought that burkeite is the most suitable candidate for seeding for the following reasons: (1) it is one of the major species and it grows relatively slowly, and (2) crystals larger than 20 μm may facilitate solids separation.

Seeding was examined in experiments involving a 3-salt solution of sodium nitrate, sodium carbonate and sodium sulfate. The main purposes of these experiments were to study the effect of seeding on product properties and to investigate potential modifications in procedures that would reduce the amount of crystal accumulation on the walls of the crystallizer. Seeded 3-salt experiments (Runs 17 and 18) used sodium sulfate and sodium carbonate crystals as seed crystals.

The objective of using burkeite seed crystals in the 3-salt crystallization experiments was to obtain larger burkeite product crystals. The seed crystals were obtained from an earlier burkeite run performed according to the simulation Lab1B.xls. The product from that run was sieved, and the crystals retained on the smallest sieve (35 to 58 μm) were used as seeds in Run 18. Unfortunately, after performing Run 18, some question as to the actual composition of the seed crystals arose and they may have instead been a physical mixture of sodium sulfate and sodium carbonate.

The amount of seed crystals added in Run 18 was 10% of the expected mass of burkeite crystal yield as predicted by the simulation. The majority of the seed crystals appeared to be

agglomerates comprised of constituent fine crystals whose shapes were similar to that of sodium sulfate. These agglomerates were close to 35 μm in size. The addition of seed crystals was expected to lead to larger product crystals. Since it was thought originally that the seed crystals were burkeite, larger crystals of this species were expected. PLM observations of the product from this run showed larger sodium carbonate and sodium sulfate crystals than in previous non-seeded 3-salt crystallization runs. There appeared to be little effect of the seed crystals on the size of the burkeite crystals in the product, and it was this observation that threw the composition of the seed crystals into question.

The product from Run 18 was washed with acetone, dried, and sieved to give the results shown in the following figure. The distribution is quite uniform and exhibits no significant post-washing agglomeration.

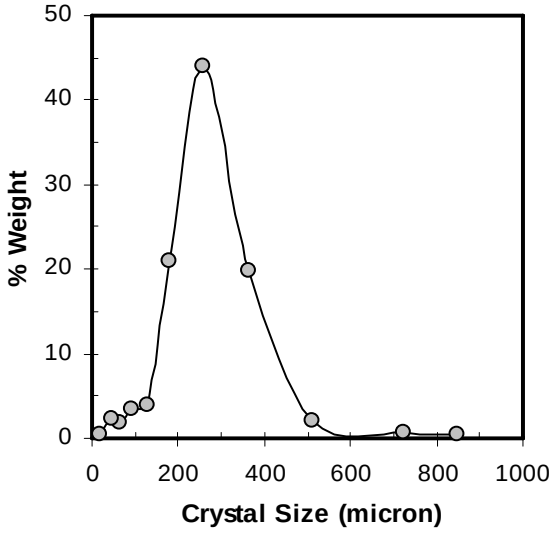


**Figure 49. Size Distribution of the Seeded 3-Salt Experiment (Run 18).**

# APPENDIX G

# EFFECT OF CRYSTAL WASHING

## G.1 WASHING EFFICIENCY

To determine qualitatively the effect of multiple wash steps on product purity, crystals recovered from run using an SST Early Feed simulant were washed and filtered four times in series. Figure G1 displays the change in color of crystals at the bottom of the sample bottles (from left to right) as the product crystals were washed.


**Figure 50. Effects of Washing on Crystal Color.**

The sample labeled –1 corresponds to the filtered slurry obtained from the crystallization and bottle 0 is a sample of the washed crystals produced in the experiment. Bottles 1 through 4 are samples taken after each of four additional wash steps. Each wash was performed by slurrying the crystals in a saturated solution of sodium nitrate. The experiment was stopped when the color between two successive samples remained unchanged. At this point the amount of adhering mother liquor and its associated impurities can be assumed negligible and the remaining color is a result of the crystal inclusions. The progression of the color to a virtually white sample after three additional washings leads to the conclusion that the majority of the remaining liquid (mother liquor remaining after the filtration operation) is present in a form other than inclusions.

The graph presented in Figure G2 shows the chromium analyses of the washed crystals. Clearly, the expected coloration of the crystals due to the presence of chromium corresponds to the visual observations described above and the quantitative analysis shown on the graph.

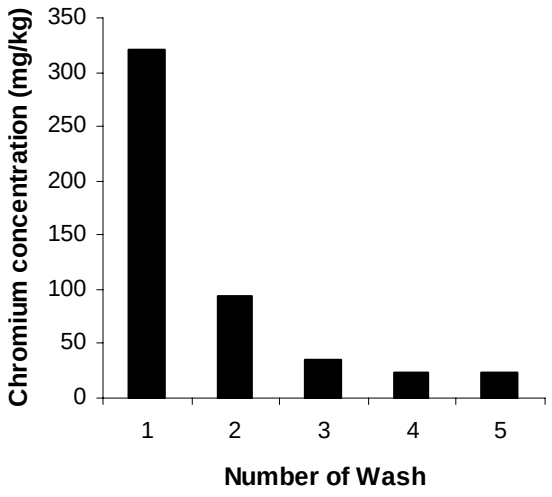


**Figure 51. Chromium Evolution with Washing.**

## REFERENCES


Aloise, Gene. United States Government Accountability Office April 6 (2006). "Hanford Waste Treatment Plant". GAO-06-602T.

Bryan, Sam.. June 12-14 (2003). "Flammable gas issue in stored Hanford Waste". American Chemical Society, Bozeman, MT. Pacific Northwest National Laboratory, Richland, WA.

Carreon, Rudy; Mauss, Billie M.; Johnson, Mike E.; Holton, Langdon K.; Wright, Todd G.; Peterson, Reid A.; Rueter, Ken J. (2002)."Selection of Pretreatment Processes for Removal of Radionuclides from Hanford Tank Waste". WM'02 Conference, February 24-28, 2002, Tucson, A.

Chapman, C.C.; Buelt, J.L.; Slate, S.C.; Katayama, Y.B.; Bunnell, L.R.. (1979). " Vitrification of Hanford wastes in a joule-heated ceramic melter and evaluation of resultant canisterized product". Abstract, Energy Res. Battelle Pac. Northwest Lab., Richland, WA, USA.

Chitry, Frederic; Pellet-Rostaing, Stephanie; Nicod, Laurence; Gass, Jean-Louis; Foos, Jacques; Guy, Alain; Lemaire, Marc. Cesium/Sodium Separation by Nanofiltration-Complexation in Aqueous Medium. Separation Science and Technology, 2001.

P. Colombo ; G. Brustatin; E. Bernardo; G. Scarinci. (2003). "Inertization and reuse of waste materials by Vitrification and fabrication of glass-based products."
Solid State and Materials Science, August 2003.

Cowley, W.L.; Vail, T.S.; Reynolds, D.A.; Herting, D.L. April 19-23 (1998). "Technical basis for selecting radionuclide concentrations for use in Hanford tank basis for interim operation source term". Technologies for the New Century topical conference, Nashville. American Nuclear Society, La grange Park, III.

DOE/EM-0319. January (1997). "Connecting the Cold War Nuclear Weapons Production Processes To Their Environmental Consequences". Linking Legacies, US Department of Energy DOE/EM-0319, United States Department of Energy, Washington, DC 20585 .

DOE/EM-0266. (1996). "Closing the Circle on the Splitting of the Atom: The Environmental Legacy of Nuclear Weapons Production and What the Department is Doing About It".

DOE/EM-0232 and DOE/EM-0290. (1995-1996). "Estimating the Cold War Mortgage: The 1995 Baseline Environmental Management report".

DOE. (1996). "Risks and the Risk Debate: Searching for Common Ground".

Felder, R. M.; Rousseau, R. W., Elementary Principles of Chemical Processes, 3rd Ed., John Wiley & Sons, Inc., New York.

Fullam, H.T.(1976). "Solubility and dissolution behavior of strontium-90 difluoride in aqueous media". ERDA Energy Res. Abstract. Battelle Pac. Northwest Lab., Richland, WA, USA.

Geniesse, Donald James; (2004). "Volume reduction of Aqueous Waste by Evaporative Crystallization of Burkeite and Sodium Salts". US Patent. Cogema Engineering Corporation, Richland, WA, USA.

Hammitt, A.P.; Schulz, W.W.. (1979). "Hot Cell Facility and Equipment for Tests of the Hanford Radionuclide Removal Process". Proceedings of the Conference on Remote Systems Technology, Volume No. 26 413-29. Rockwell Hanford Oper., Richland, WA, USA.

Hassan, N.M.; McCabe, D.J.; King, W.D.; Hamm, L.L.; Johnson, M.E.. Ion exchange removal of cesium from Hanford tank waste supernates with SuperLig® 644 resin. Journal of Radioanalytical and Nuclear Chemistry. Vol. 254, No. 1 (2002), pp. 33-40.

Herting, D; Cook, G; Warrant, R; Document Number HNF-11585 "Identification of Solid Phases in Saltcake from Hanford Site Waste Tanks," Richland, Washington (2002).

Herting, D.L. (1992). "Identification of crystals in Hanford nuclear waste using polarized light microscopy". Energy Res. Abstract, 17(08), Abstract No. 22486. Westinghouse Hanford Co., Richland, WA, USA.

Herting, Dan. June 12-14 (2003). "Inorganic tank waste speciation". Abstracts, 58th Northwest Regional Meeting of the American Chemical Society.

Herting, Daniel L. September 7-11 (1997). "Clean salt process for Hanford nuclear waste treatment". Book of Abstracts, 214th ACS National Meeting, Las Vegas, NV. American Chemical Society, Washington, D.C.

P.Hrma, J.V. Crum, D.J. Bates, P.R. Bredt, L.R. Greenwood, H.D. Smith. (2005). "Vitrification and testing of a Hanford high-level waste sample. Part 1: Glass fabrication, and chemical and radiochemical analysis."Journal of Nuclear Materials 345 (2005) 19-30

P.Hrma, J.V. Crum, P.R. Bredt, L.R. Greenwood, B.W. Arey, H.D. Smith. (2005). "Vitrification and testing of a Hanford high-level waste sample. Part 2: Phase identification and waste form leachability."Journal of Nuclear Materials 345 (2005) 31-40

Huang, Frank H.; Mitchell, Dolores E.; Conner, John M.. (1994). "Low-Level Radioactive Hanford Wastes Immobilized by Cement-Based Grouts". Nuclear Technology. Westinghouse Hanford Company, Richland, WA,USA.

Kaldor, R.A.; McDaniel, E.W.; Treat, R.L.. September 7-11 (1985). "Immobilization of Selected Low-Level Hanford Wastes in Grout". Waste Management (Tucson, Arizona). Pacific Northwest Lab., Richland, WA, USA.

Kaminski, Michael D.; Nunez, Luis. Cesium Extraction from a Novel Chemical Decontamination Process Solvent Using Magnetic Microparticles. Separation Science and Technology Vol. 37, No. 16 2002.

Lewis, R E.; Butler, T.A.; Lamb, E. (1965). "Recovery of 137Cs from fission-product wastes and transport by an aluminosilicate ion exchanger". U.S. At. Comm. Oak Ridge Natl. Lab., Oak Ridge, TN, USA.

Mika. M; Patek. M; Maixner.J; Randakova.S; Hrma.P;. (2001)."The effect of temperature and composition on spinel concentration and crystal size in high-level radioactive waste vitrification." Proceedings of the International Conference on radioactive Waste Management and Environmental Remediation, 2001.

Ponder, Sherman M.; Helkowski, Robert; Mallouk, Thomas E. Continuous-Flow Process for the Separation of Cesium from Complex Waste Mixtures. Ind. Eng. Chem. Res. Vol. 40, No. 15 2001.

Rabiger K. ; Keldenich K. ; Scheffer J.. Glastech Ber. (1995). "Experience in operation of a pilot plant melting residual substances."
Glass Sci technol, Vol. 68, 84-90, 1995.

Reynolds, D.A.; Herting, D.L. (1985). "Solubilities of Sodium Nitrate, Sodium Nitrate, Sodium Nitrite, and Sodium Aluminate in simulated nuclear waste ". Energy Res. Abstr.. Rockwell Hanford Oper., Rockwell Int. Corp., Richland, WA, USA.

Robert A. Smith ; David H. Nyman; B. Nick Anderson. (1990) "Getting ready to build the Hanford Waste Vitrification Plant." Nuclear Engineering International, Vol. 35, No 428, 40-43, March 1990.

Thompson, LE.; Lowery, P.S. (2003). "Development of the bulk vitrification treatment process for the low activity fraction of Hanford single shell tank waste"
Conference, February 23-27,2003 Tucson, AZ

Toghiani, Rebecca K.; Lindner, Jeff S.; Herting, D.L. March 11-14 (2002). "Modeling of Hanford saltcake dissolution". American Institute of Chemical Engineers, Spring National Meeting, New Orleans, LA, USA.

Tyree Geoff.."First glass made at Hanford via bulk vitrification."
CH2M Hill Hanford group Publication

Vance, E.R.; Hart, K.P.; Carter, M.L.; Hambley, M.J.; Day, R.A.; Begg, B.D.(1998). "Further studies of Synroc immobilization of HLW sludges and Tc for Hanford tank waste remediation". Materials Research Society. Materials Division, ANSTO, Menai, Australia.

Wilson.B.K; Hrma.P; Alton.J; Plaisted.T.J; Vienna.J.D . (2002). “The effect of composition on spinel equilibrium and crystal size in high-level waste glass.” Journal of Materials Science, Vol 37 (24), 5327-5331, 2002.